Cell merger, Cold pool, and mid-level dry air of the afternoon thunderstorms at Taipei on 14 June 2015

Ming-Jen Yang 楊明仁
National Taiwan University

Acknowledgement: Mr. Jyong-En Miao

Seminar at University of Hawaii

3:30 pm, Wednesday, 20 January 2021

News report of urban flooding for this event

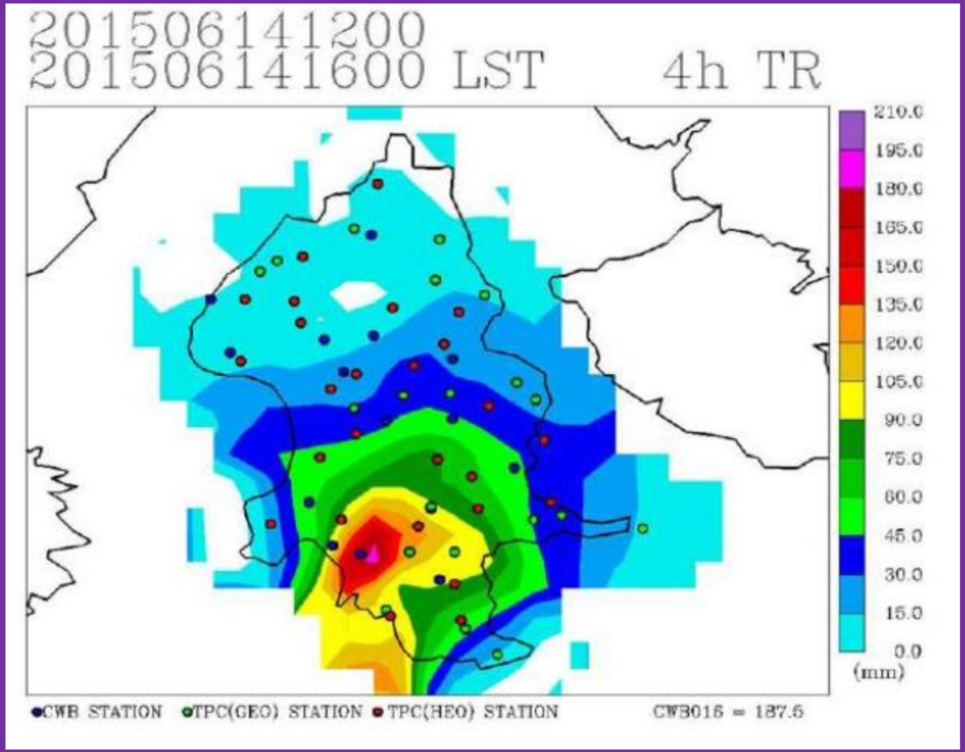

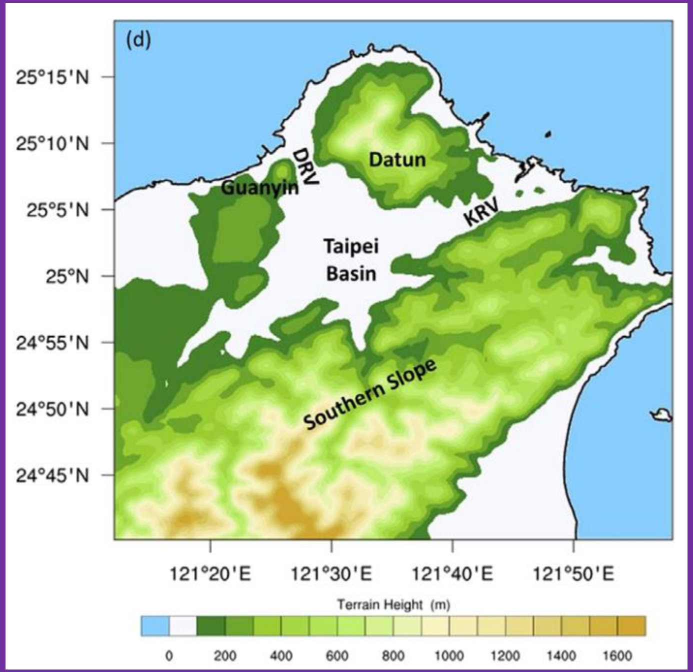

Weak Synoptic Forcing
& Moderate Thermodynamic Instability

Surface

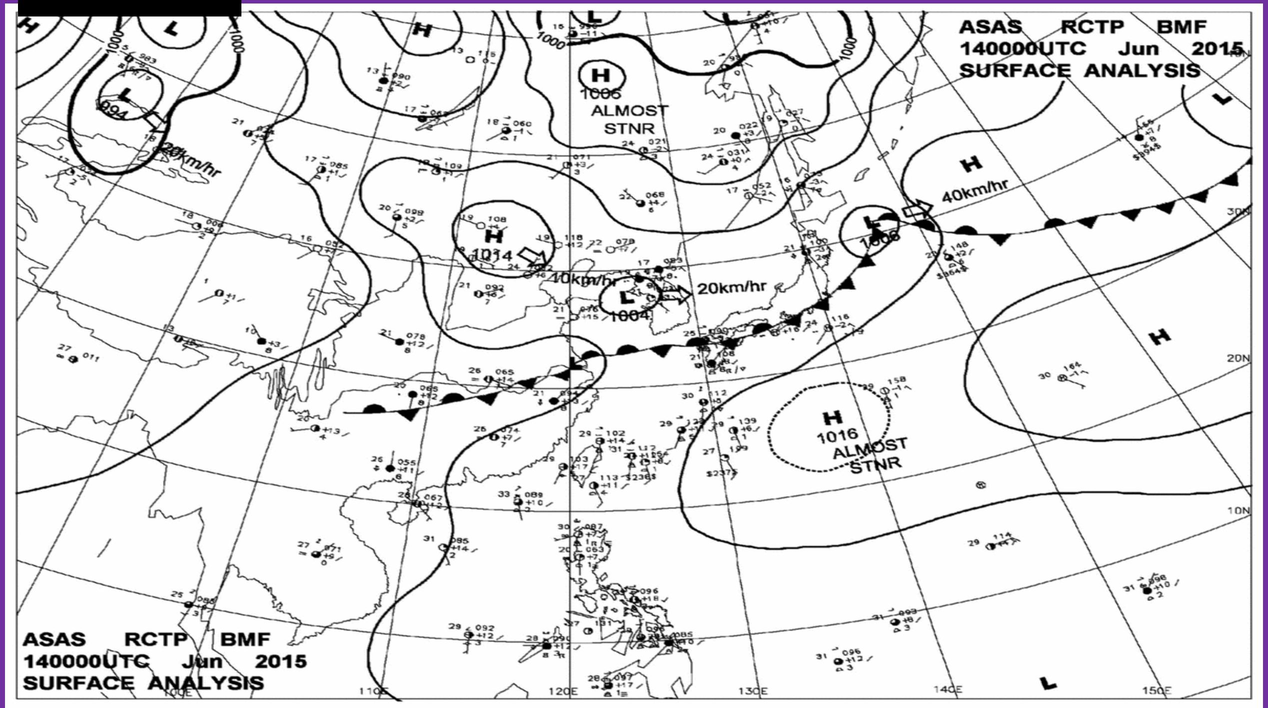

CWB Synoptic Analysis

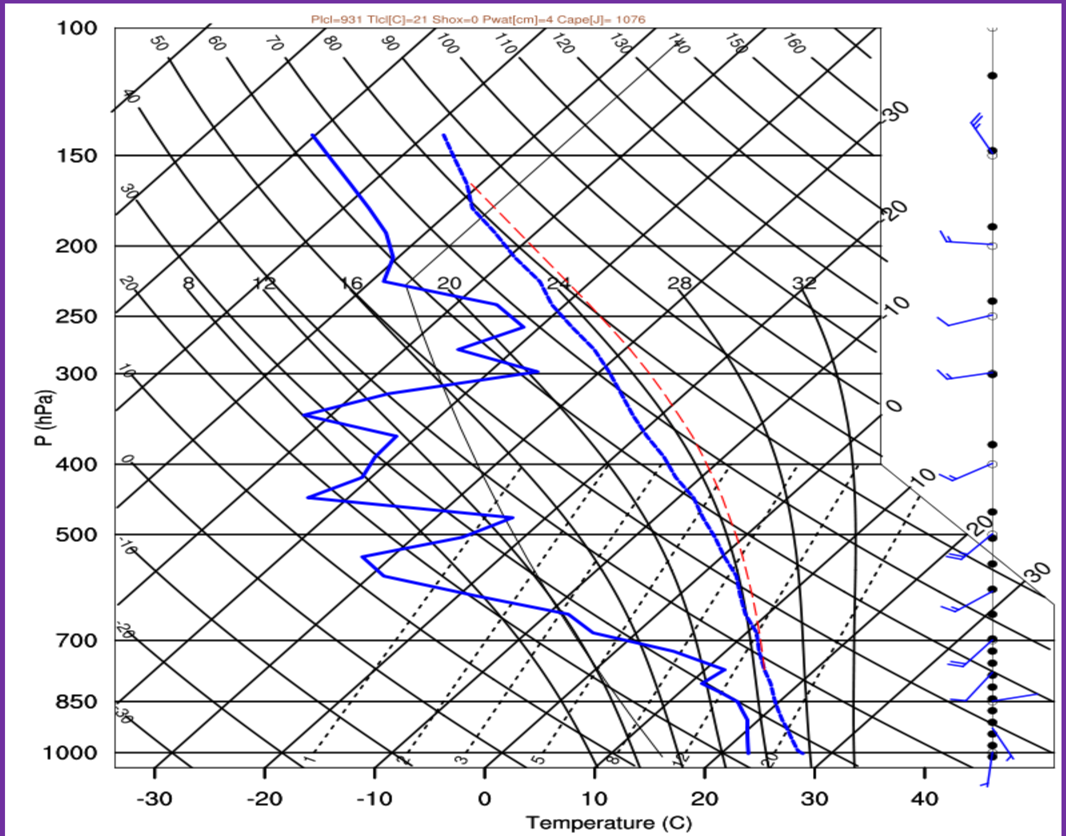

CAPE = 1076 J/kg at 08 LST for Banchiao sounding
=> Moderate instability

Synoptic Conditions at Upper Levels

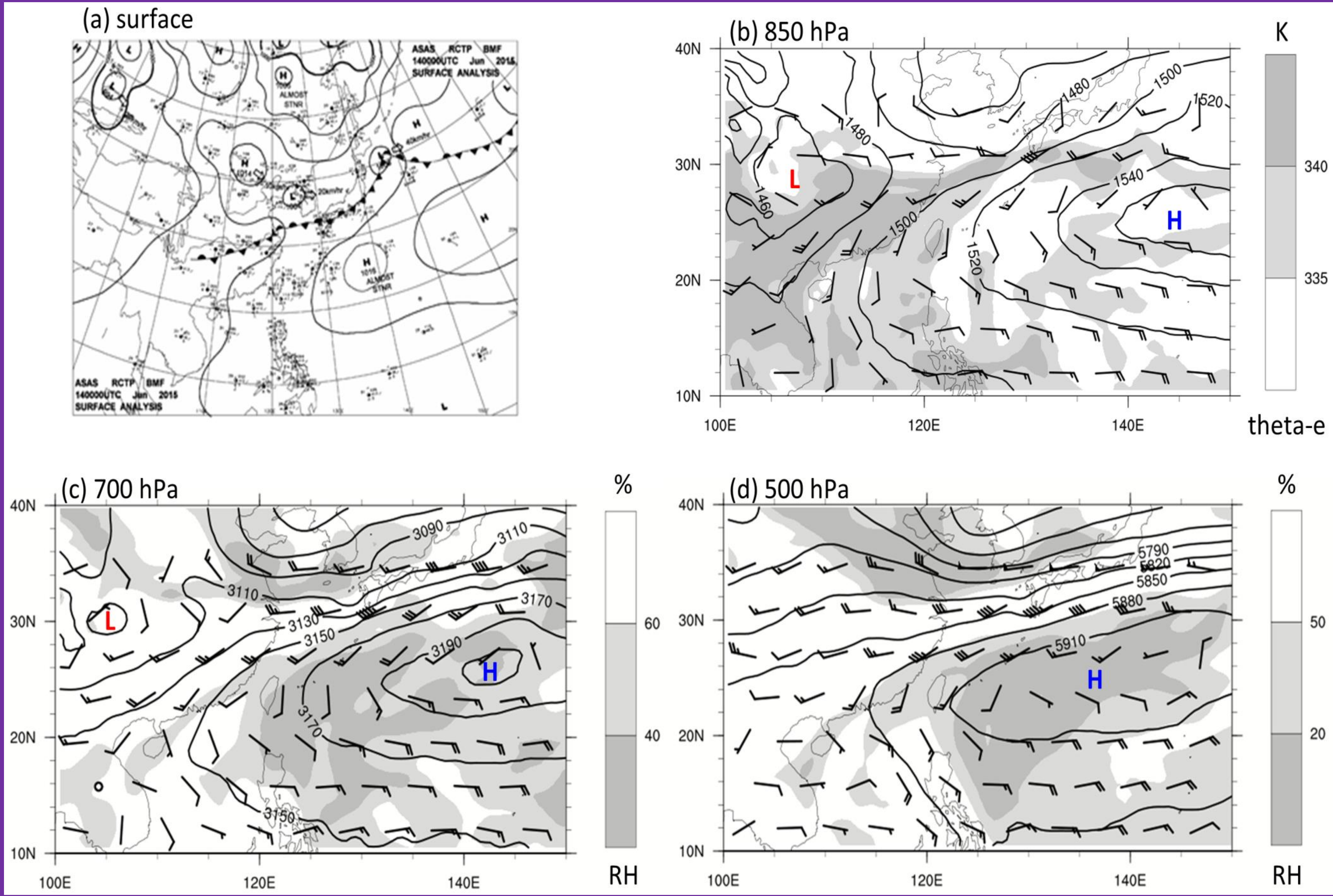

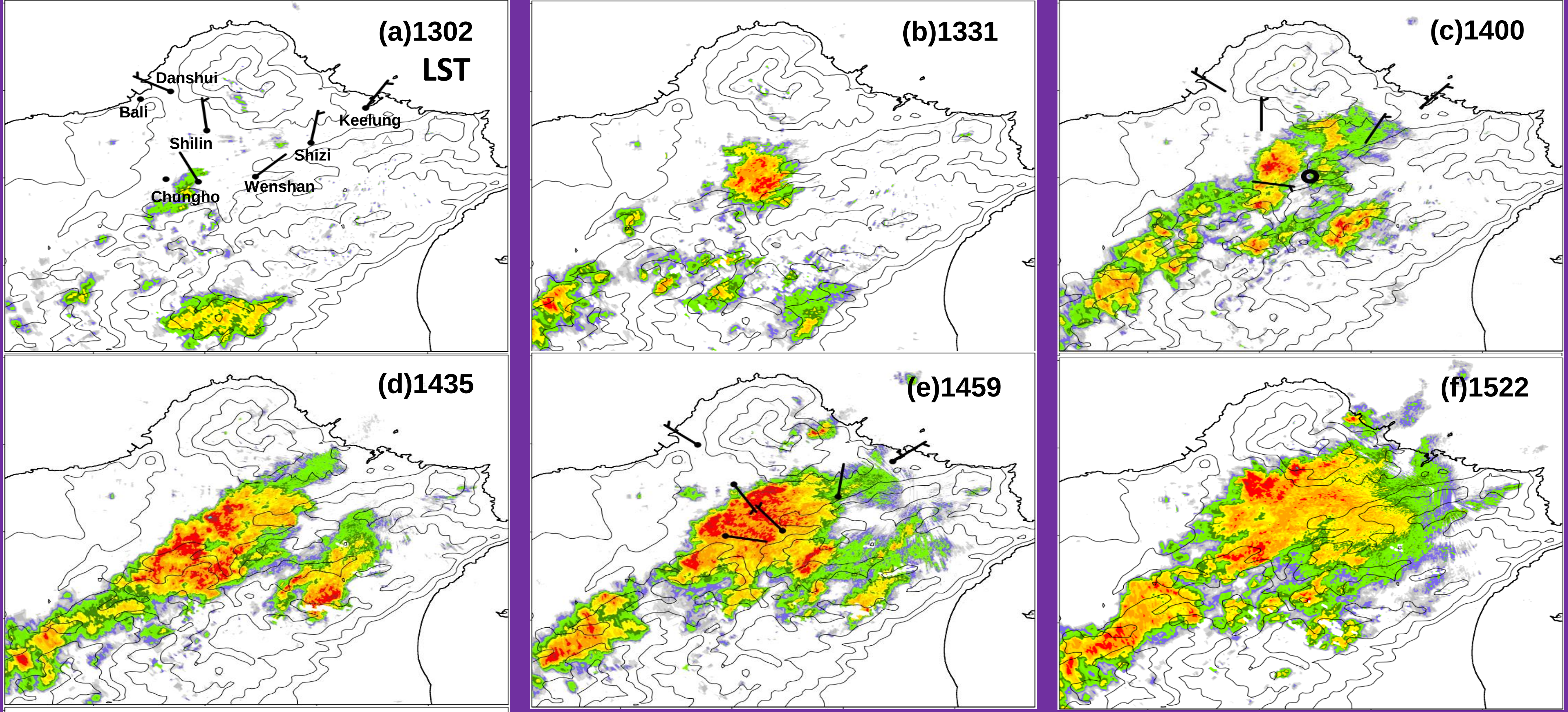

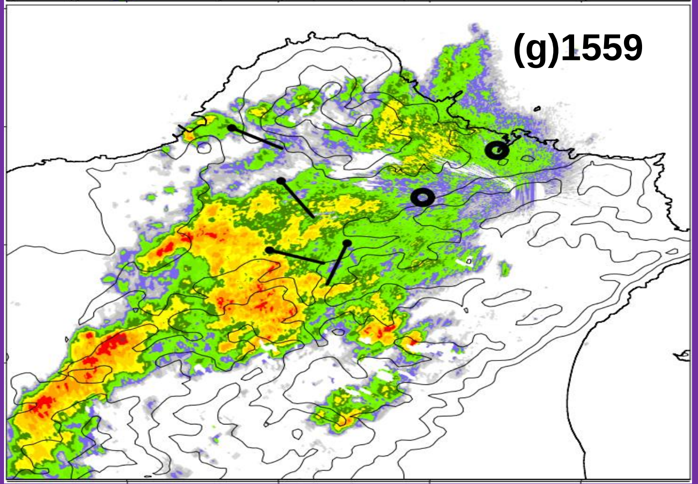

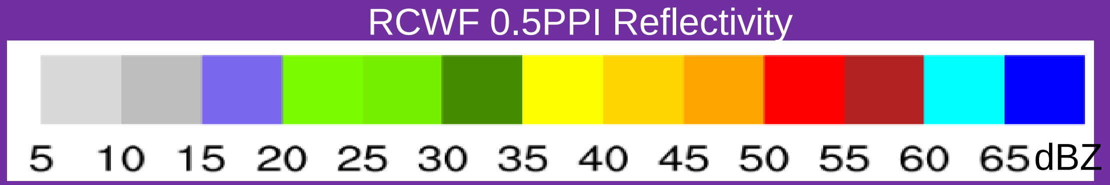

Evolution of Lowest Elevation-Angle Radar Reflectivity PPI observed by RCWF Radar from 1300 LST to 1600 LST

Time series of rainfall rate
at Gongkung rain-gauge station

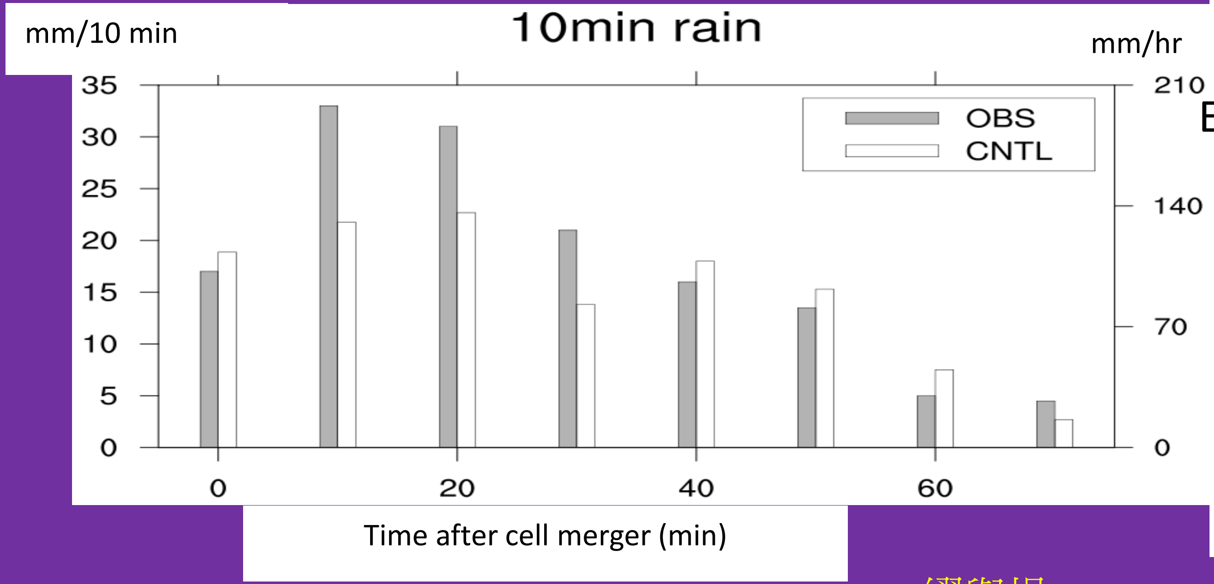

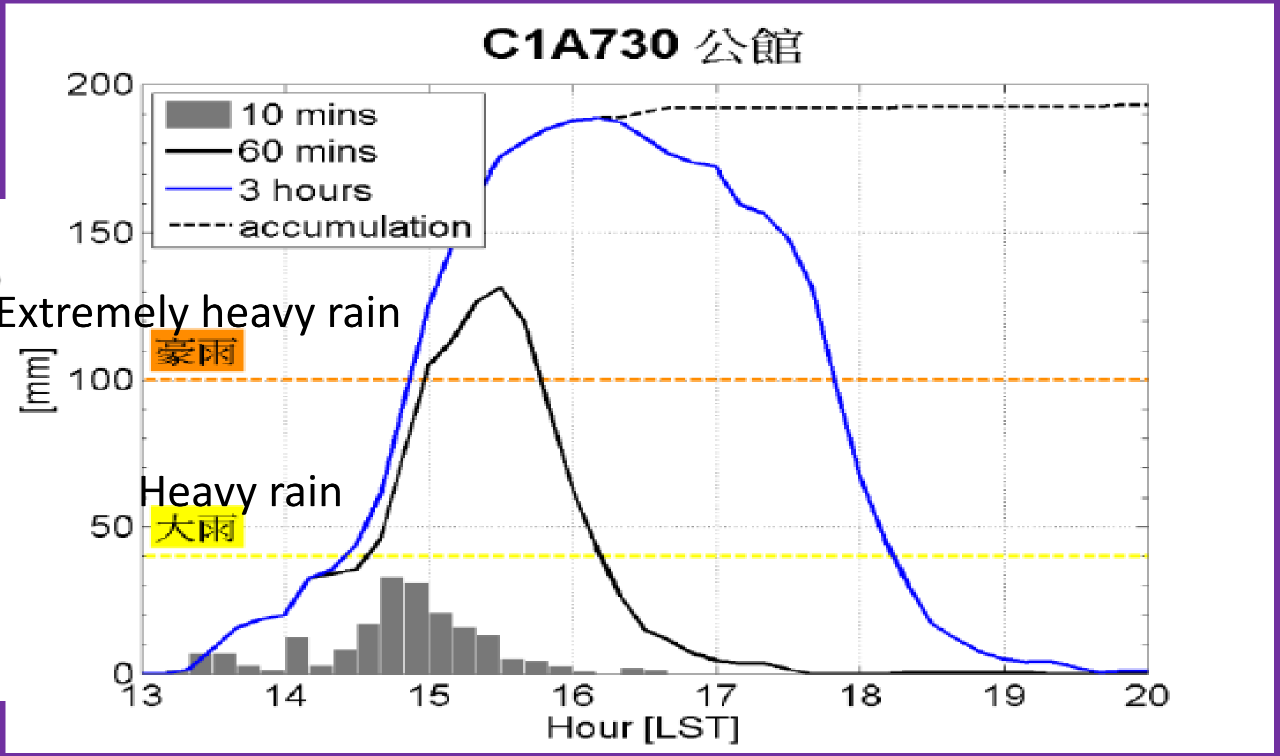

繆與楊
(2018; 大氣科學)

周等人
(2016; 大氣科學)

=> Both observation and model simulation show that rainfall rate increased significantly after cell merger.

Model Configuration

- Version 3.4 of WRF ARW
- two-way interactive 4 nested domains: 13.5, 4.5, 1.5 , **0.5 km**
- **55 vertical levels (8 layers within PBL)**
- **Kain-Fritsch cumulus on D1 only**
- microphysics scheme: WDM6
- Dudhia shortwave radiation
- RRTM longwave radiation
- Noah land surface model
- YSU PBL
- Landuse data: MODIS
- ECMWF ERA-Interim 0.75°x0.75°
- initial time: 6/13 12Z
- forecast hour: 24hr ( at t = 15hr)

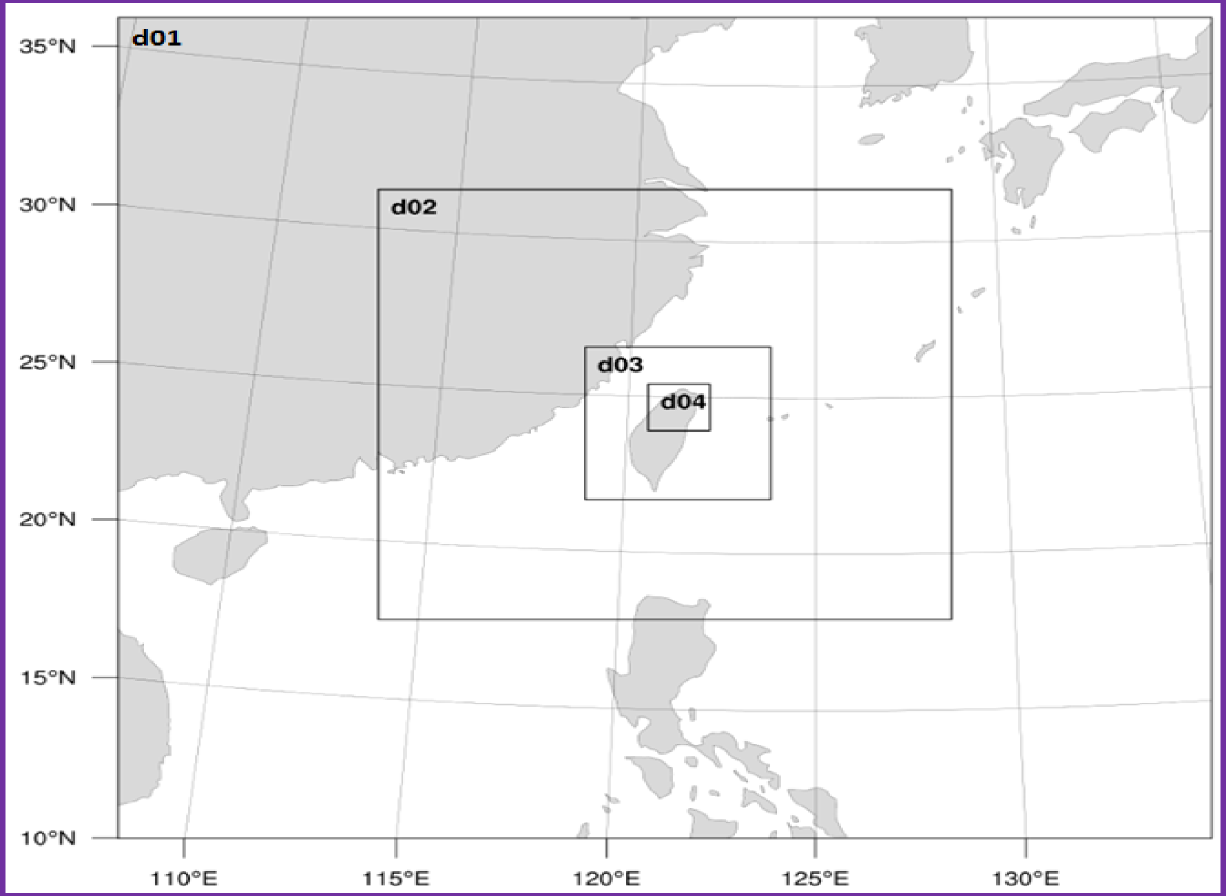

Comparison between the simulated and observed soundings

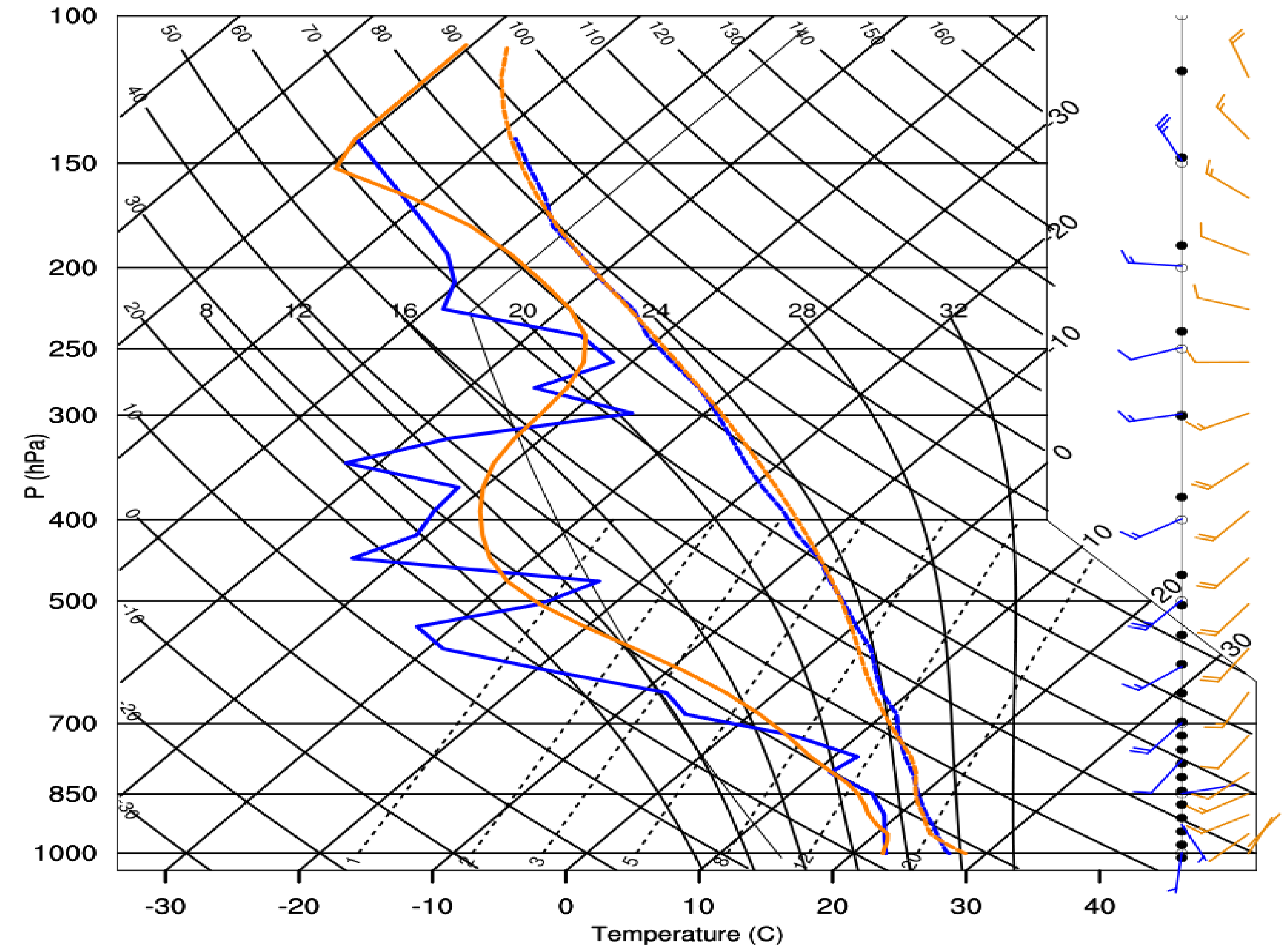

Banchiao sounding at 0800 LST

OBS **WRF-CNTL**

CAPE comparison:

=> OBS: 1076 J/kg

CNTL: 885 J/kg

Both indicate a mid-level dry layer!

Both show the southwesterly between 850 hPa and 400 hPa, and also westerly at upper level.

OBS

WRF-CNTL

2-m Temp.
& Wind

1200-1800 LST
rainfall

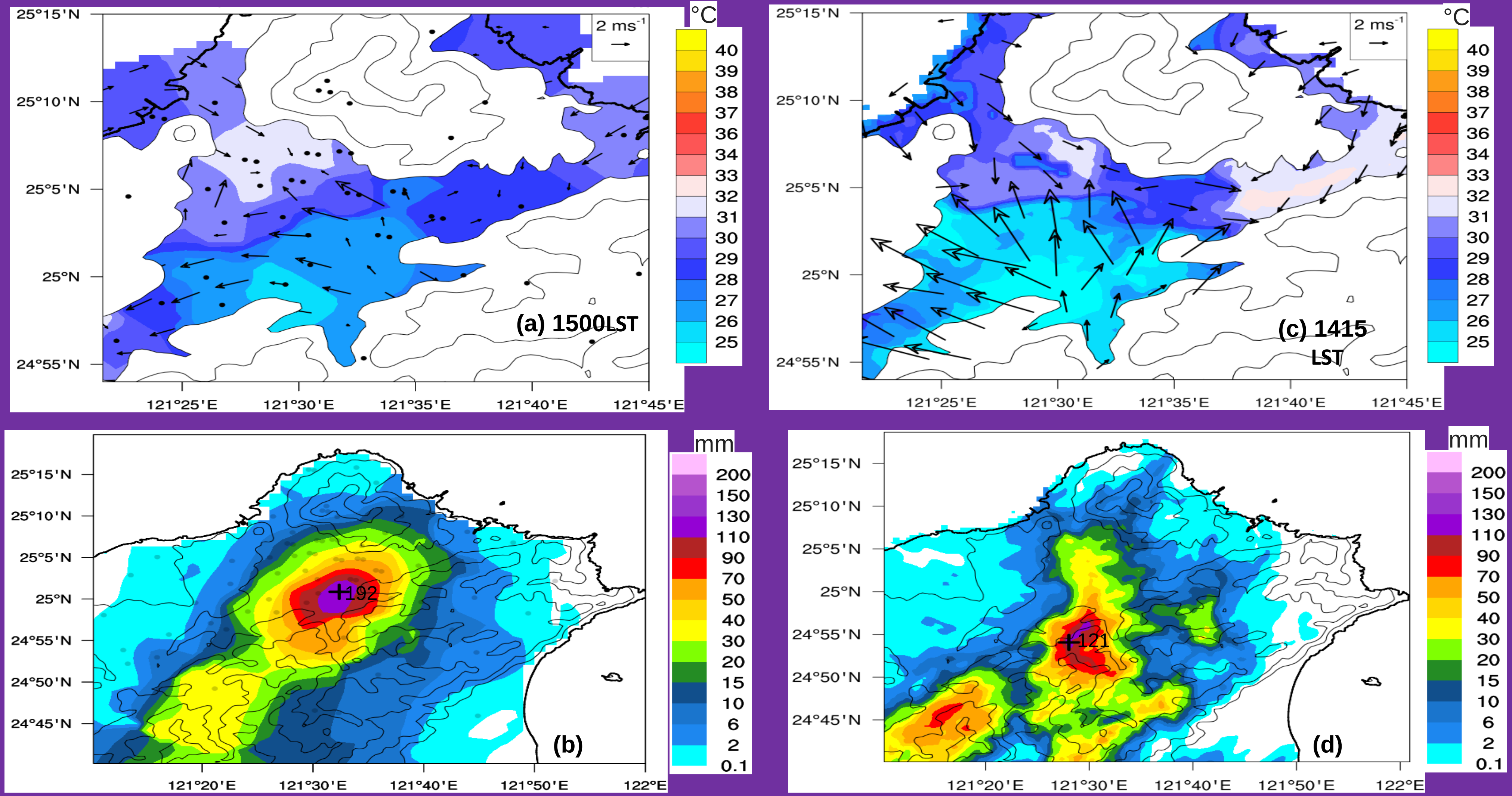

繆與楊
(2018; 大氣科學)

=> Low-level convergence produced by sea-breeze circulation and thunderstorm cold-air outflow at Taipei City

Water vapor comparison (OBS vs. WRF-CNTL)

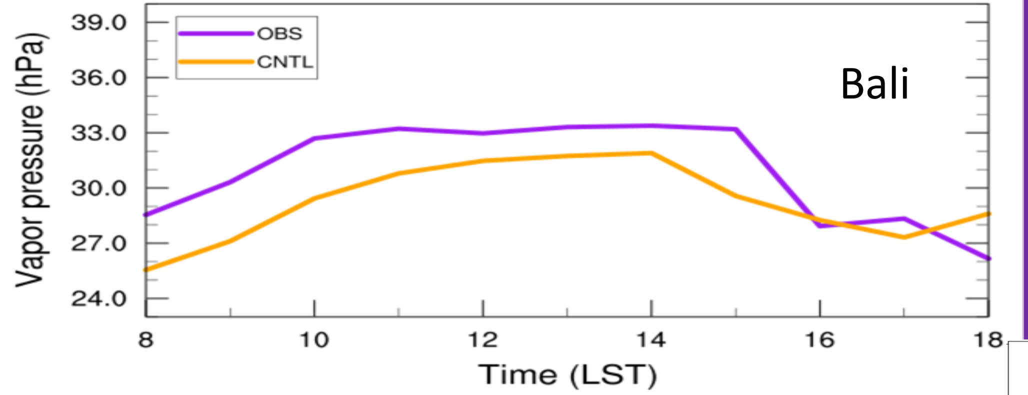

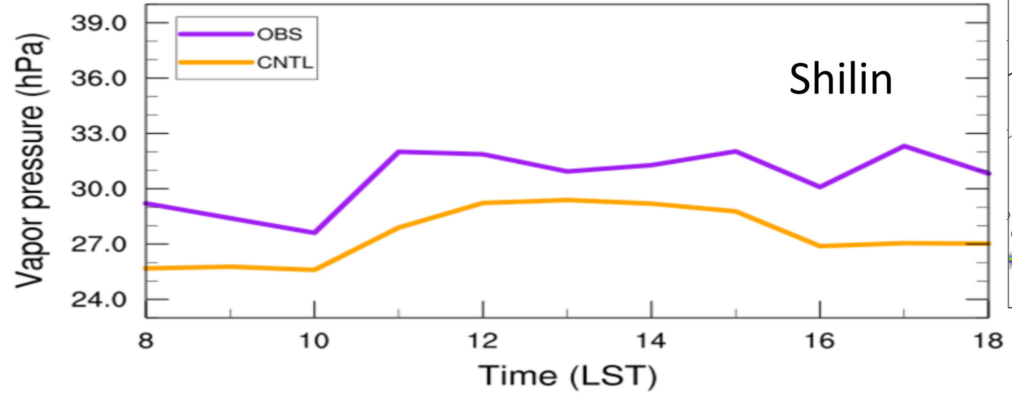

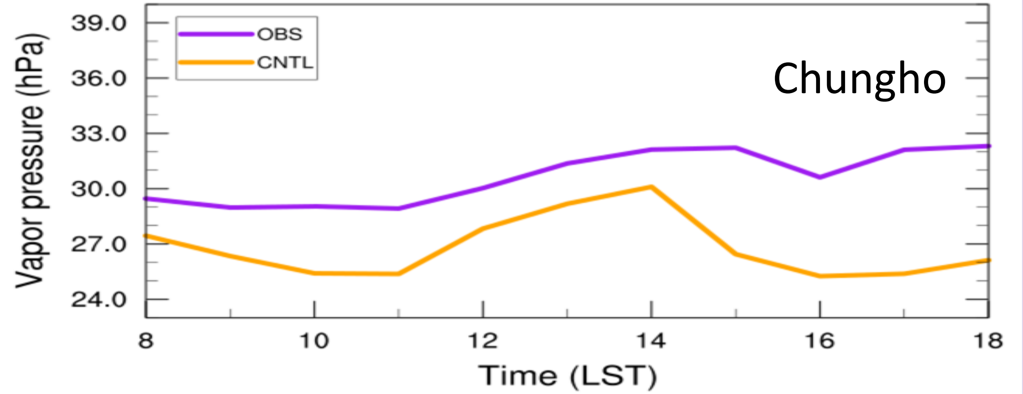

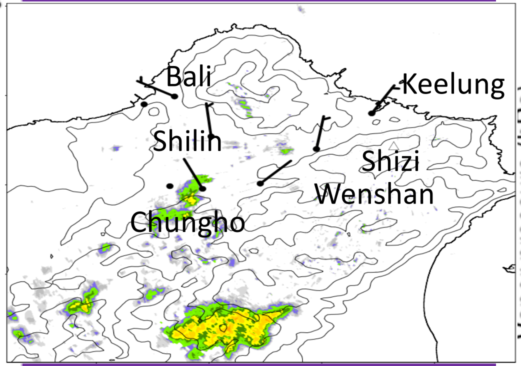

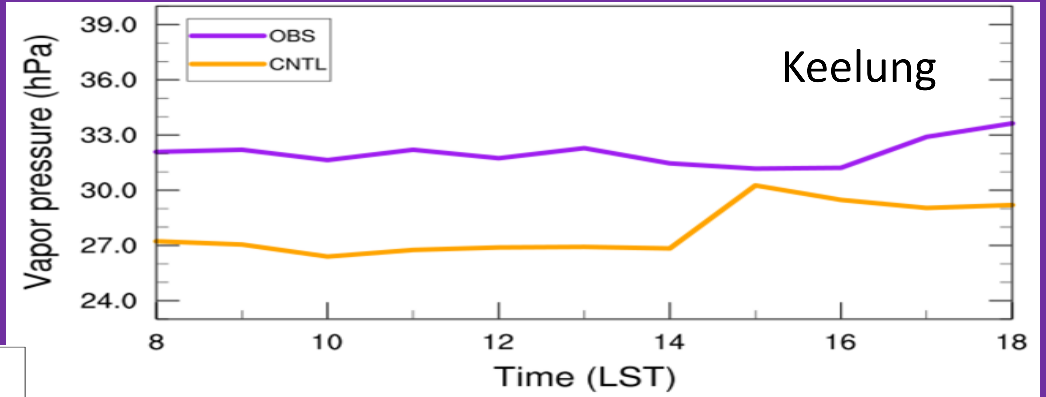

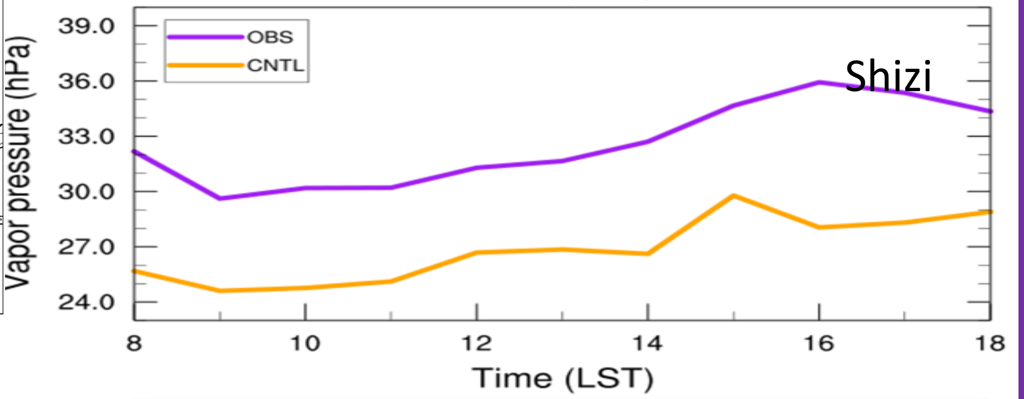

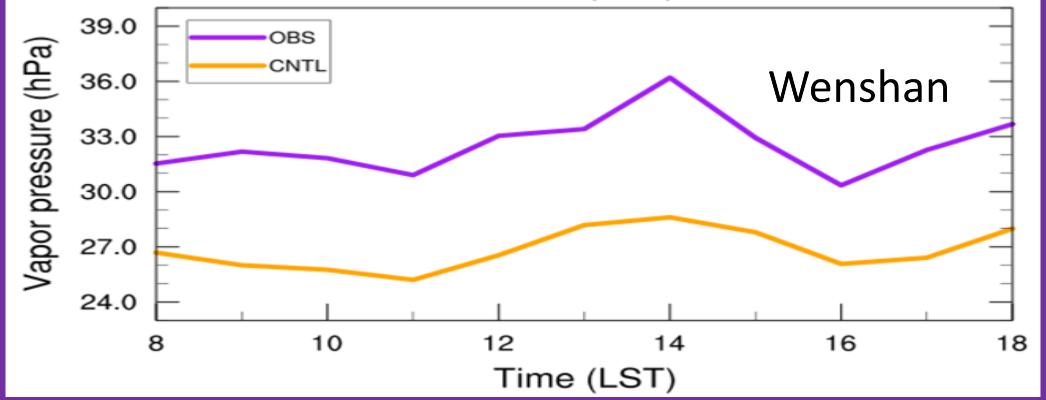

OBS

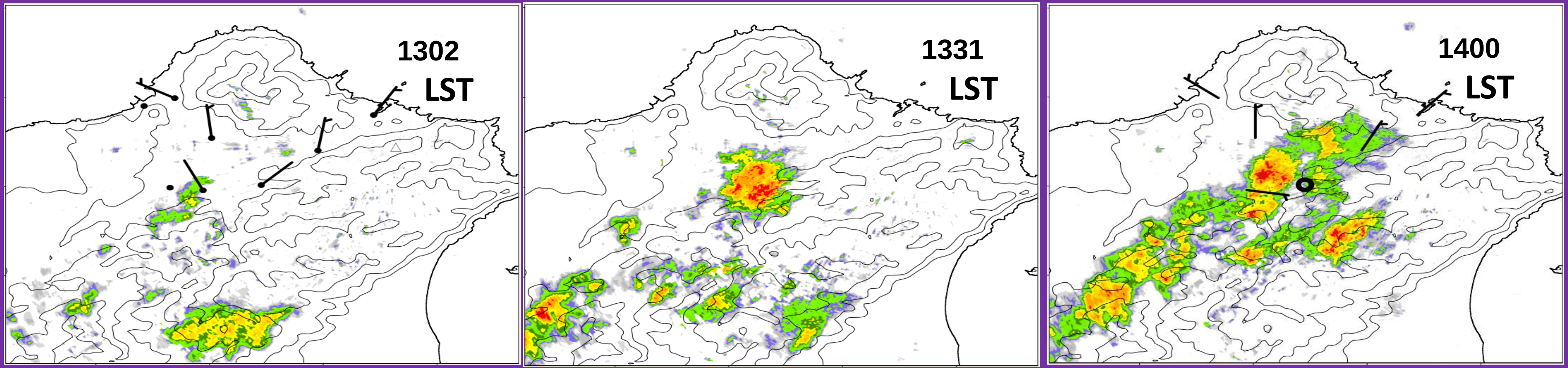

Reflectivity PPI at 0.5 deg. elevation

WRF

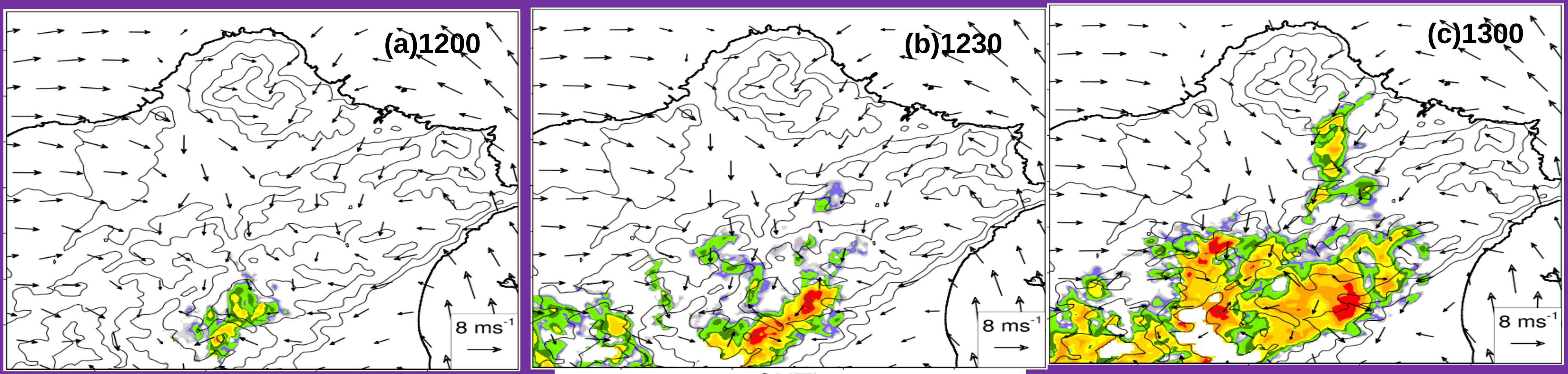

CNTL
Reflectivity at z=1.5km

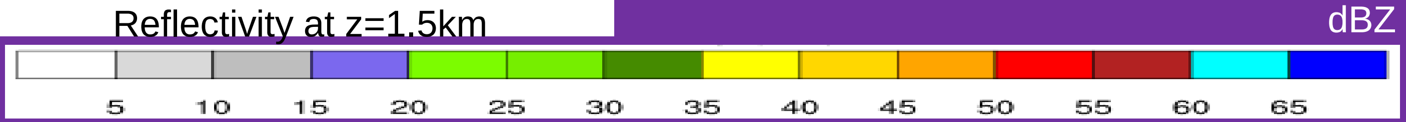

=> Simulated thunderstorms occurred one hour earlier than the observed.

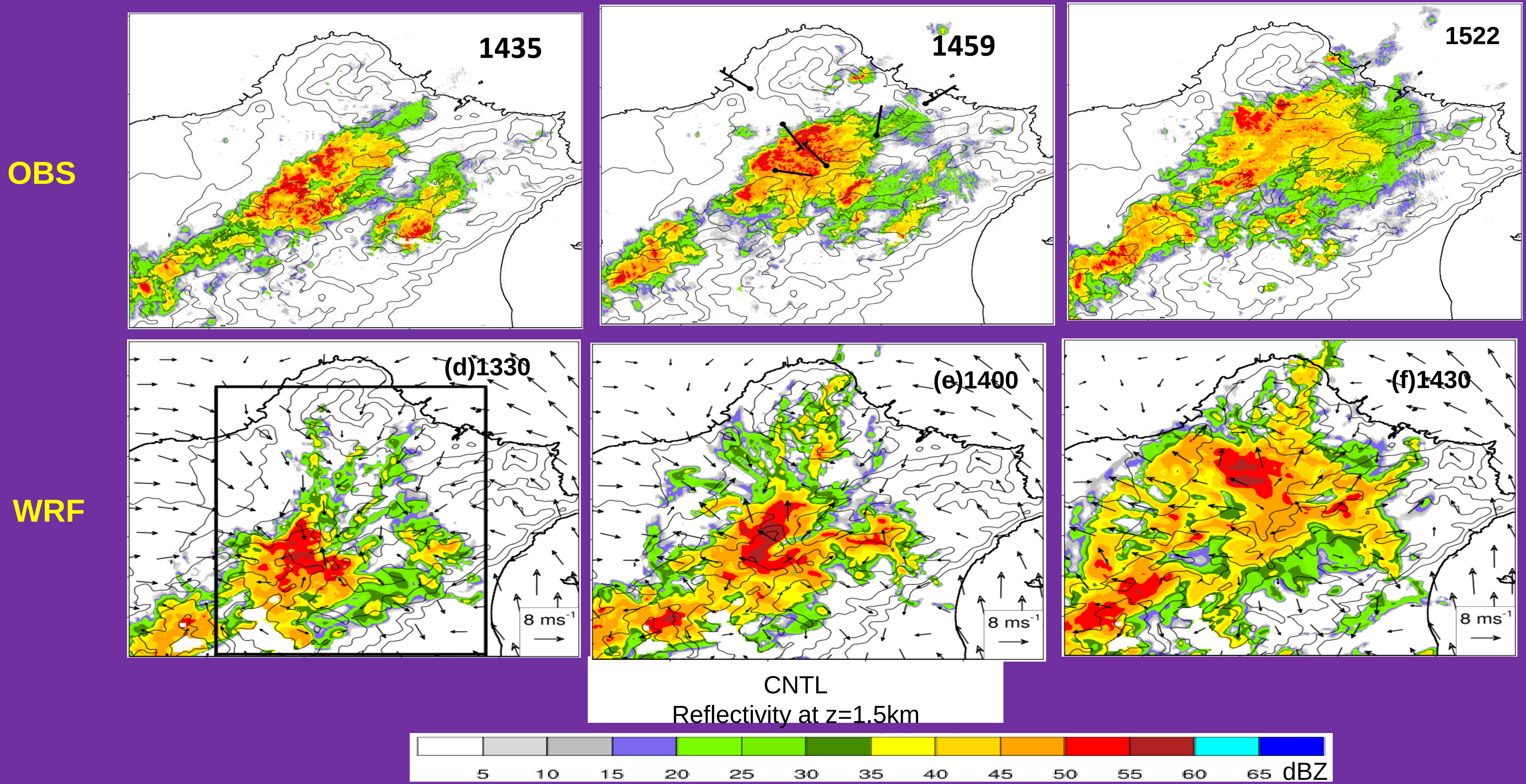

=> Simulated thunderstorms occurred one hour earlier than the observed.

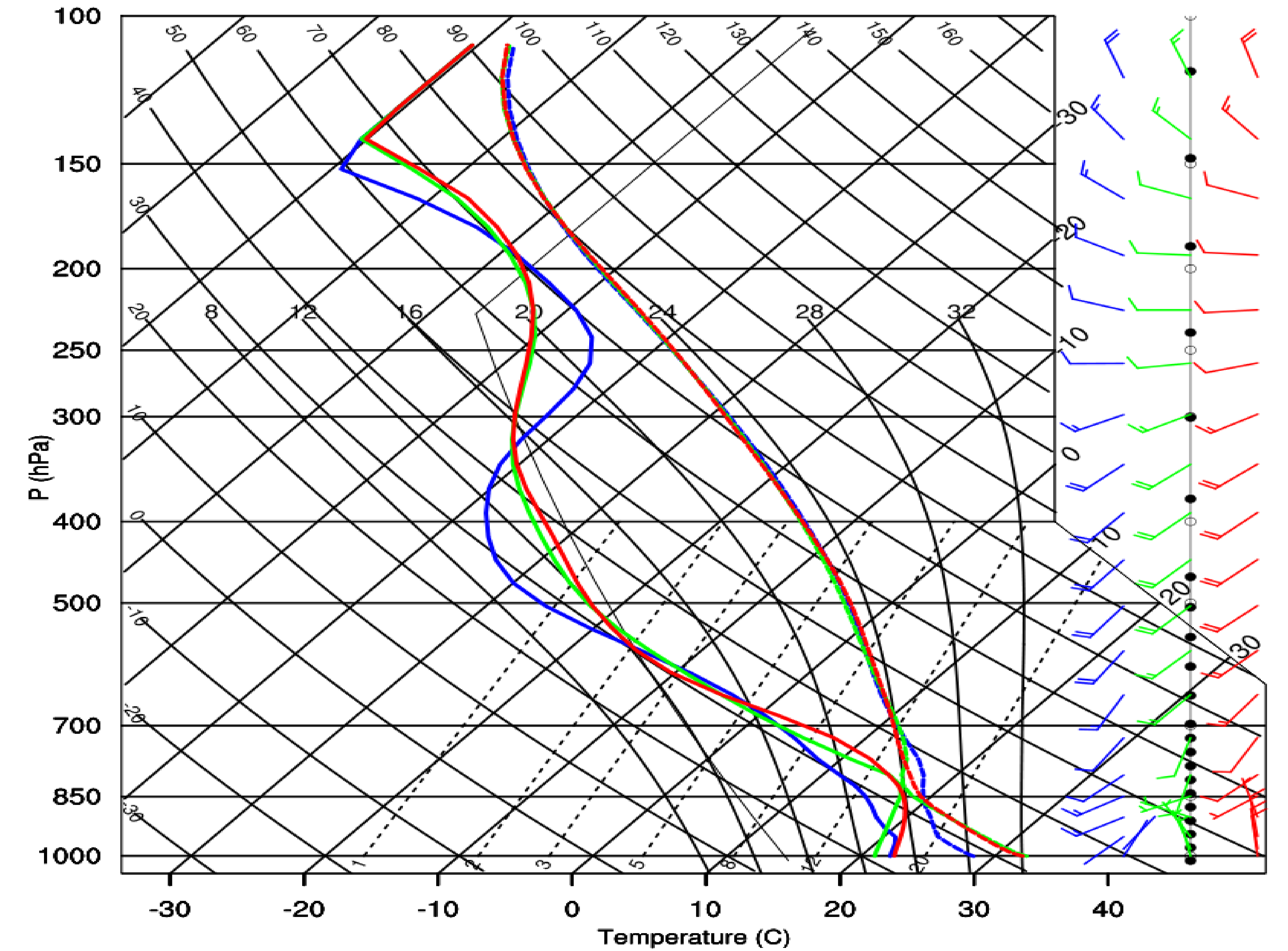

CAPE evolution

0800 LST

1100 LST

1200 LST

0800 LST:
CAPE = 885 J/kg

1100 LST:
CAPE = 1833 J/kg
Well-mixed PBL
Wind turns to northerly below 1km

1200 LST:
CAPE = 3268 J/kg
Dewpoint increases
Wind turns to northerly below 1.3 km.

Cell Merger Mechanisms

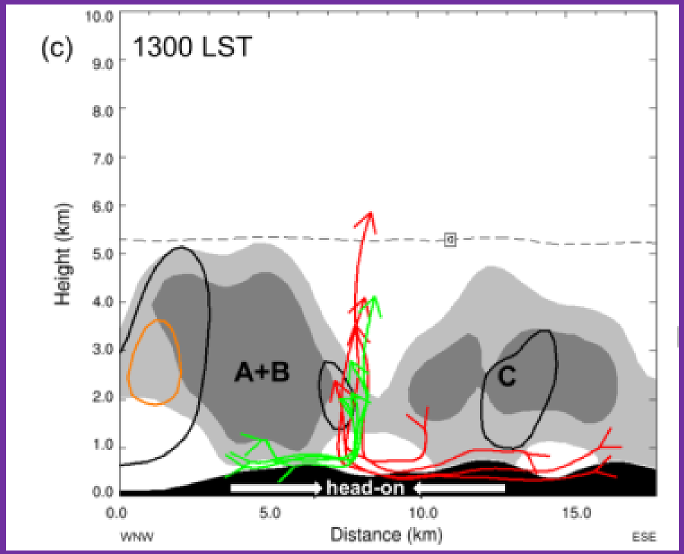

Cell Mergers in Radar Observation

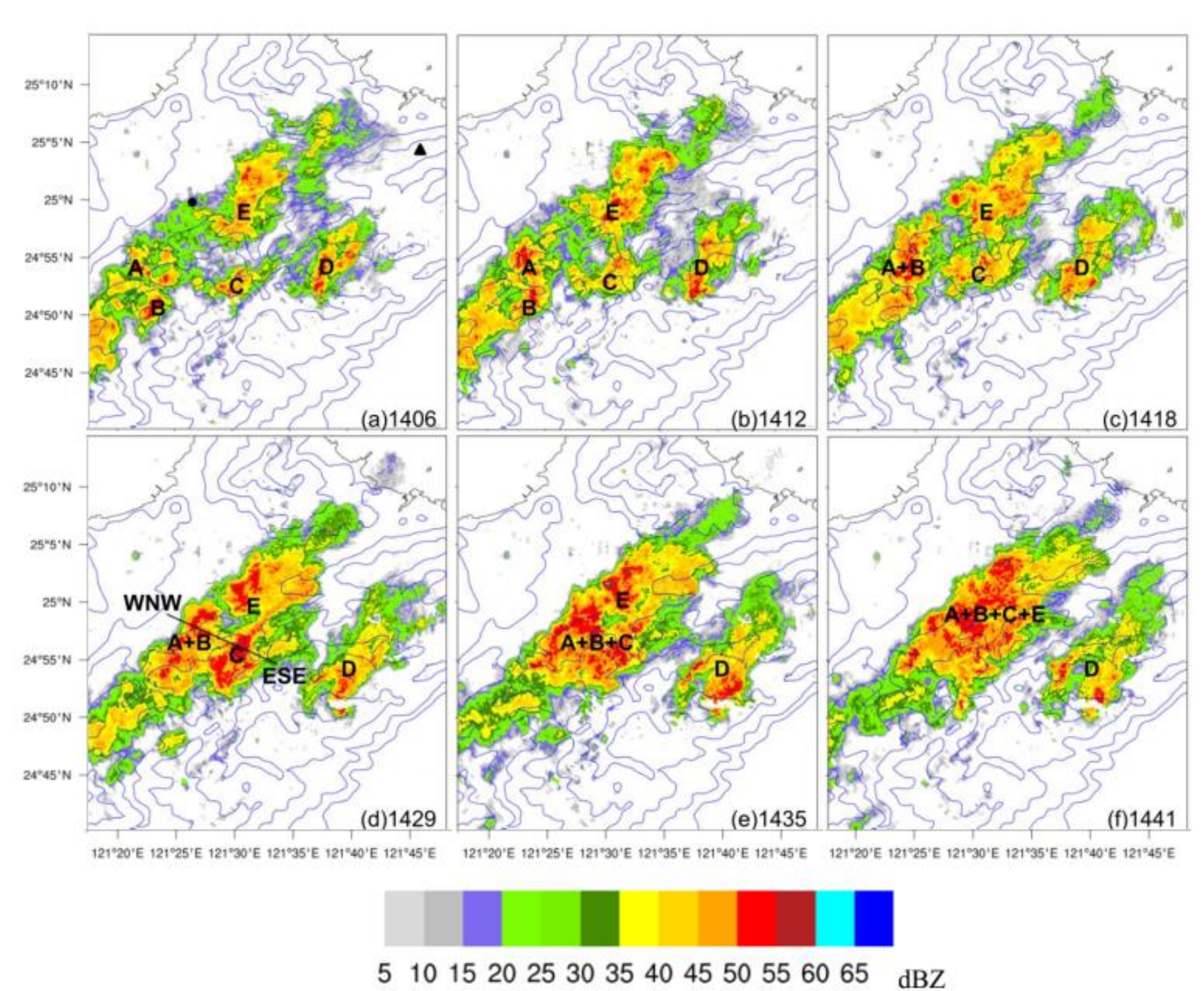

繆與楊
(2018; 大氣科學)

Cell Mergers in Radar Observation

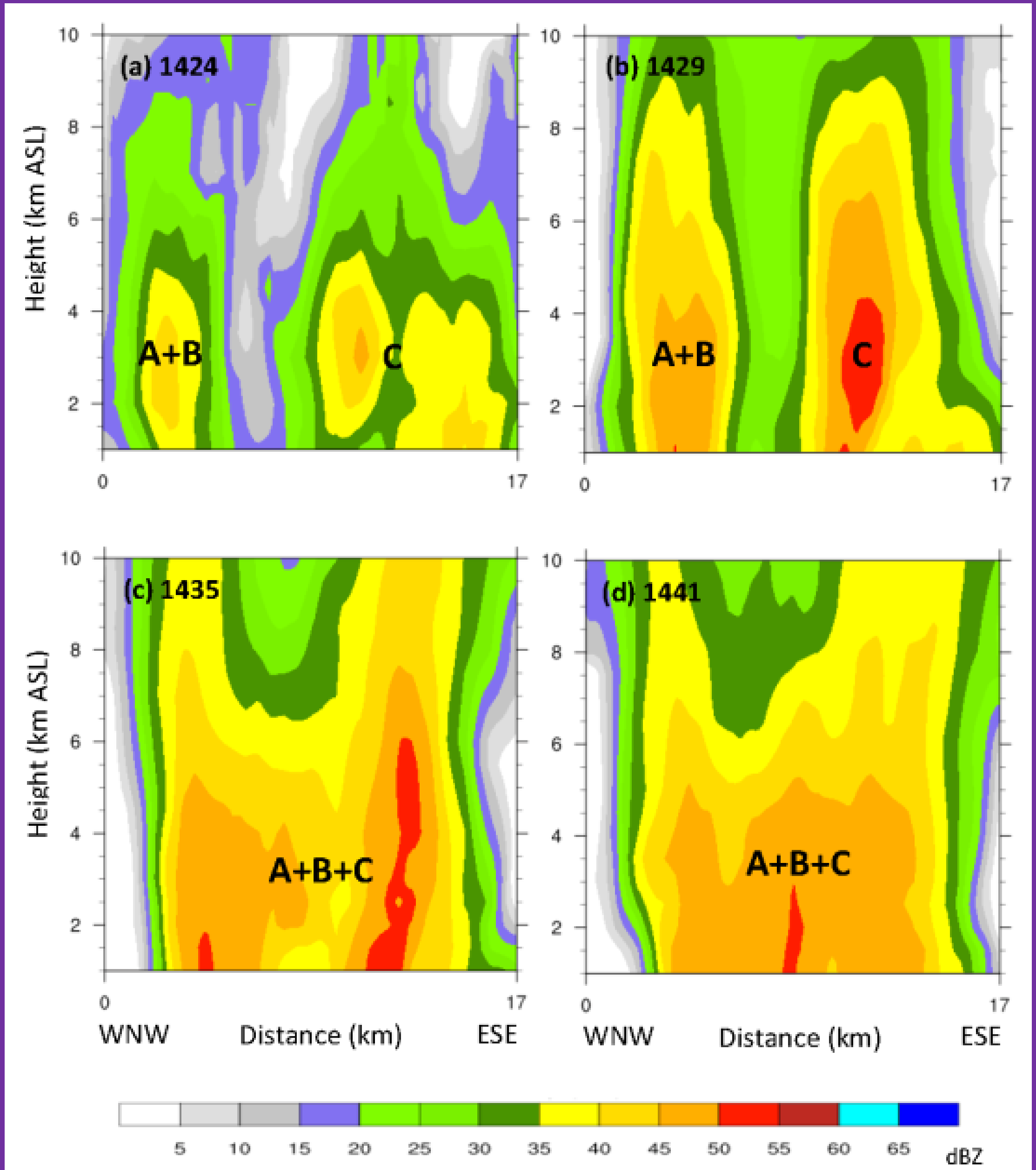

繆與楊
(2018; 大氣科學)

Cell Mergers in CNTL Simulation

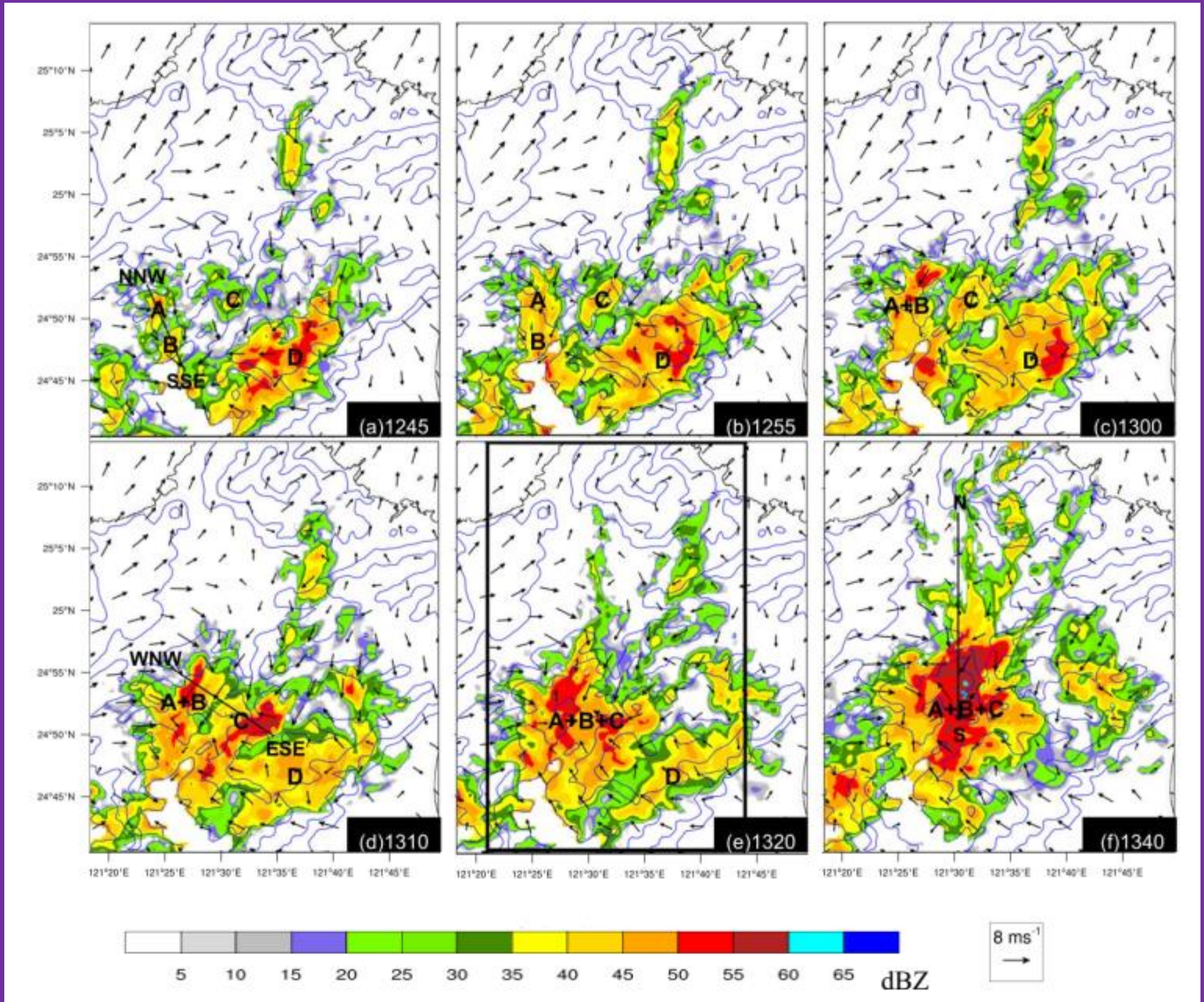

繆與楊
(2018; 大氣科學)

Cell Mergers in CNTL Simulation

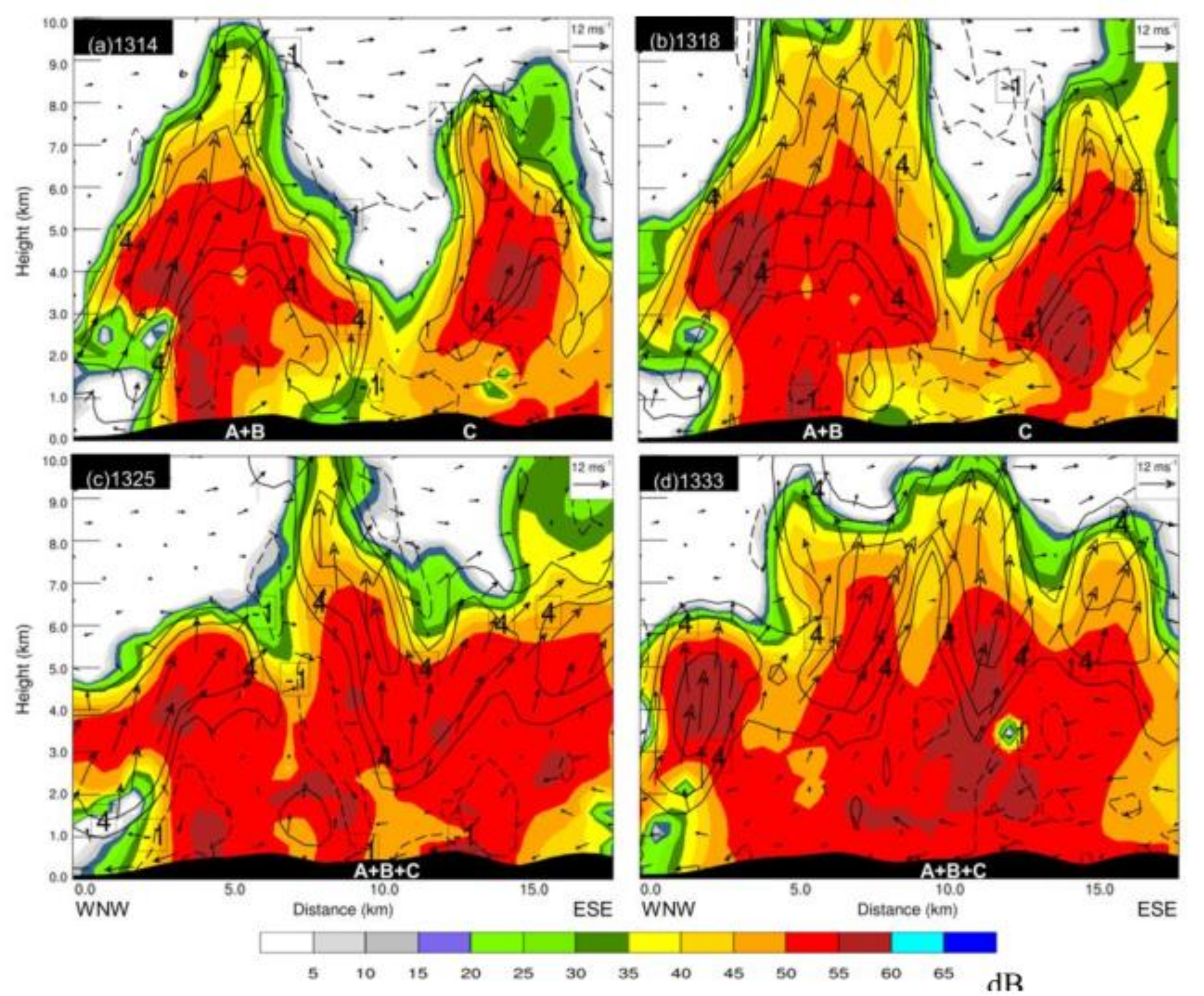

繆與楊
(2018; 大氣科學)

Analysis of 80 trajectories => Difference in Propagation Speeds for the Merger of Cell A and Cell B

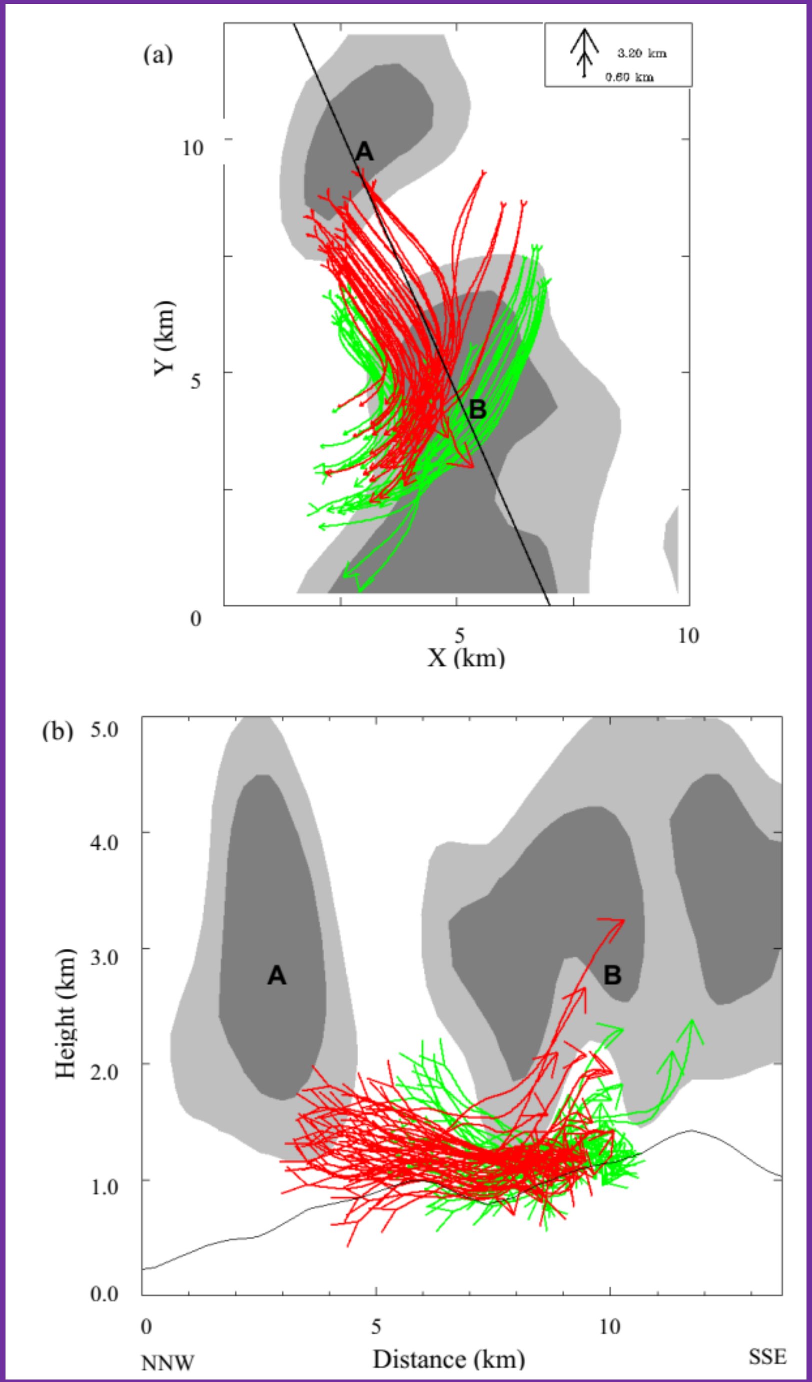

繆與楊
(2018; 大氣科學)

Analysis of 80 trajectories
=> Difference in Propagation Directions for the Merger of Cell A+B and Cell C

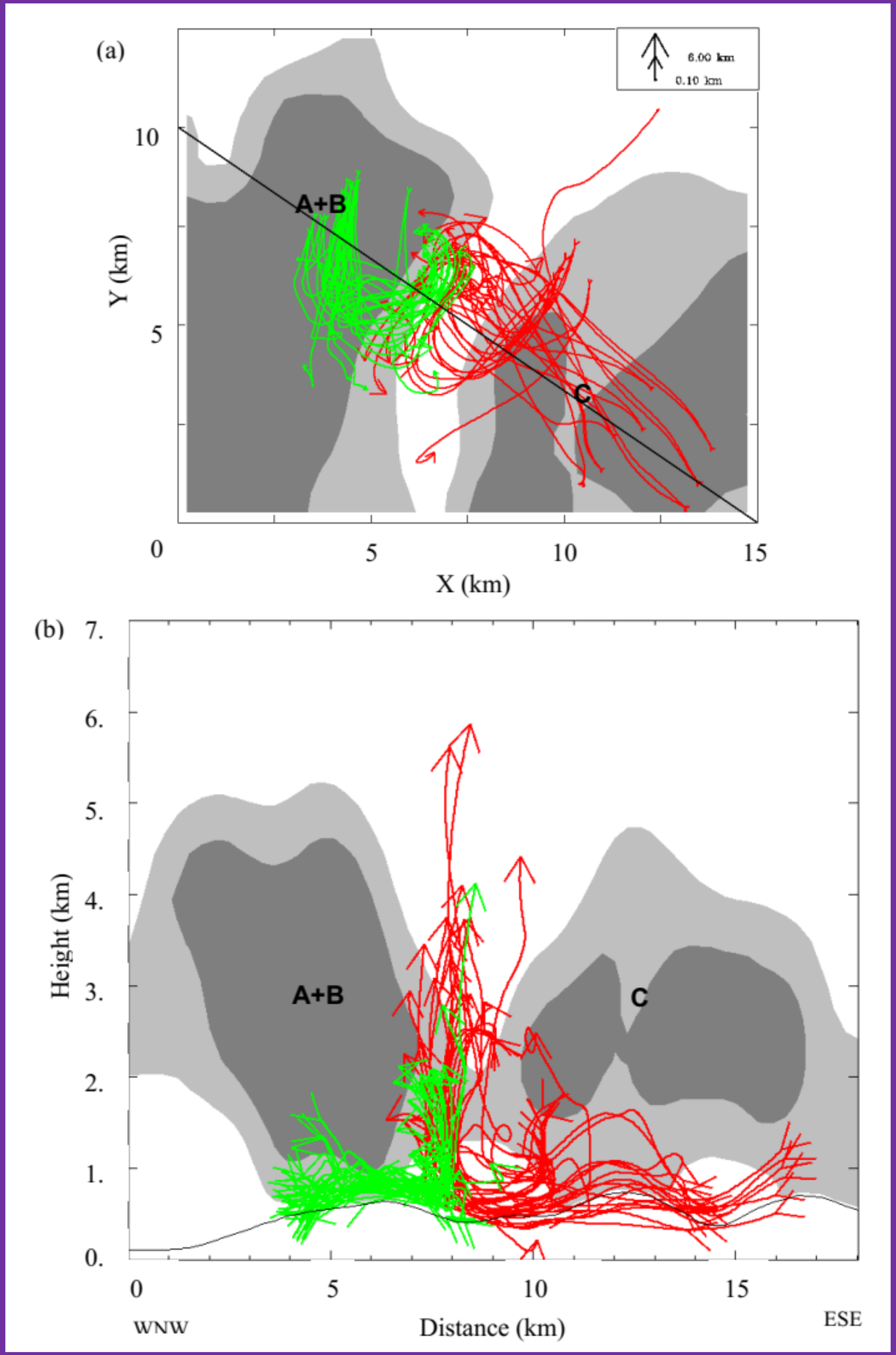

繆與楊
(2018; 大氣科學)

Conceptual Model for Cell-Merger Mechanism

Merger of Cell A and Cell B
=> Rear-end Collision

Merger of Cell A+B and Cell C
=> Head-end Collision

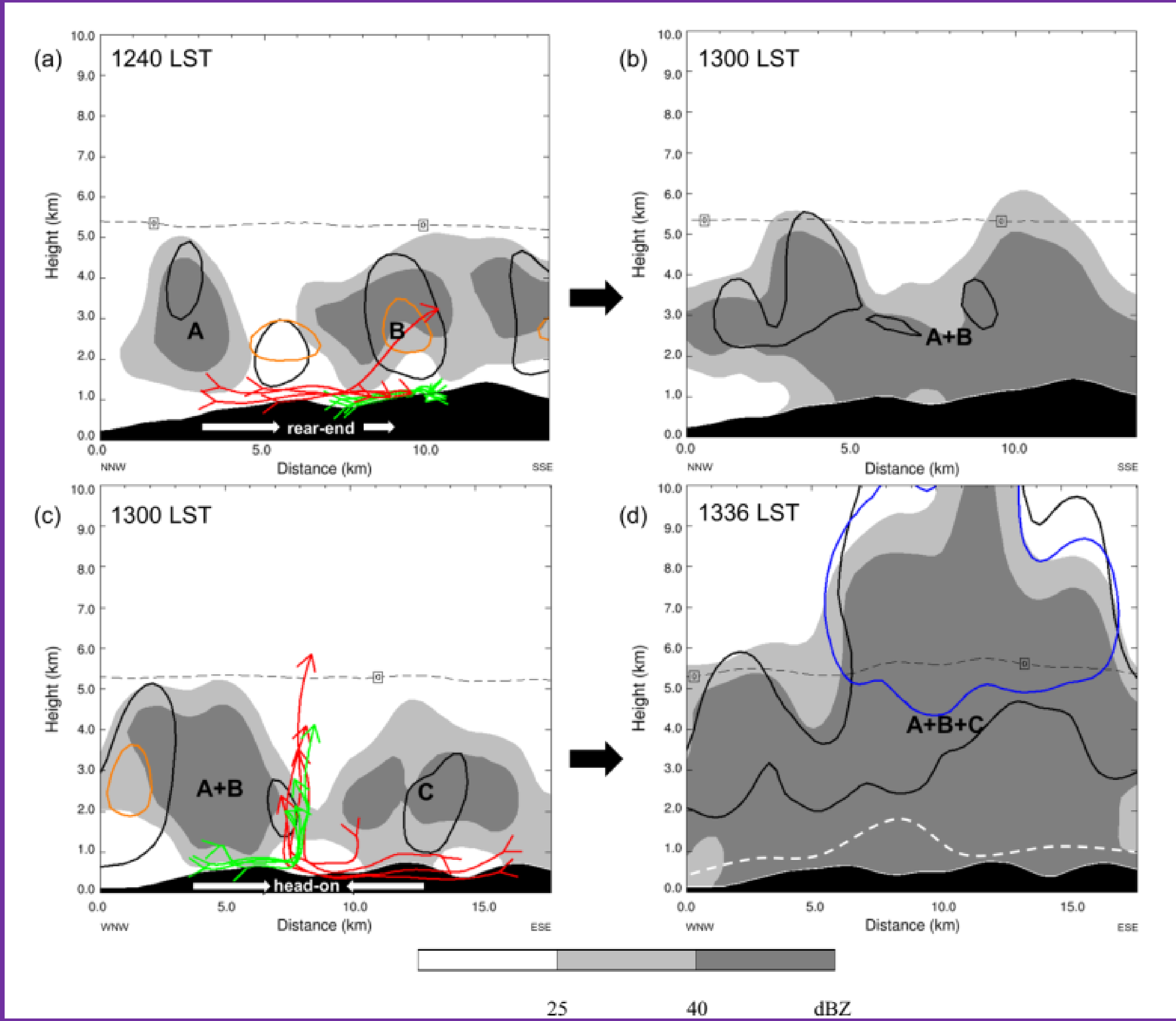

繆與楊
(2018; 大氣科學)

Cold-Pool Dynamics

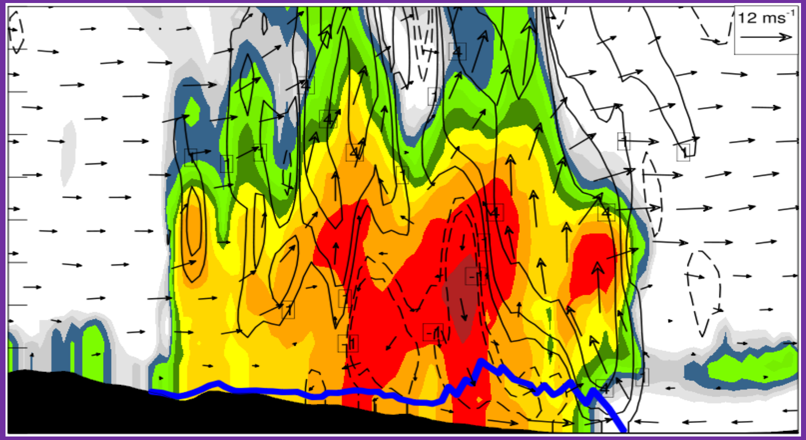

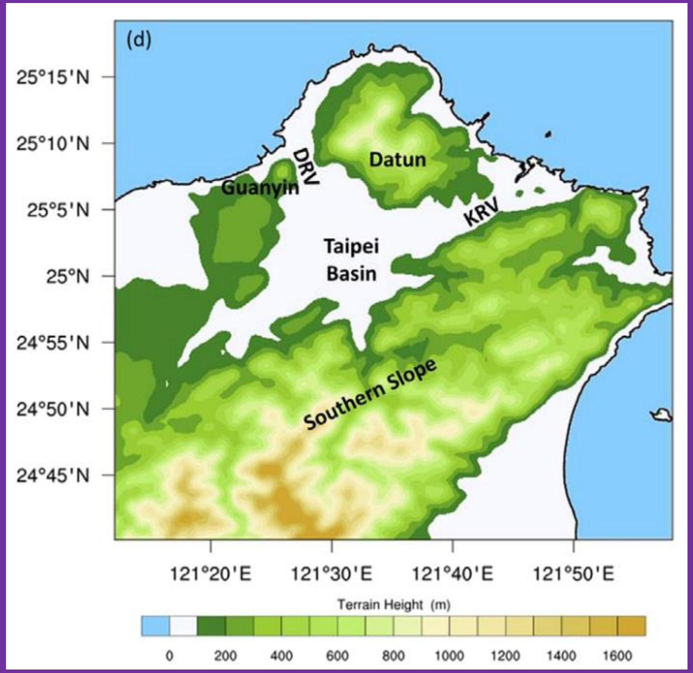

Vertical Cross Section along the Danshui River Valley

Colored: meridional wind

Contour: equivalent potential temperature

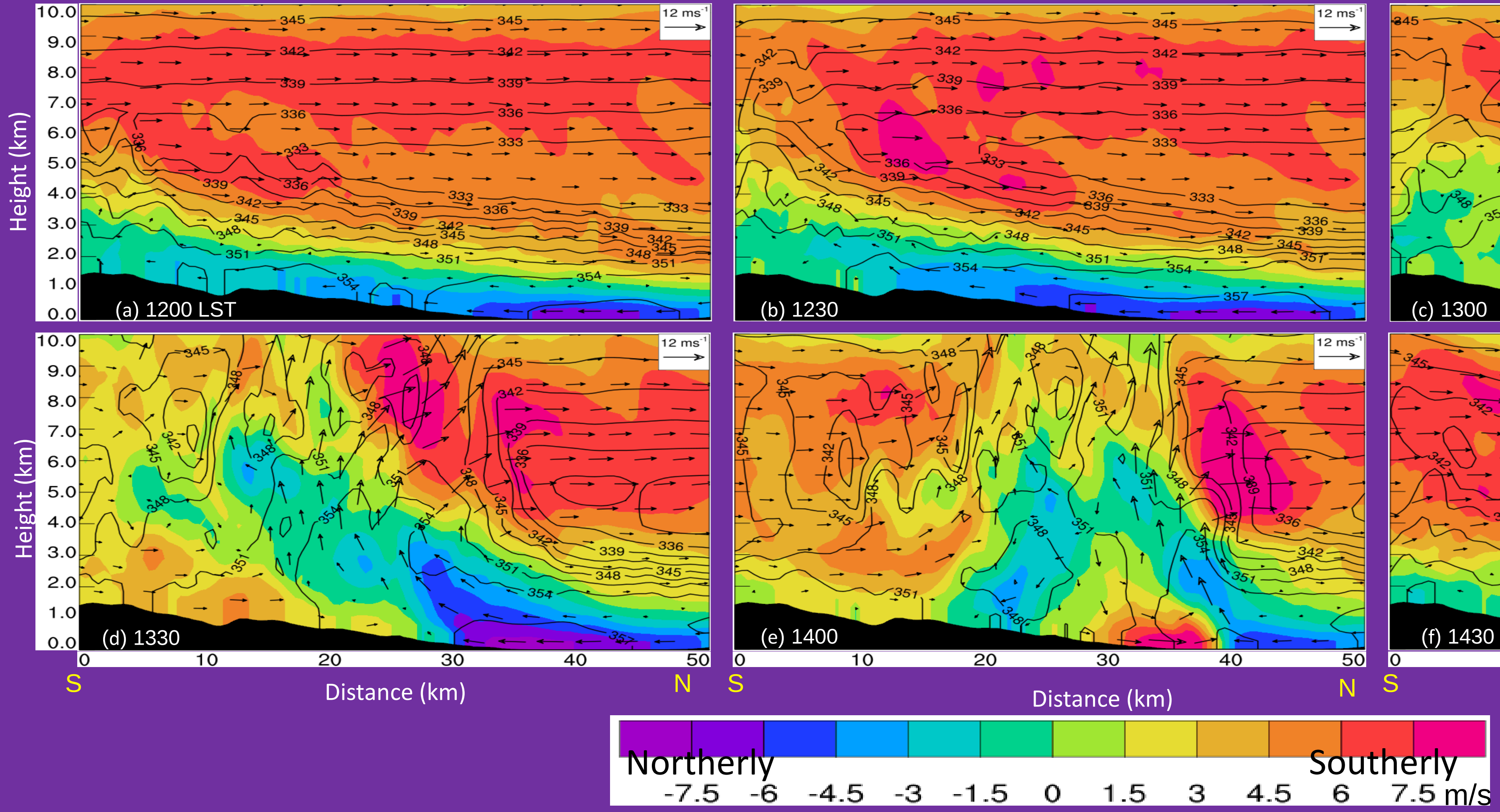

Miao and Yang (2020; JMSJ)

Vertical Cross Section along the Danshui River Valley

Shaded: radar reflectivity

Contour: vertical velocity = { -1, -0.5, 1, 2, 4, 8 } m/s

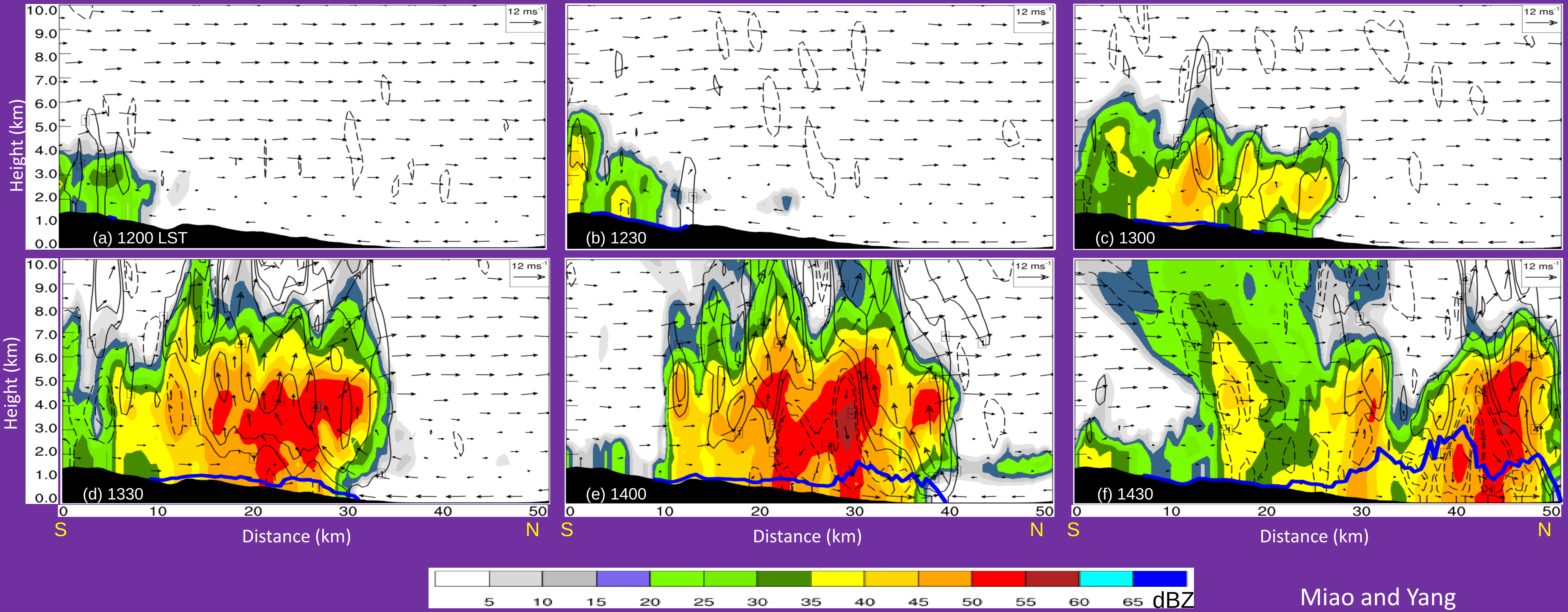

Miao and Yang (2020; JMSJ)

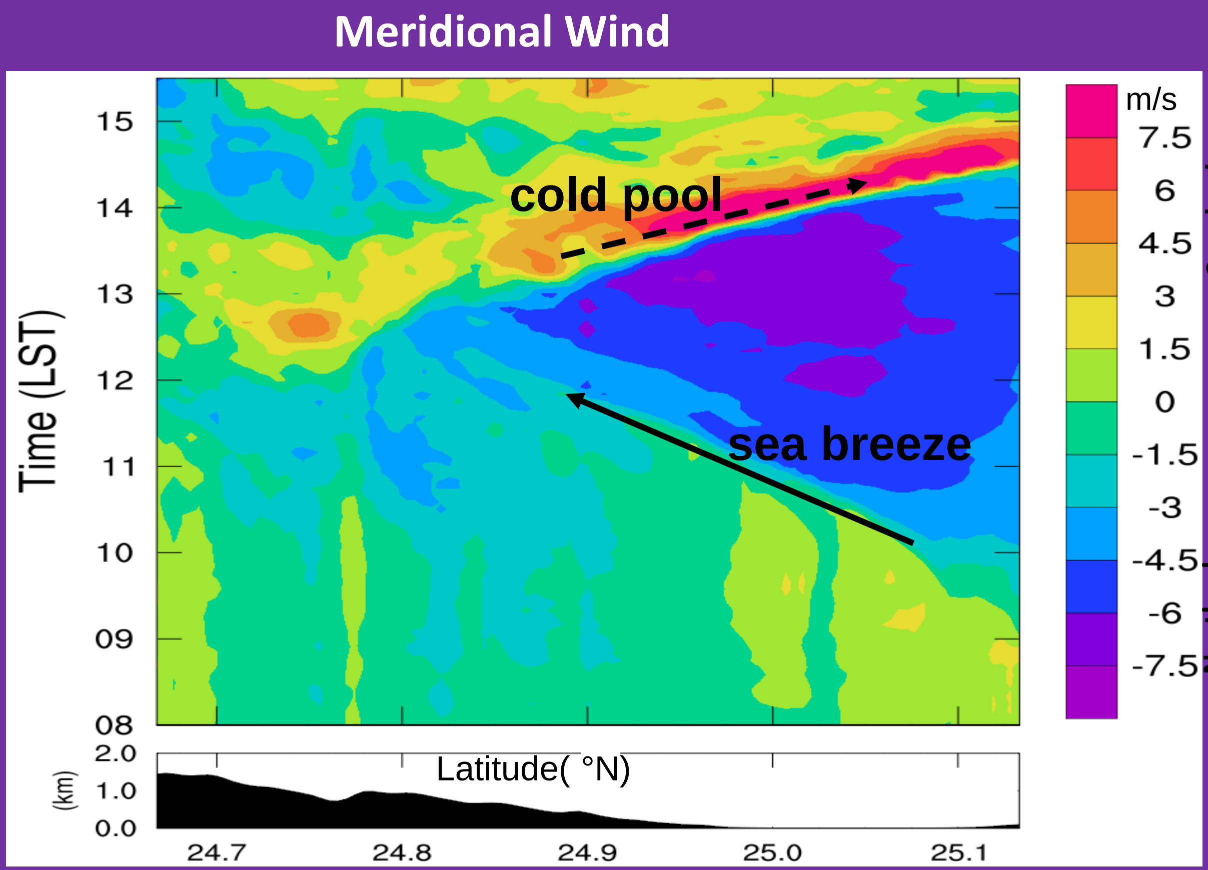

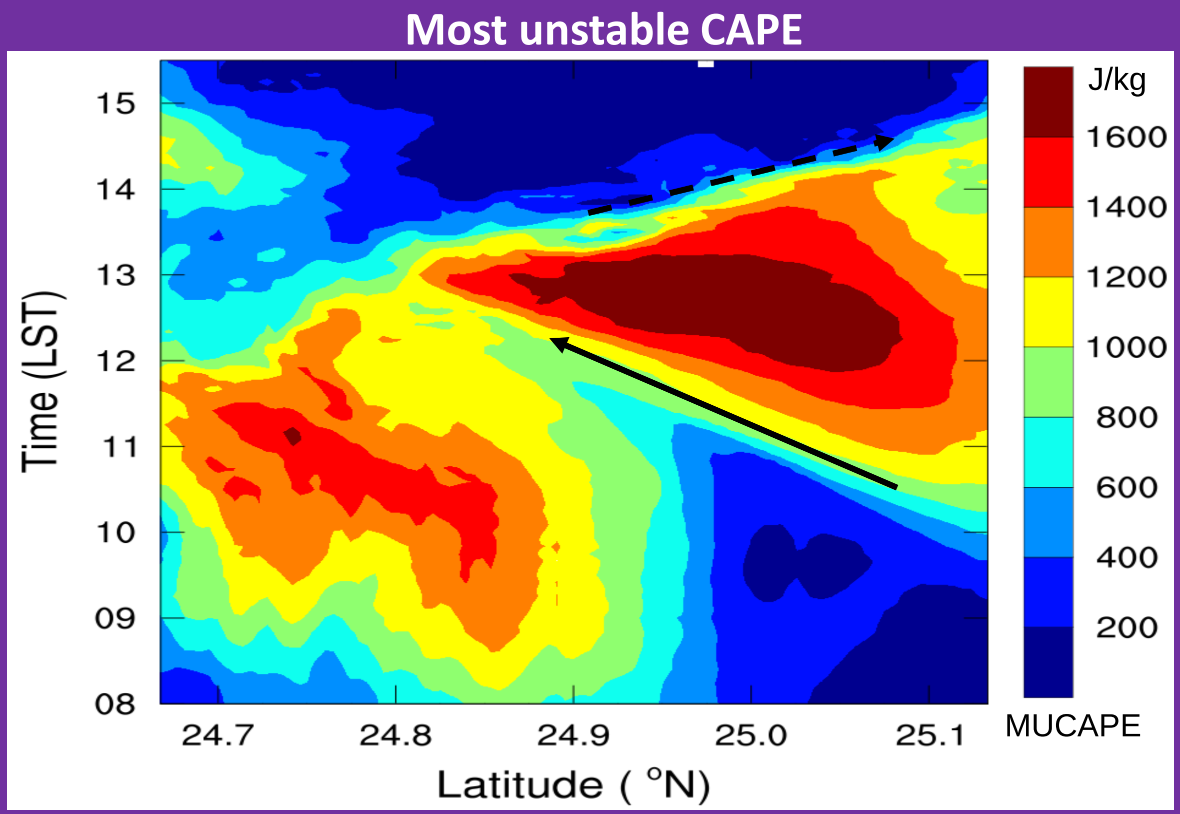

Hovmöller diagrams along the Danshui River Valley

=> sea-breeze propagation speed ~4.6 m/s
cold-pool propagation speed ~ 6.5 m/s

=> MUCAPE is highly related to the meridional wind which is associated with sea-breeze circulation

Miao and Yang (2020; JMSJ)

Table 1. Design of control and sensitivity experiments.

Run	Initial time	Description
CNTL	20 LST 13 Jun. 2015	full physics
NMLT	20 LST 13 Jun. 2015	no melting cooling of graupel after 08 LST 14 June 2015
NEVP	20 LST 13 Jun. 2015	no evaporative cooling of rainwater after 08 LST 14 June 2015
NDAT	20 LST 13 Jun. 2015	full physics with Mt. Datun removal

Experiments: CNTL: full physics; NMLT: No melting cooling of graupel
NEVP: No evaporative cooling of rainwater; NDAT: No Mt. Datun

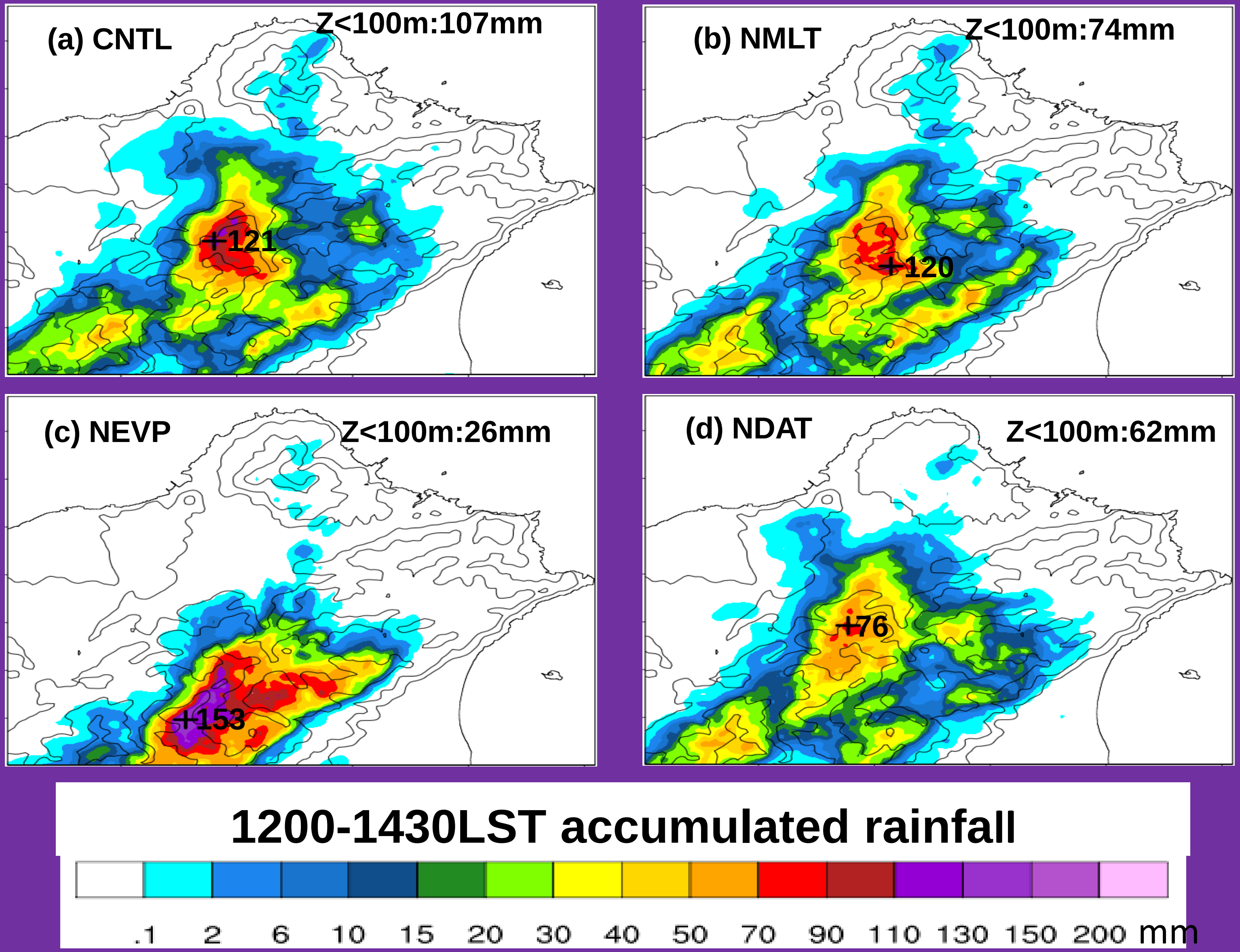

Miao and Yang (2020; JMSJ)

Z=1.5km@1430 LST

Vertical Cross Section @1430 LST

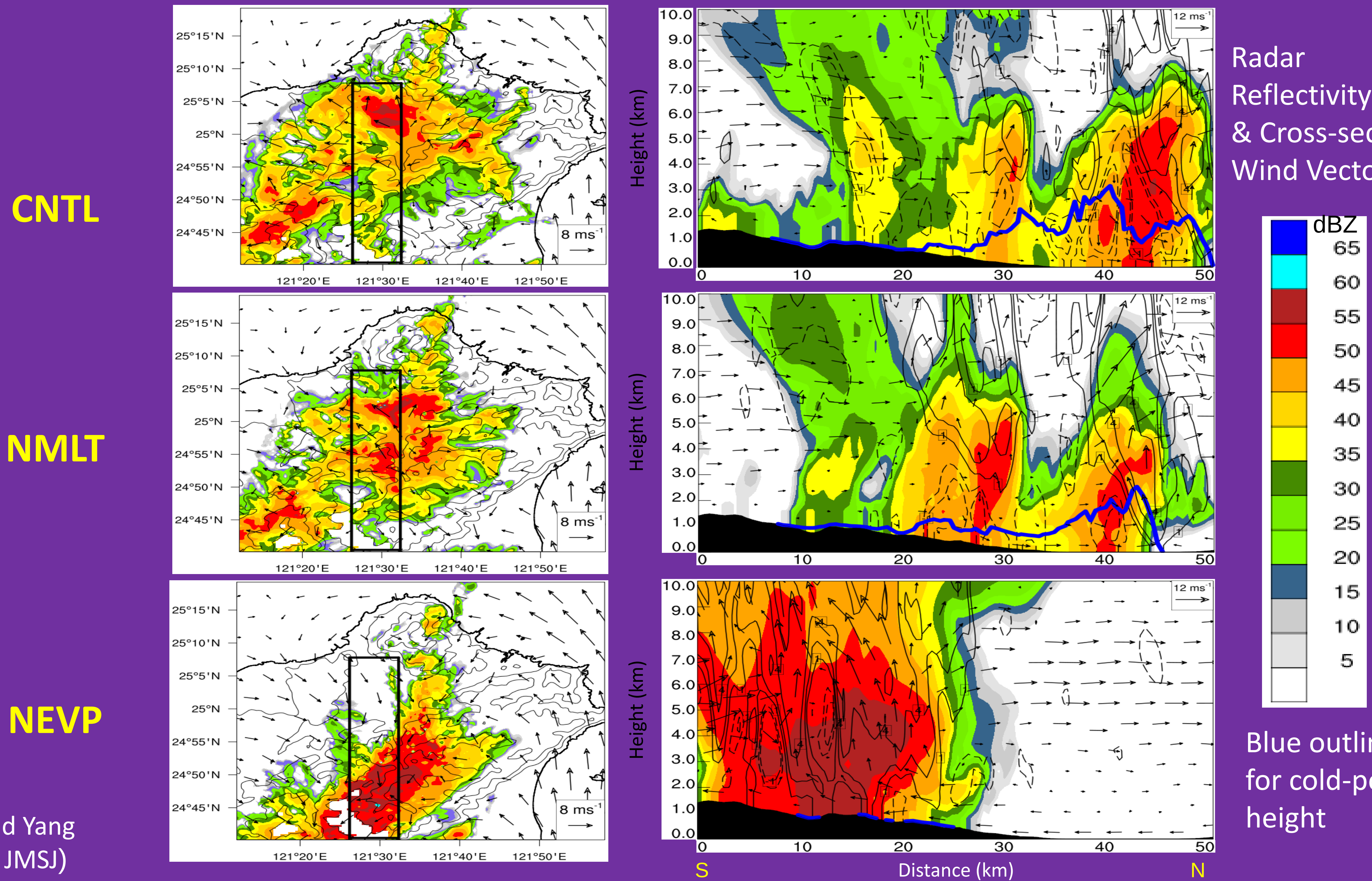

Radar Reflectivity & Cross-section Wind Vectors

Blue outline for cold-pool height

Miao and Yang (2020; JMSJ)

Southerly

MUCAPE

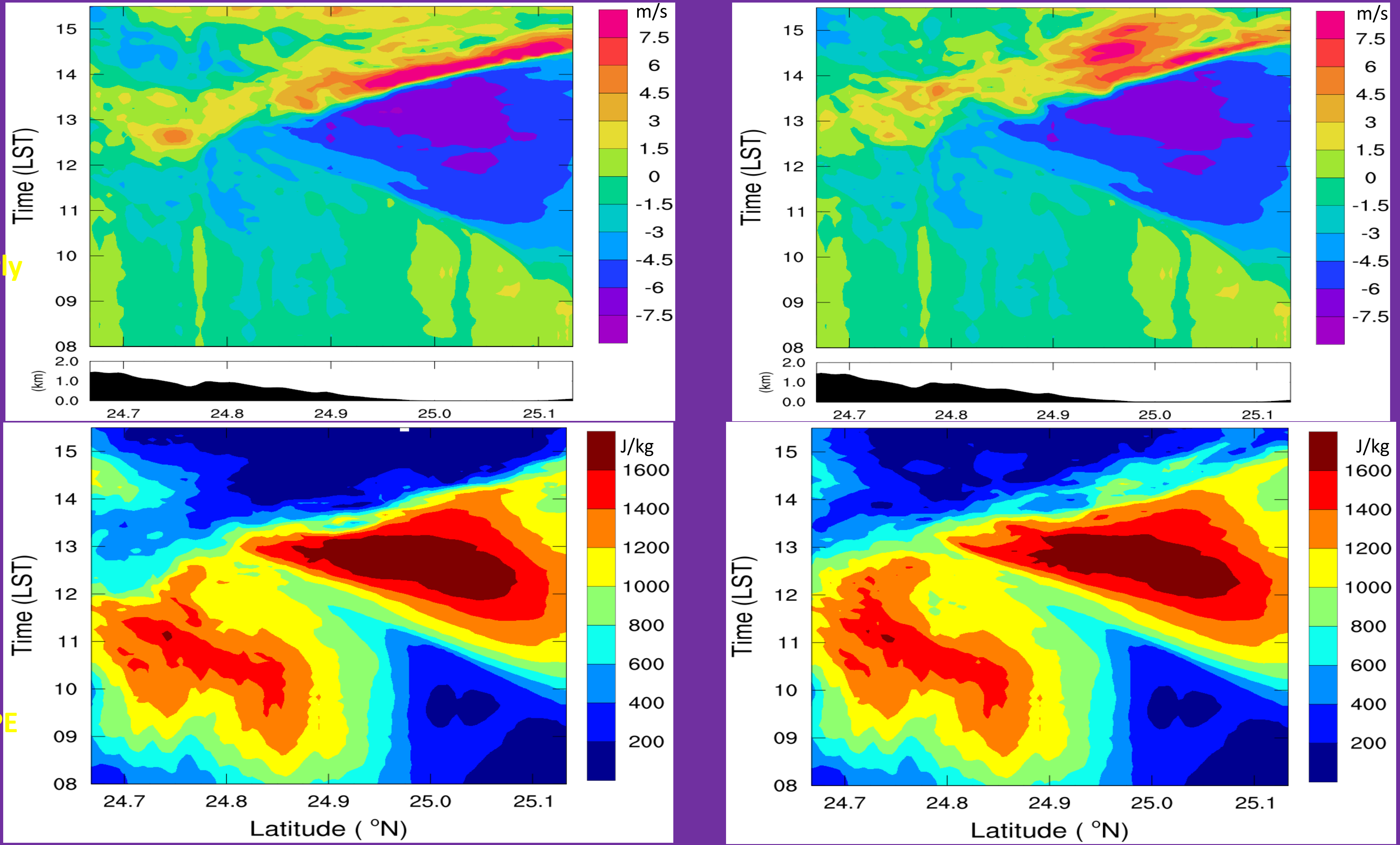

Sea Breeze from Danshui

CNTL

NMLT

Southerly

MUCAPE

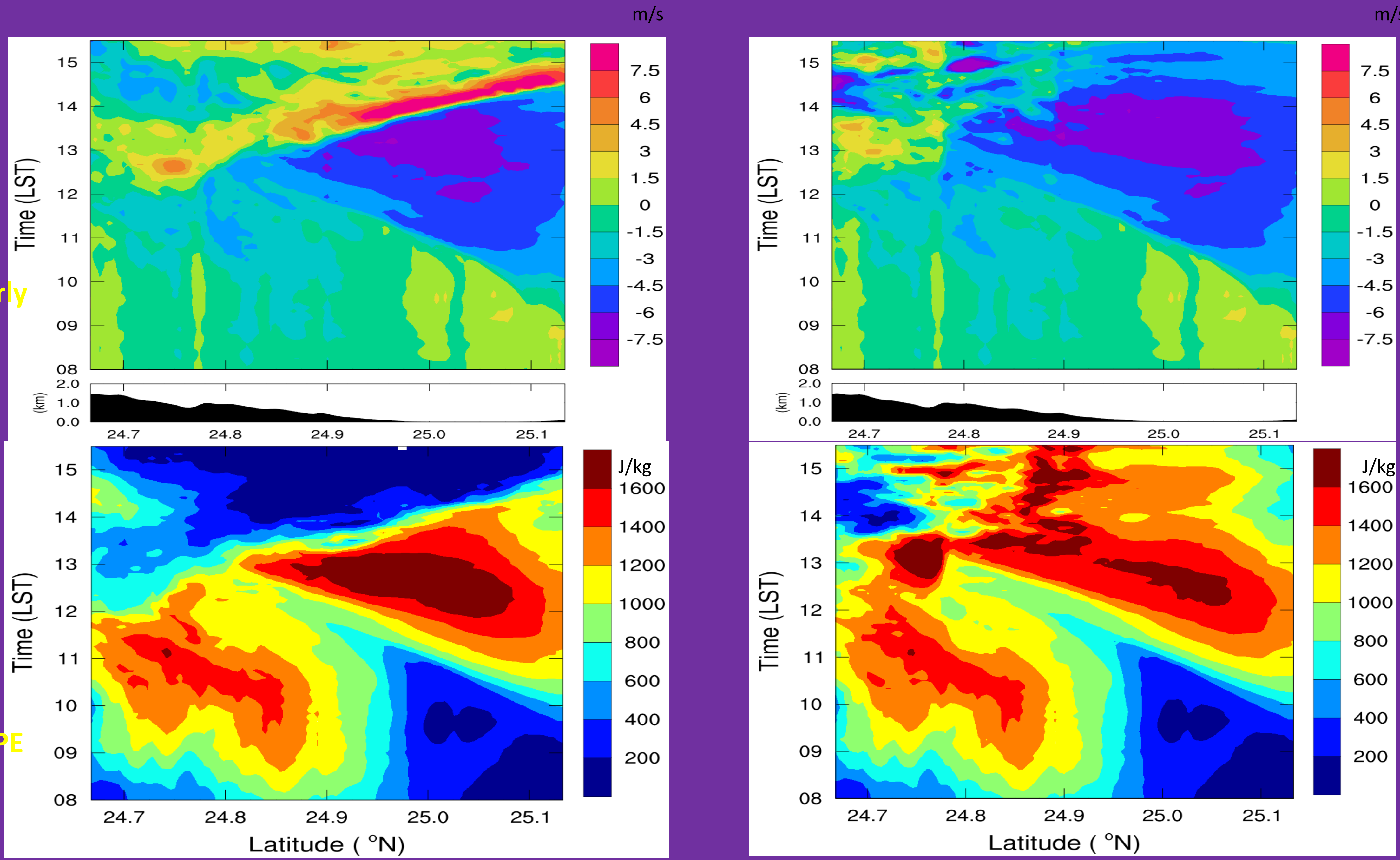

Sea Breeze from Danshui

CNTL

NEVP

Taipei Basin Statistics

Buoyancy

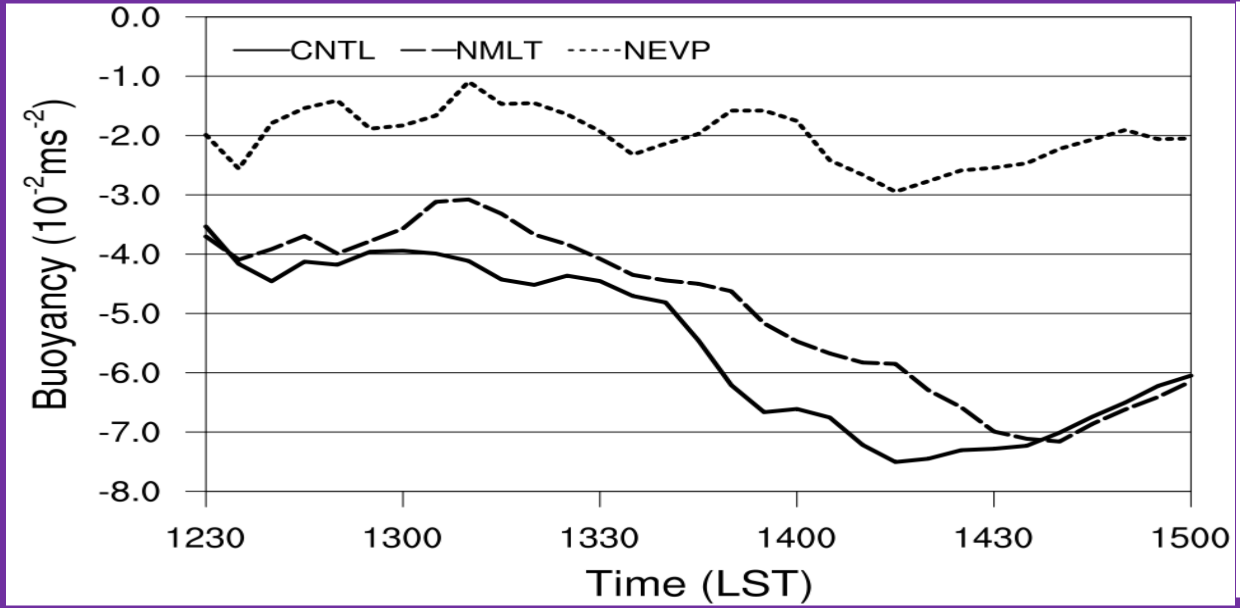

Cold-pool propagation speed

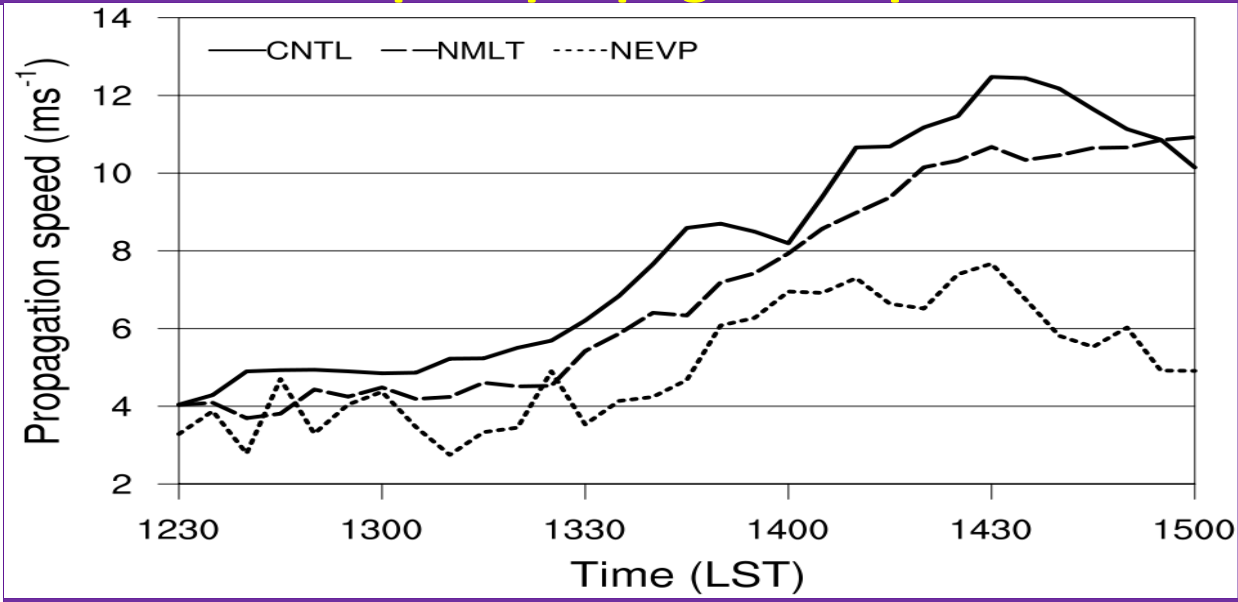

Cold-pool depth

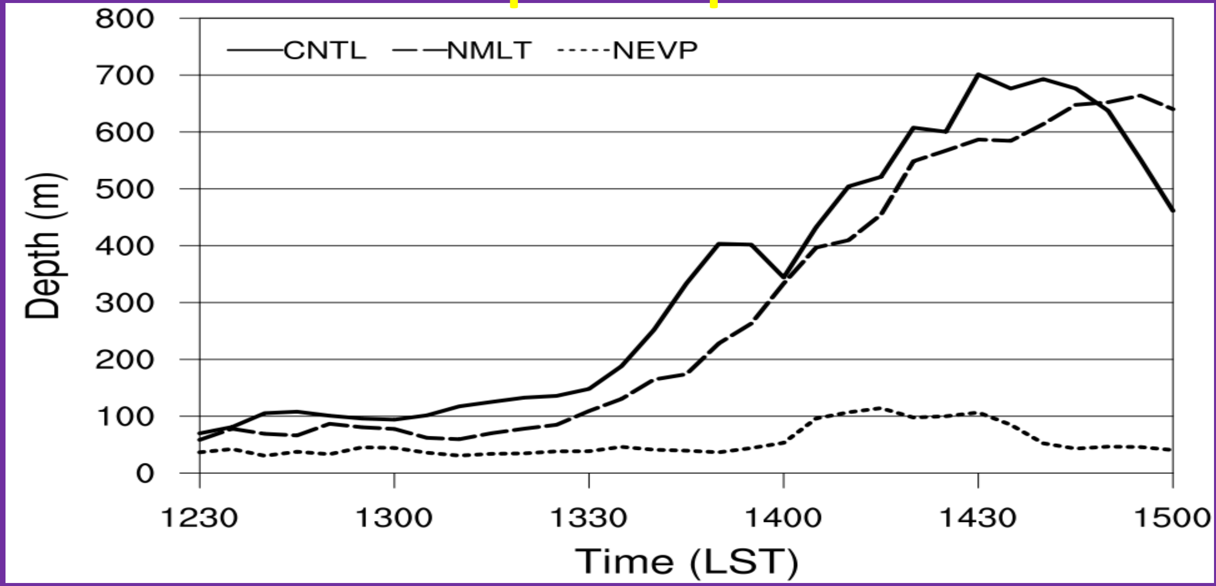

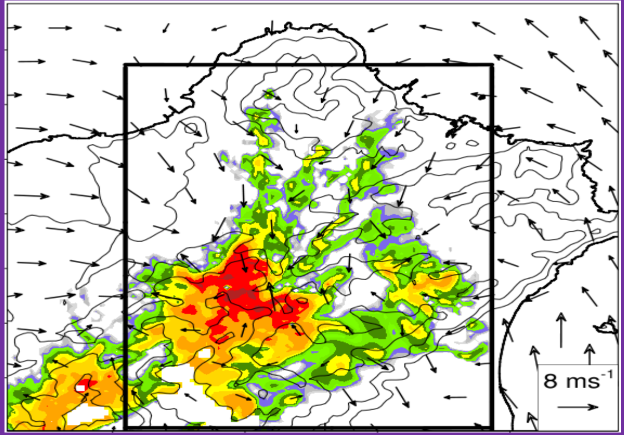

The effect of Mount Datun on increasing local convergence and enhancing convection within Taipei Basin

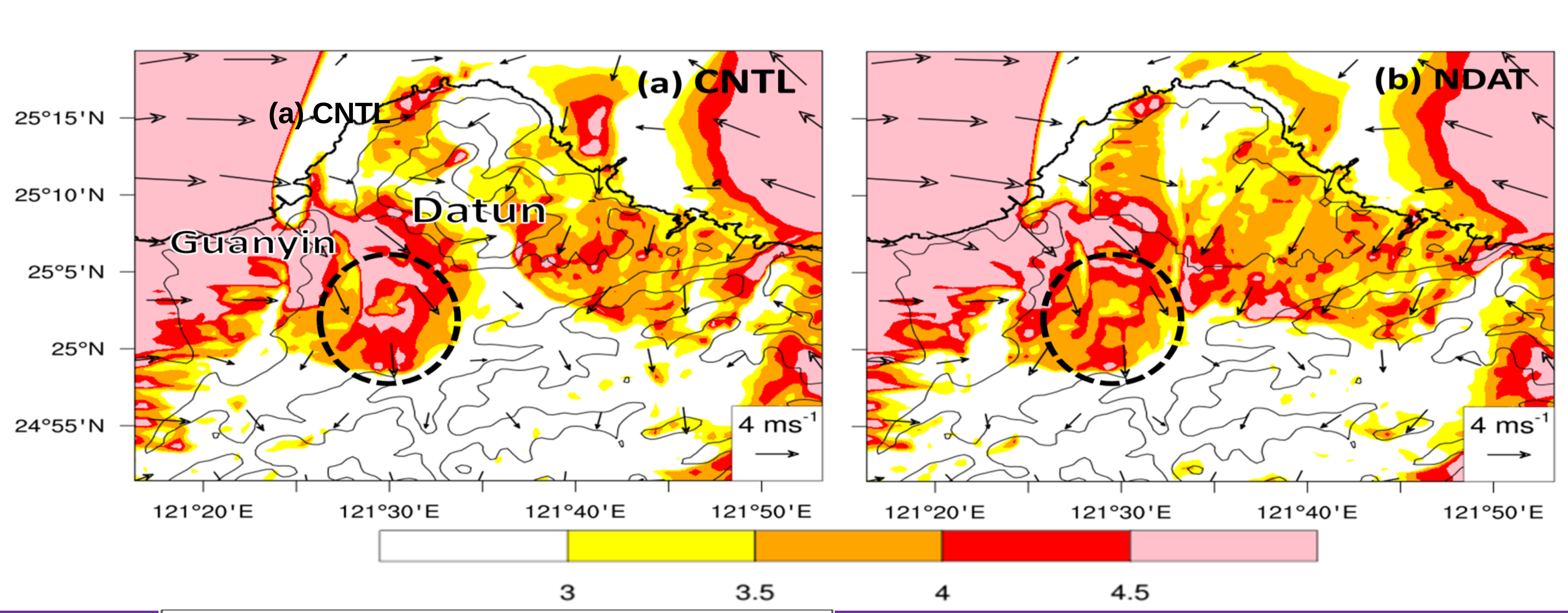

1200-1430LST accumulated rainfall

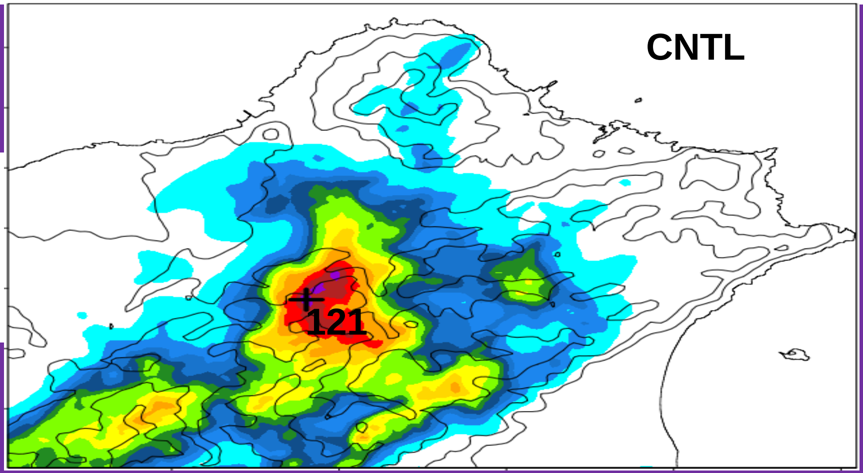

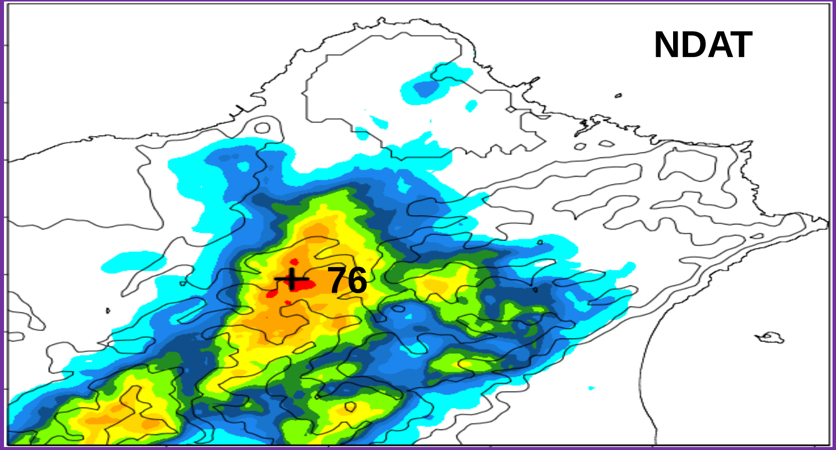

Miao and Yang (2020; JMSJ)

- CAPE difference

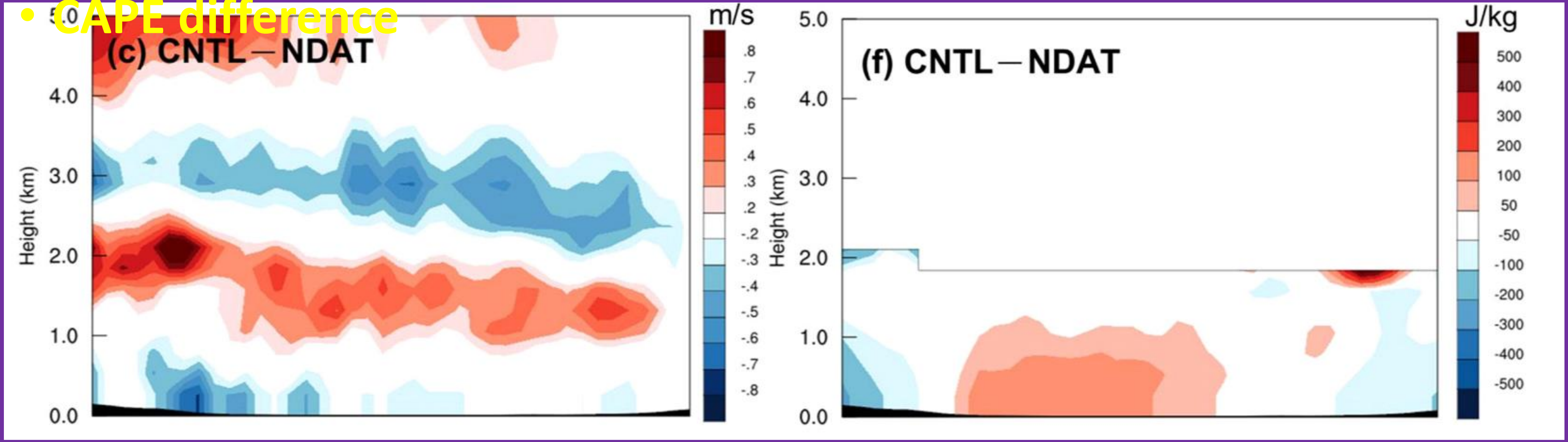

Meridional wind difference

CAPE difference

Miao and Yang (2020; JMSJ)

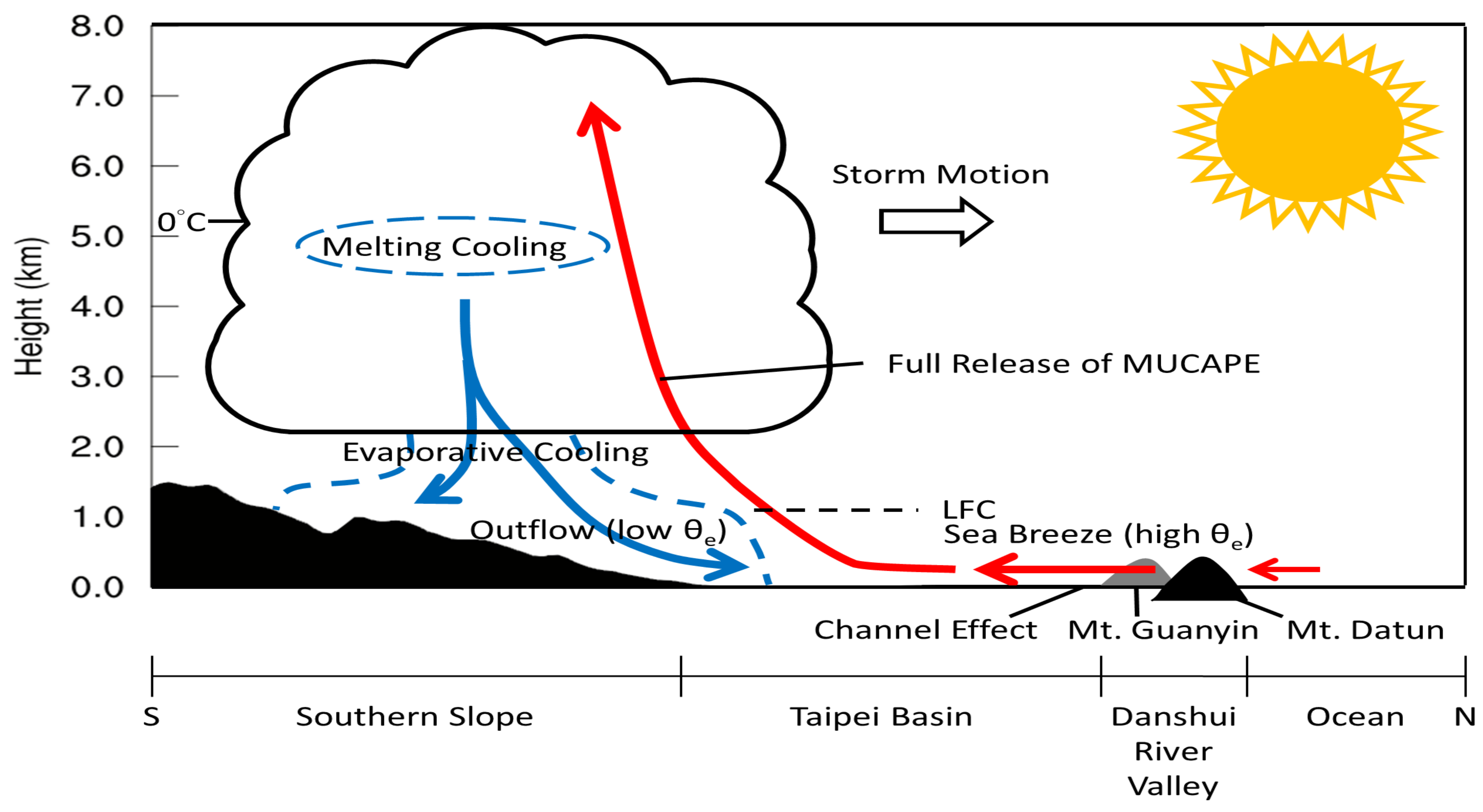

Schematic diagram of the interactions between sea breeze, cold pool and coastal terrain for the development of afternoon thunderstorm over Taipei basin.

Miao and Yang (2020; JMSJ)

Impacts of Mid-Level Dry Air

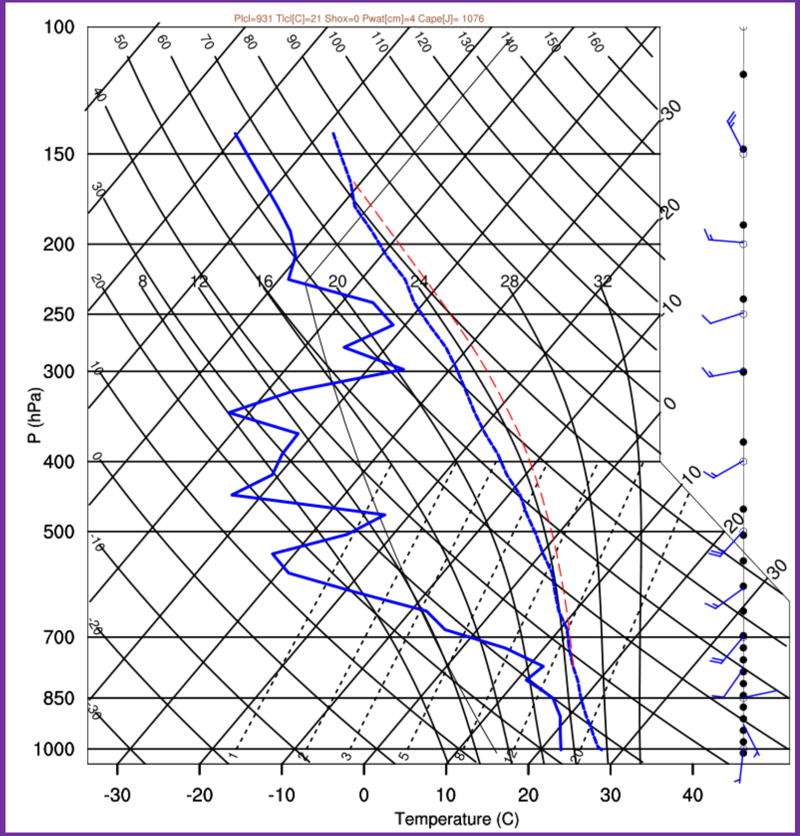

Taipei Soundings at Initial time

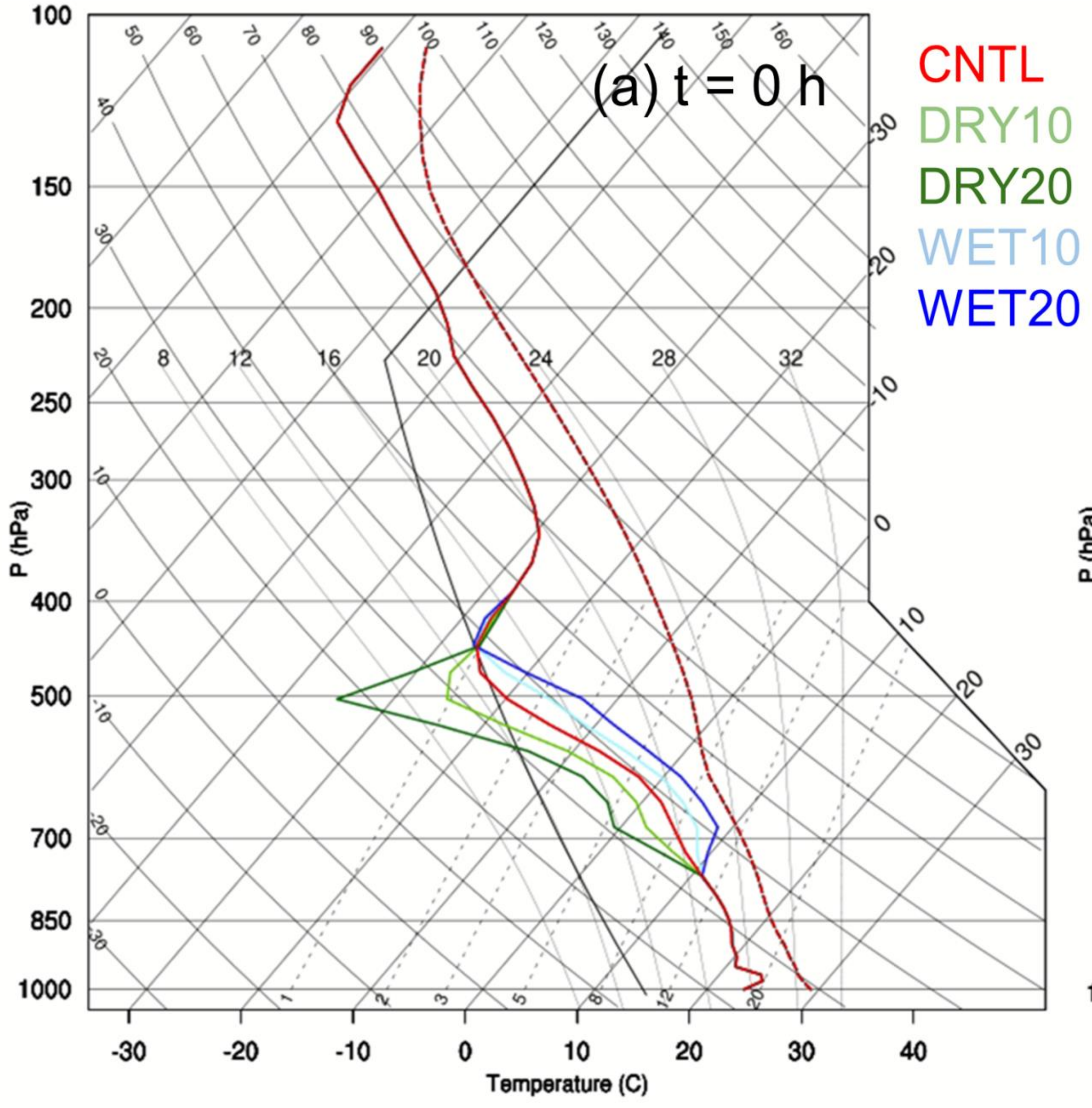

Taipei Soundings 12 hours later

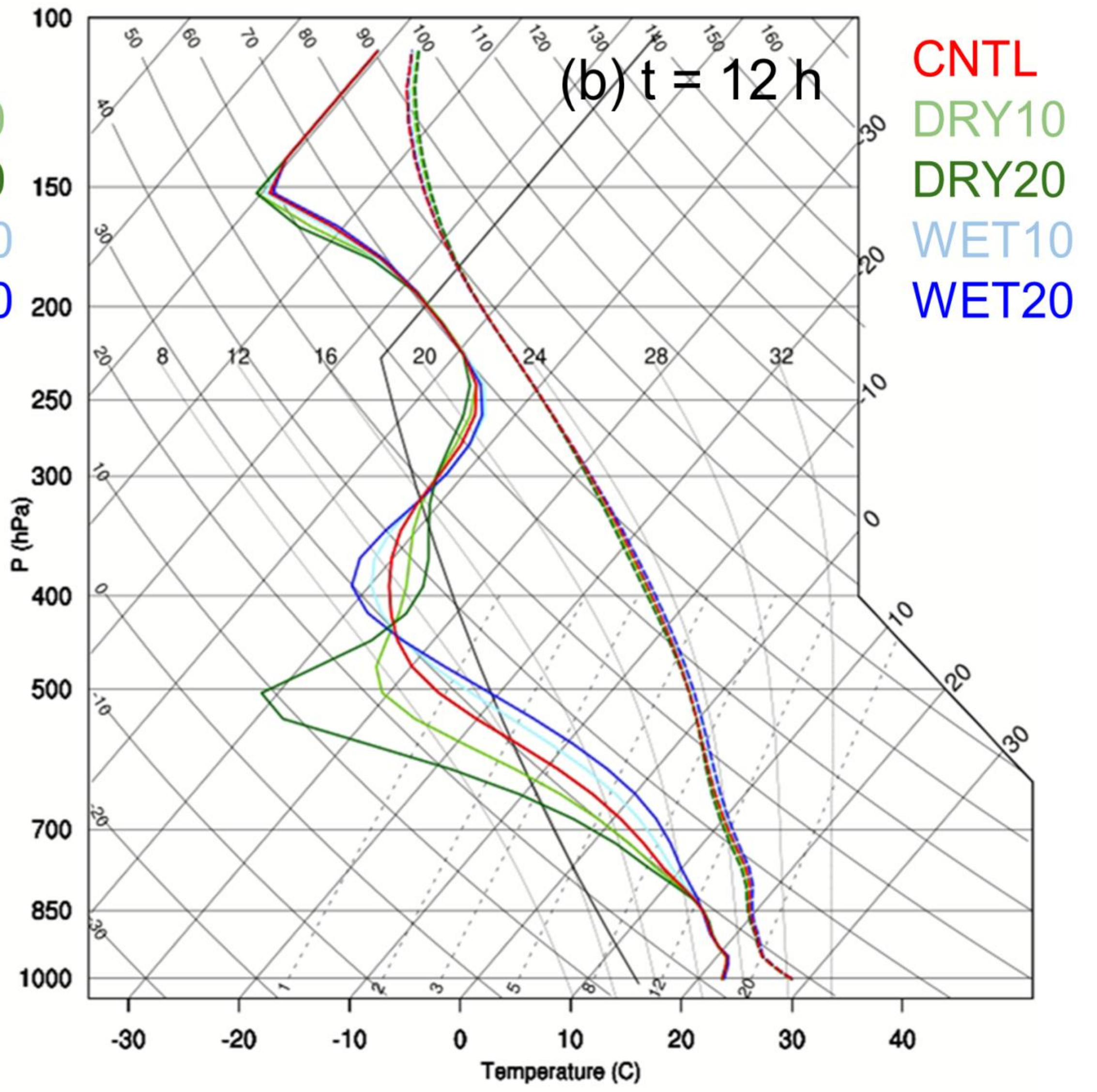

Table 1. 700 and 500-hPa dewpoint departure, 700–500 hPa mean relative humidity, DCAPE and precipitable water (PW) for the simulation experiments at t = 12 h.

Experiment	500/700 hPa T–Td (K)	500–700 hPa mean RH (%)	DCAPE (J kg^{-1})	PW (mm)
CNTL	22.9 / 8.9	35%	1166	45.7
DRY10	27.8 / 10.4	27%	1318	43.6
DRY20	37.7 / 12.0	19%	1489	41.6
WET10	20.4 / 7.6	41%	1046	47.6
WET20	19.0 / 6.4	46%	949	49.4

Phase 1 Phase 2 Phase 3

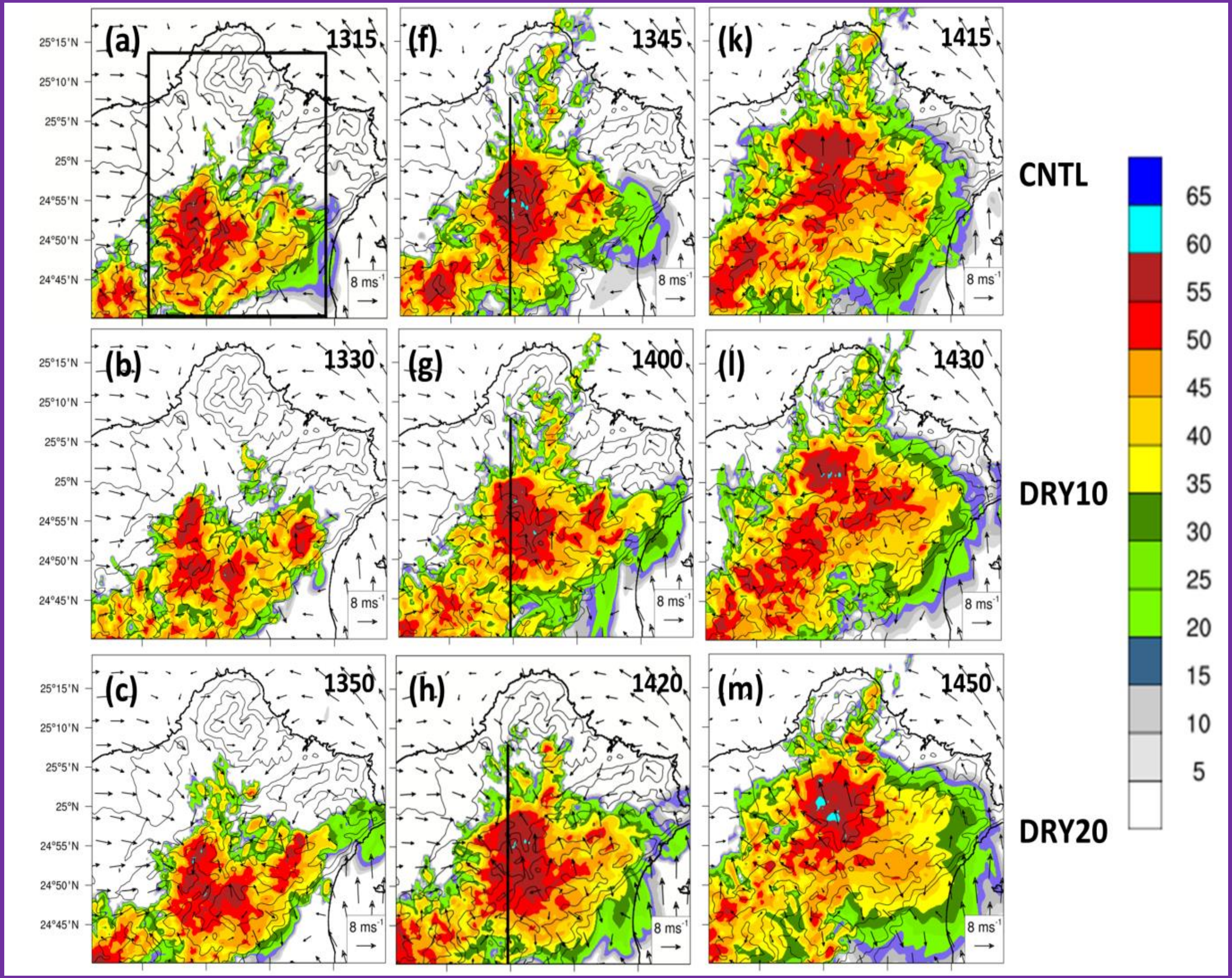

=> Convection is stronger and more organized in CTL, DRY10, and DRY20 than in WET10 and WET20

Phase 1 Phase 2 Phase 3

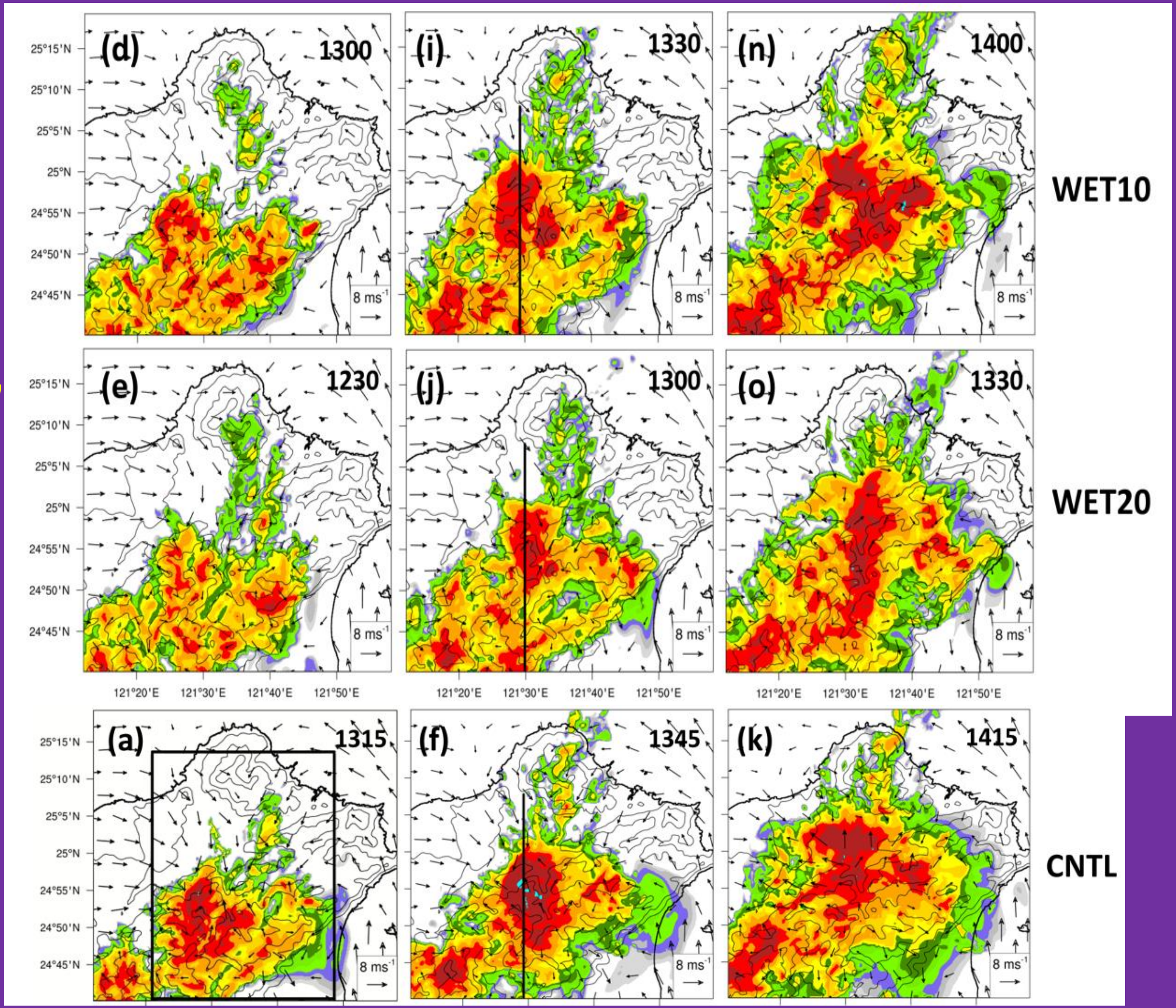

=> WET20 had the earliest convection, followed by WET10, CNTL, DRY10, and DRY20

=> A moister mid-level will have an earlier convection initiation

Convection Organization defined as
a) Connected area with column-max. Z > 55 dBZ
b) Connected area with upper-level W > 3 m/s

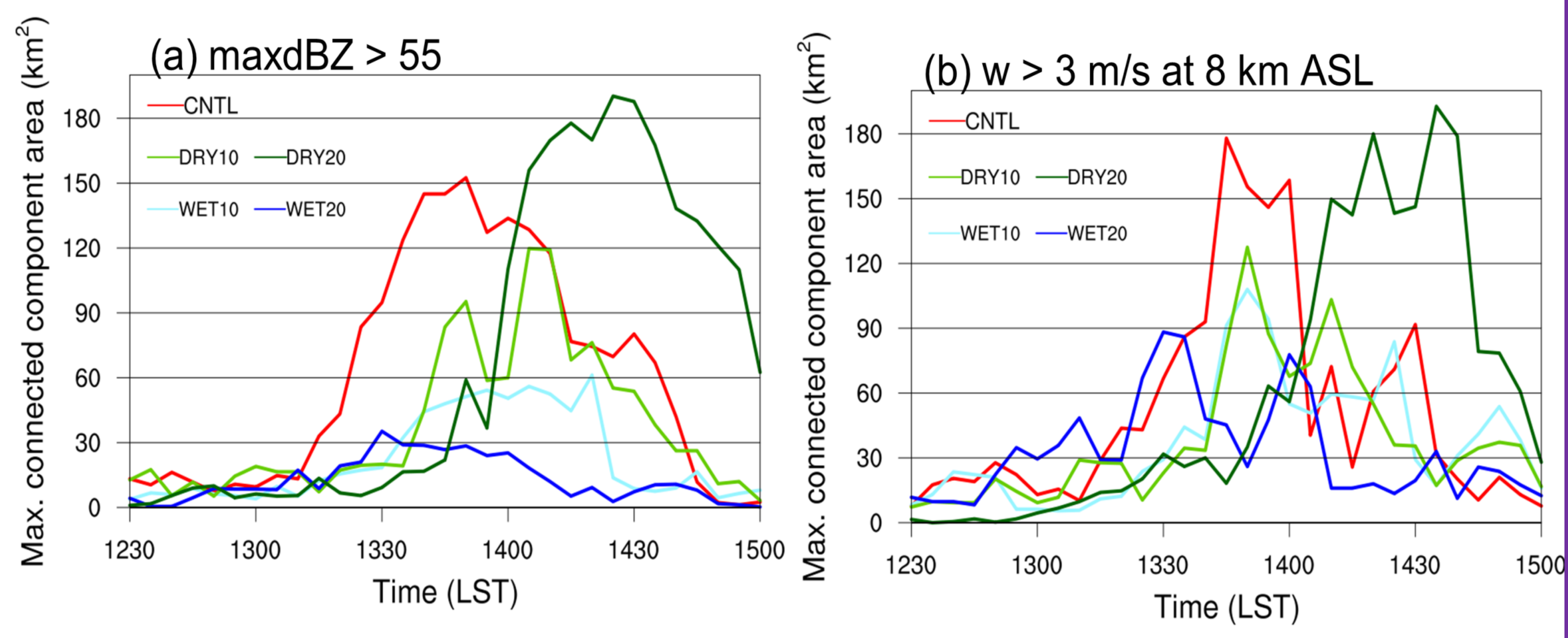

Order of convection organization:
DRY20 > CNTL >DRY10 >WET10 > WET20

Order of bain-accumulated rainfall:
WET20 > CNTL > WET10 > DRY10 > DRY20

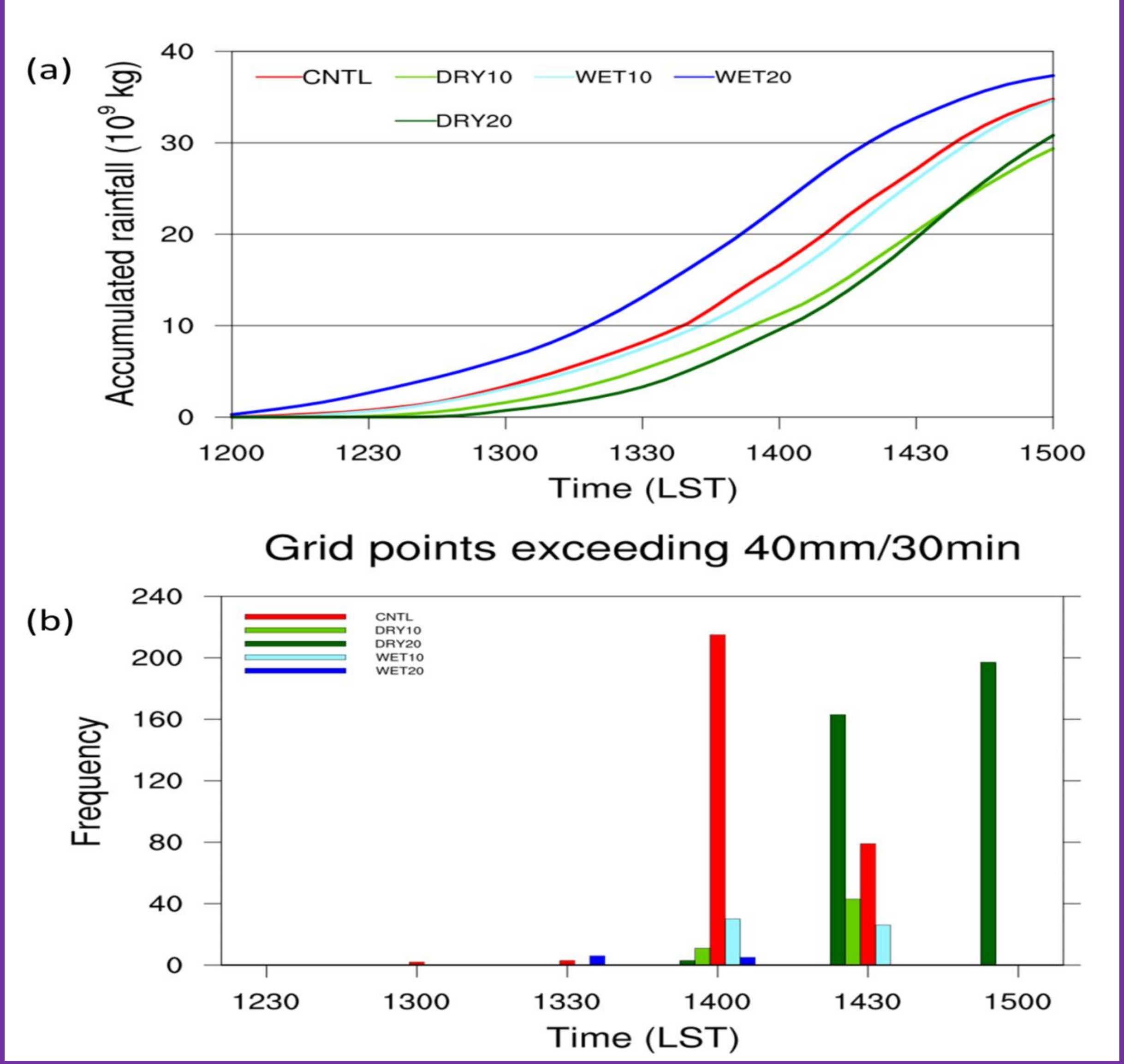

Order of area with intense rainfall rate (> 40 mm / 30 min):
DRY20 > CNTL > DRY10 ~ WET10 > WET20

=> Accumulated rainfall is not positively related to rainfall rate!

Updraft mass flux for five experiments

=> Upper-level updraft flux maxima were associated with depositional heating, and low-level updraft flux maxima were by lifting above the cold pool

Order of low-level updraft mass flux: DRY20 > CNTL > DRY10 > WET10 > WET20

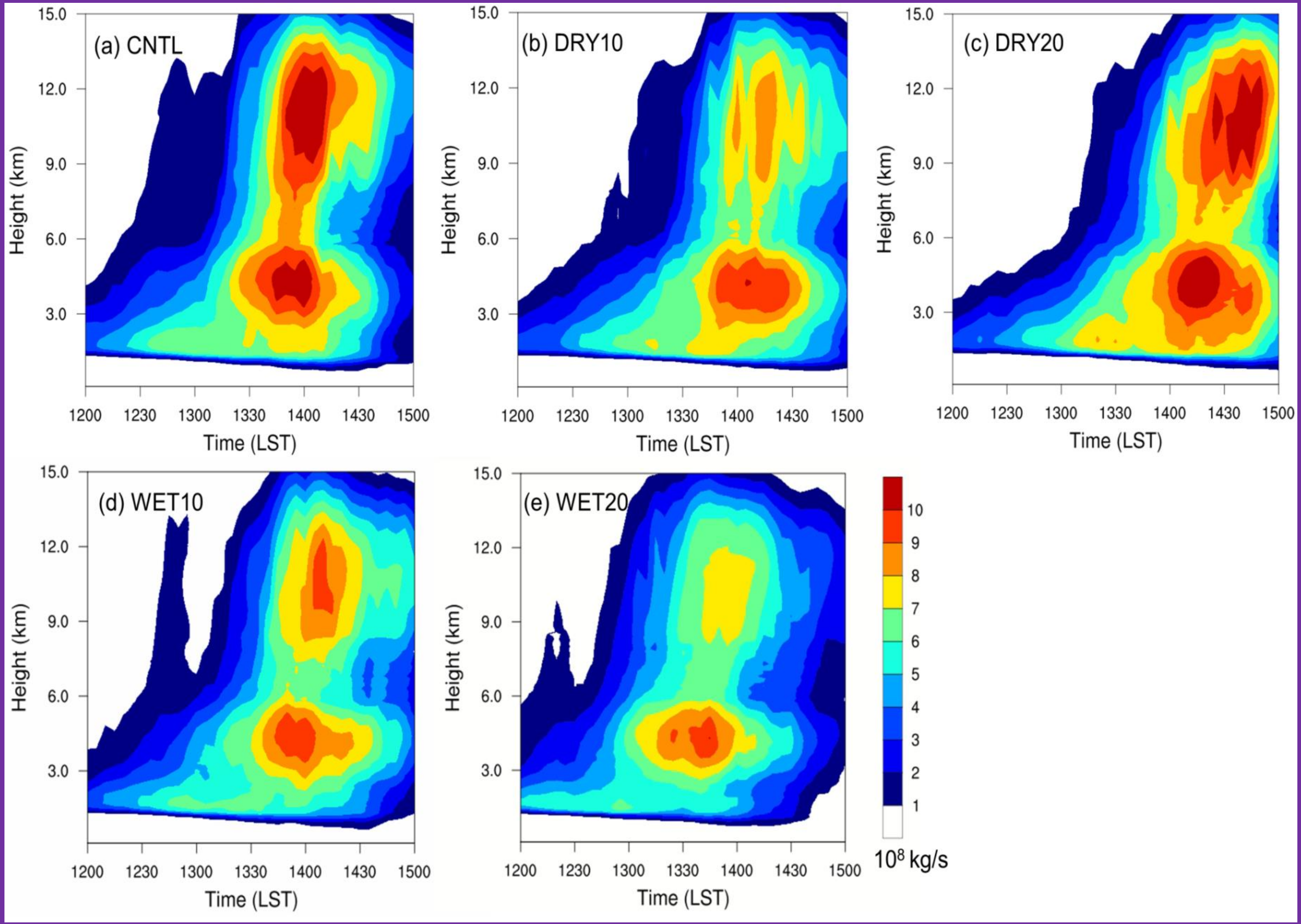

Downdraft mass flux for five experiments

Low-level downdraft flux maxima were associated with evaporative cooling

Order of low-level updraft mass flux: CNTL > DRY20 > WET10 > DRY10 > WET20

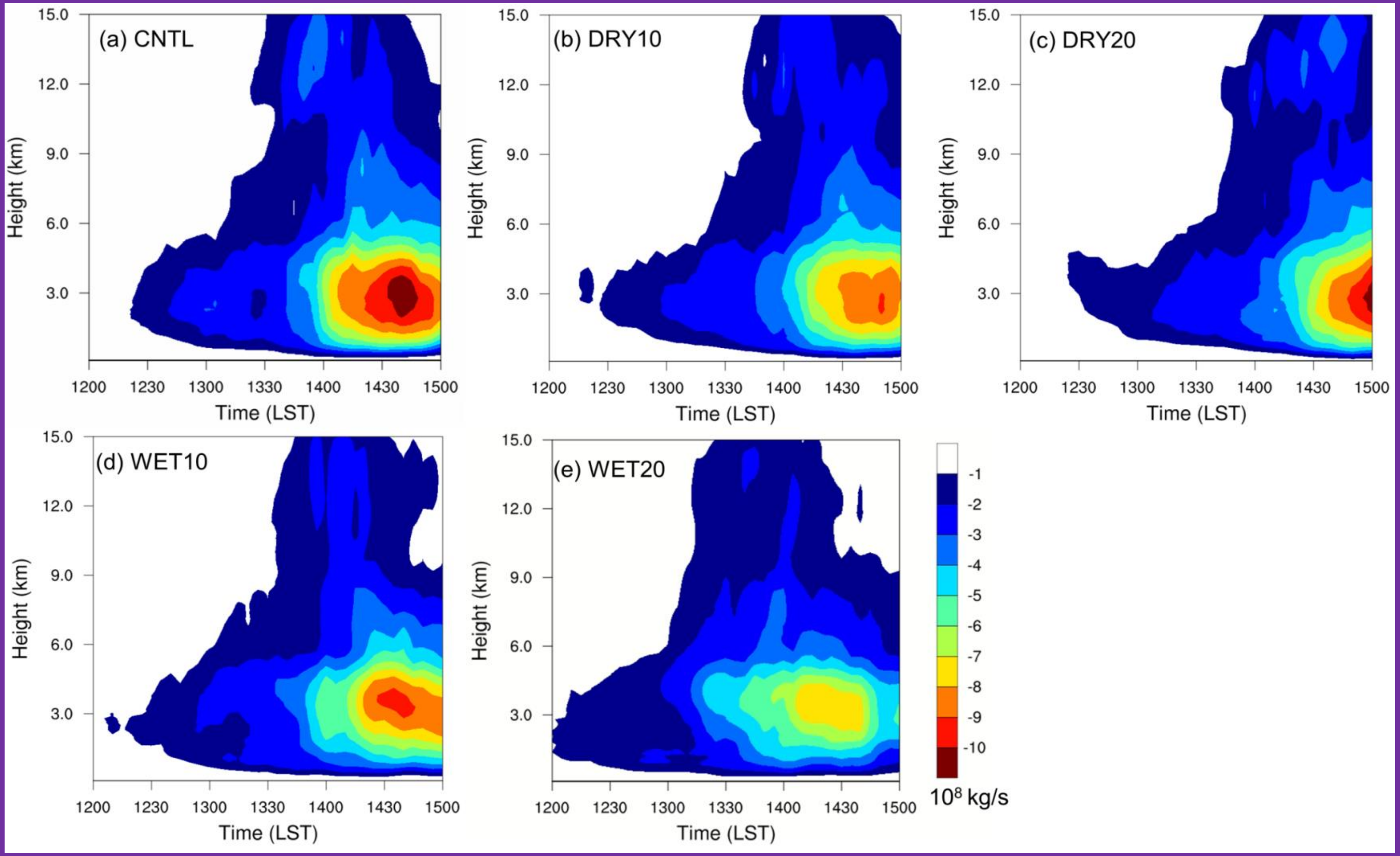

Bulk entrainment rate for five experiments

The decrease of entrainment rate was associated with the increase of storm organization at 1330 -1430 LST for CNTL, DRY10, and DRY20 experiment.

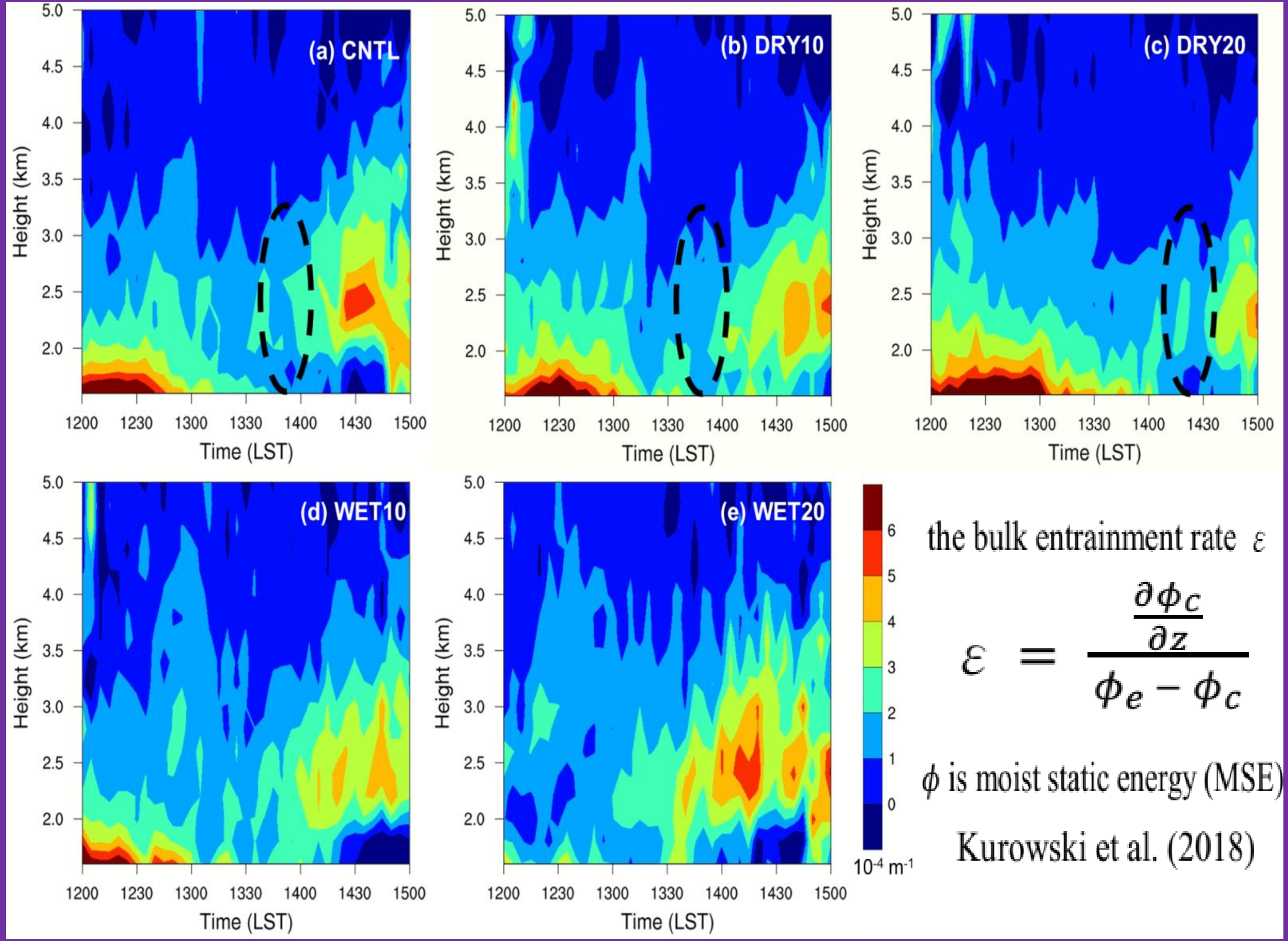

For WET10 and WET20 experiments, The entrainment rate did not increase with the increase of updraft mass flux.

Statistics of peak intensity and theta-e within updrafts for five experiments

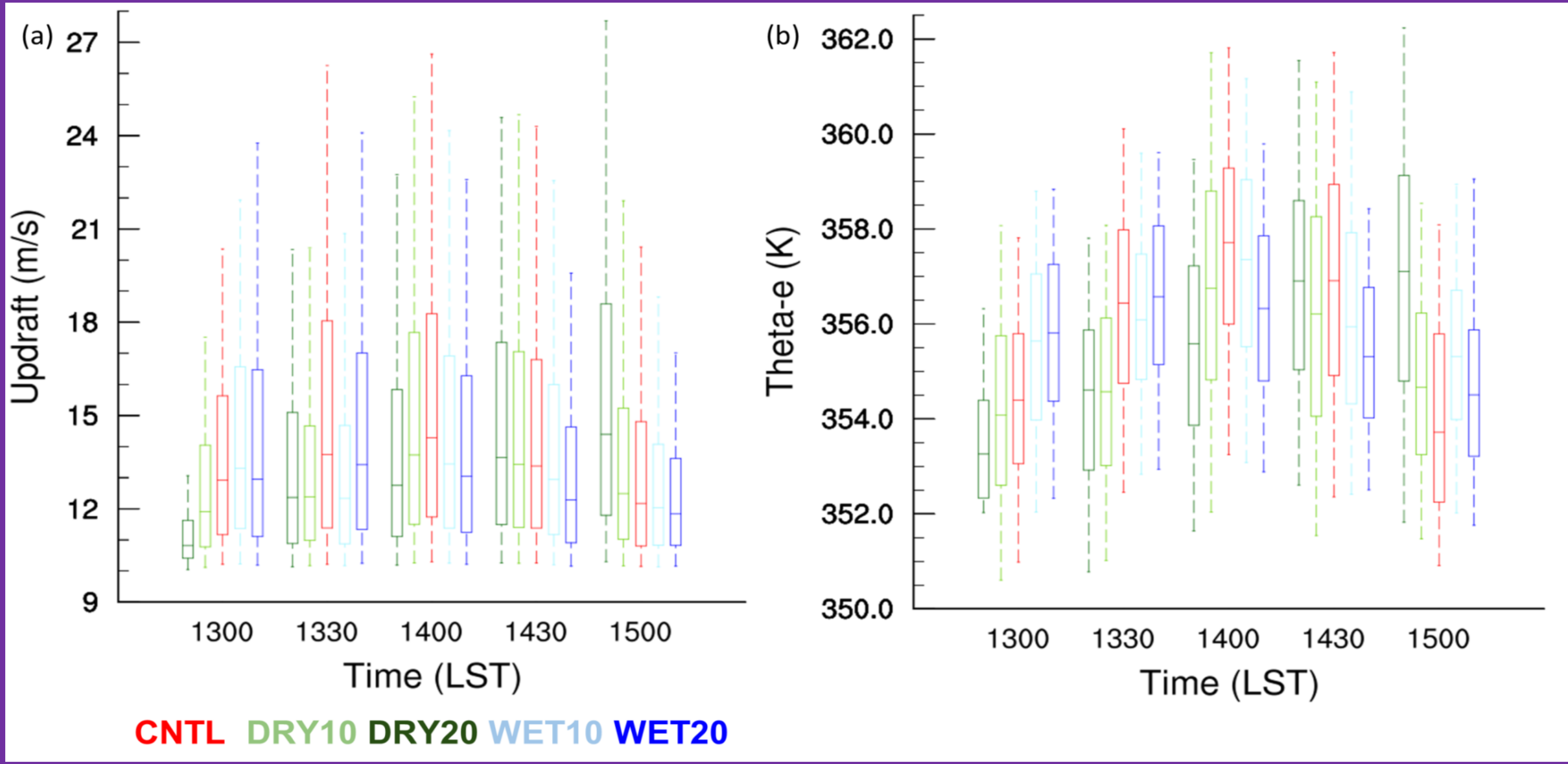

=> CNTL, DRY10, and DRY20 experiments have stronger updrafts than WET10 and WET20 runs

=> These stronger updrafts are associated with higher theta-e air

Statistics of peak intensity within downdrafts for five experiments

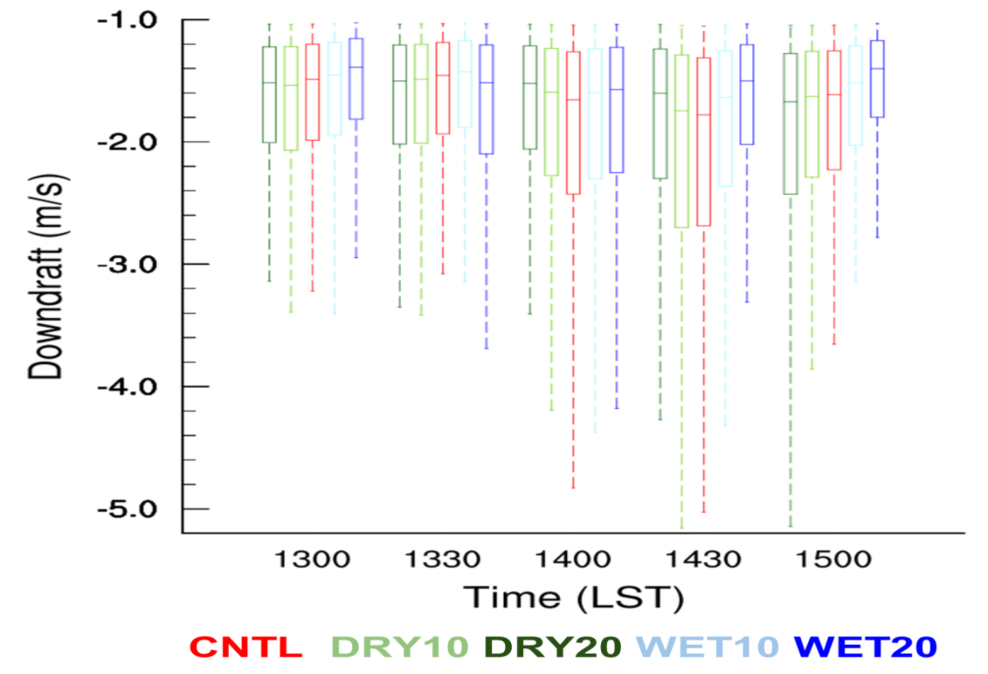

=> CNTL, DRY10, and DRY20 experiments have stronger downdrafts than WET10 and WET20 runs

=> Downdraft enhancement in direr mid-level environments

Vertical cross section along Danshui River Valley for five experiments

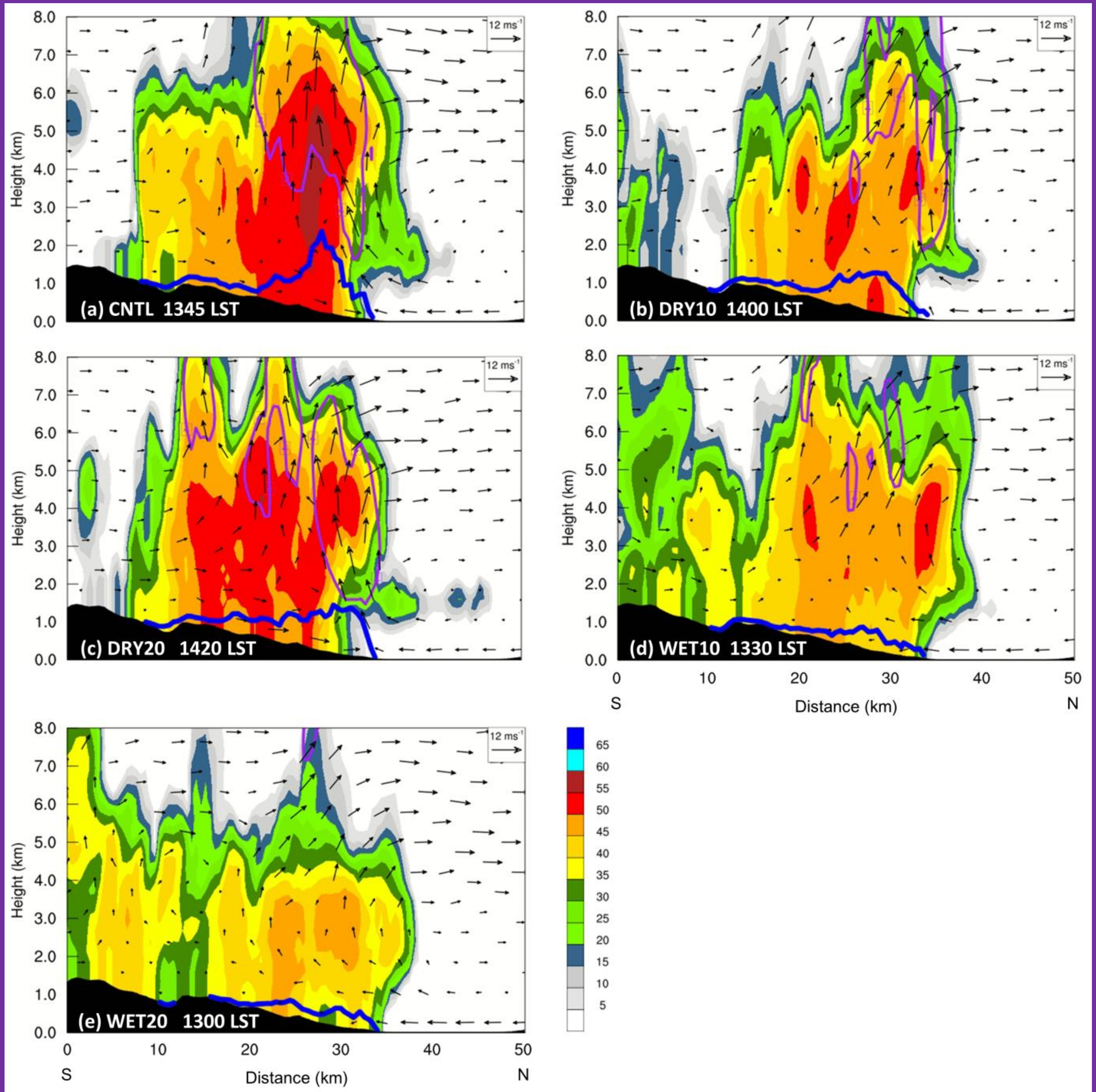

=> CNTL and DRY20 have stronger radar echos, but WET10 and WET20 have weaker echoes

=> CNTL and DRY20 have deeper cold pools and stronger lifting, but WET10 and WET20 have shallower ones and weaker lifting

Analysis of 200 air parcel 30-min forward trajectories lifted near the surface within Taipei Basin

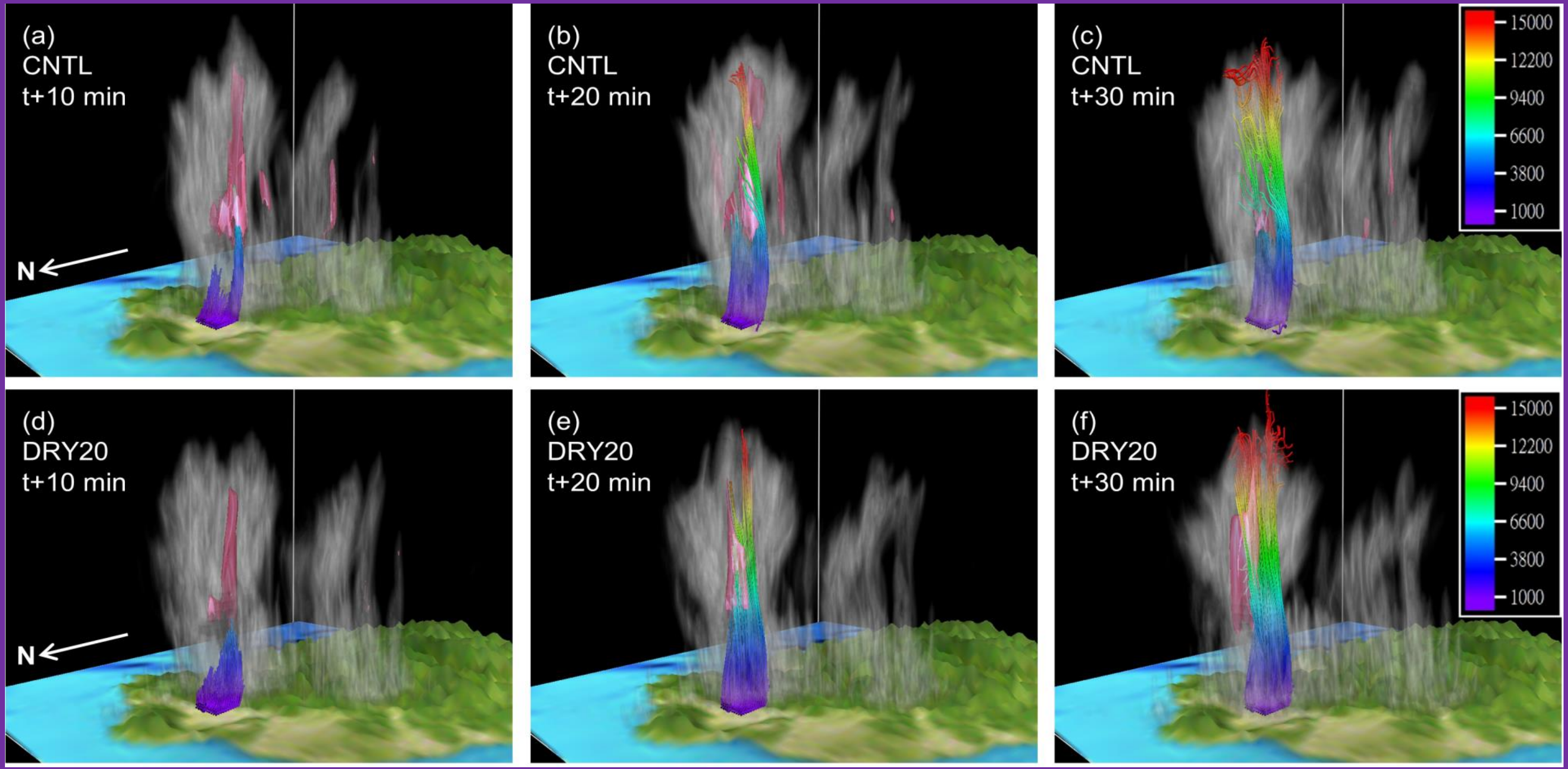

=> Trajectories in CNTL and DRY20 runs can overshoot the tropopause

=> Lots of graupel particles at middle levels in CNTL and DRY20

Analysis of 200 air parcel 30-min forward trajectories lifted near the surface within Taipei Basin

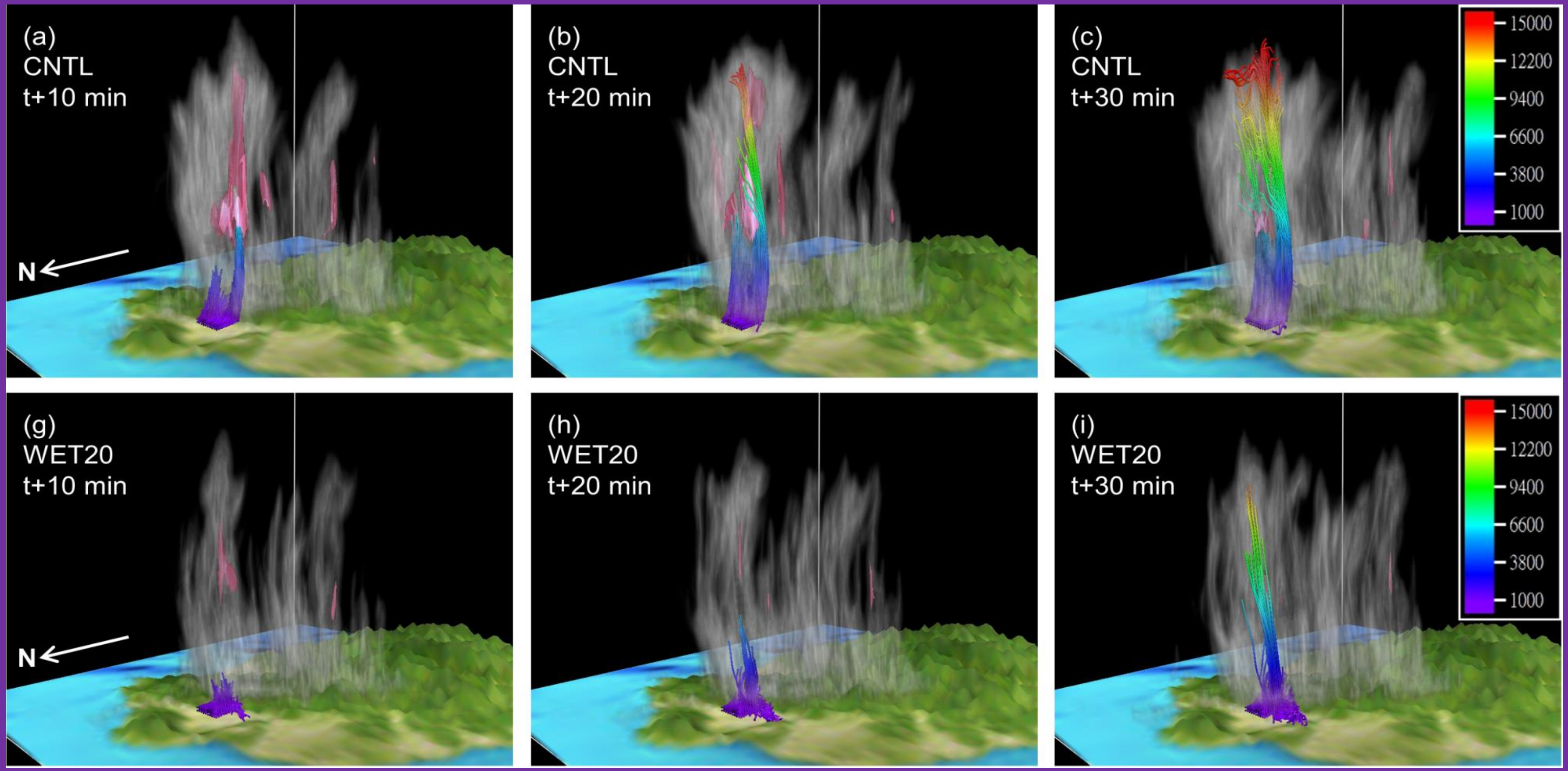

=> Most trajectories in WET20 remained trapped below the melting level

=> Fewer graupel particles in WET20

Histogram of final heights of air parcels for CNTL, DRY20, and WET20

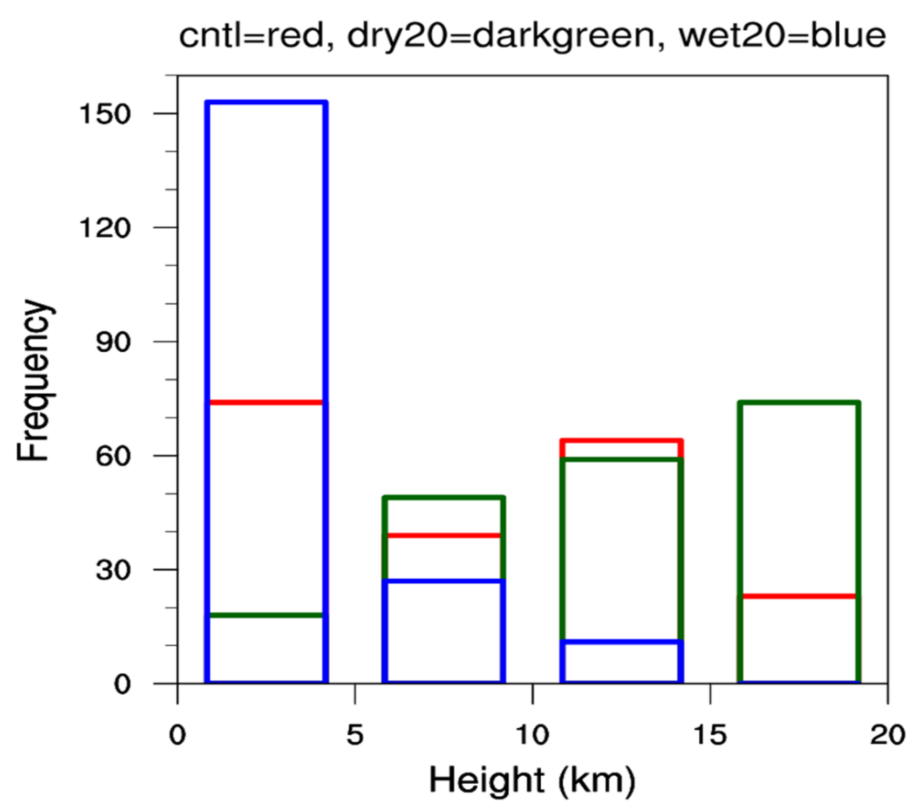

=> 91% of parcels in DRY20 can reach above 5 km (melting level)
=> 63% of parcels in CNTL can reach 5 km, but only 24% of parcels in WET20 can reach the melting level

CAPE (colored) and Cold-Pool Height (Contoured)

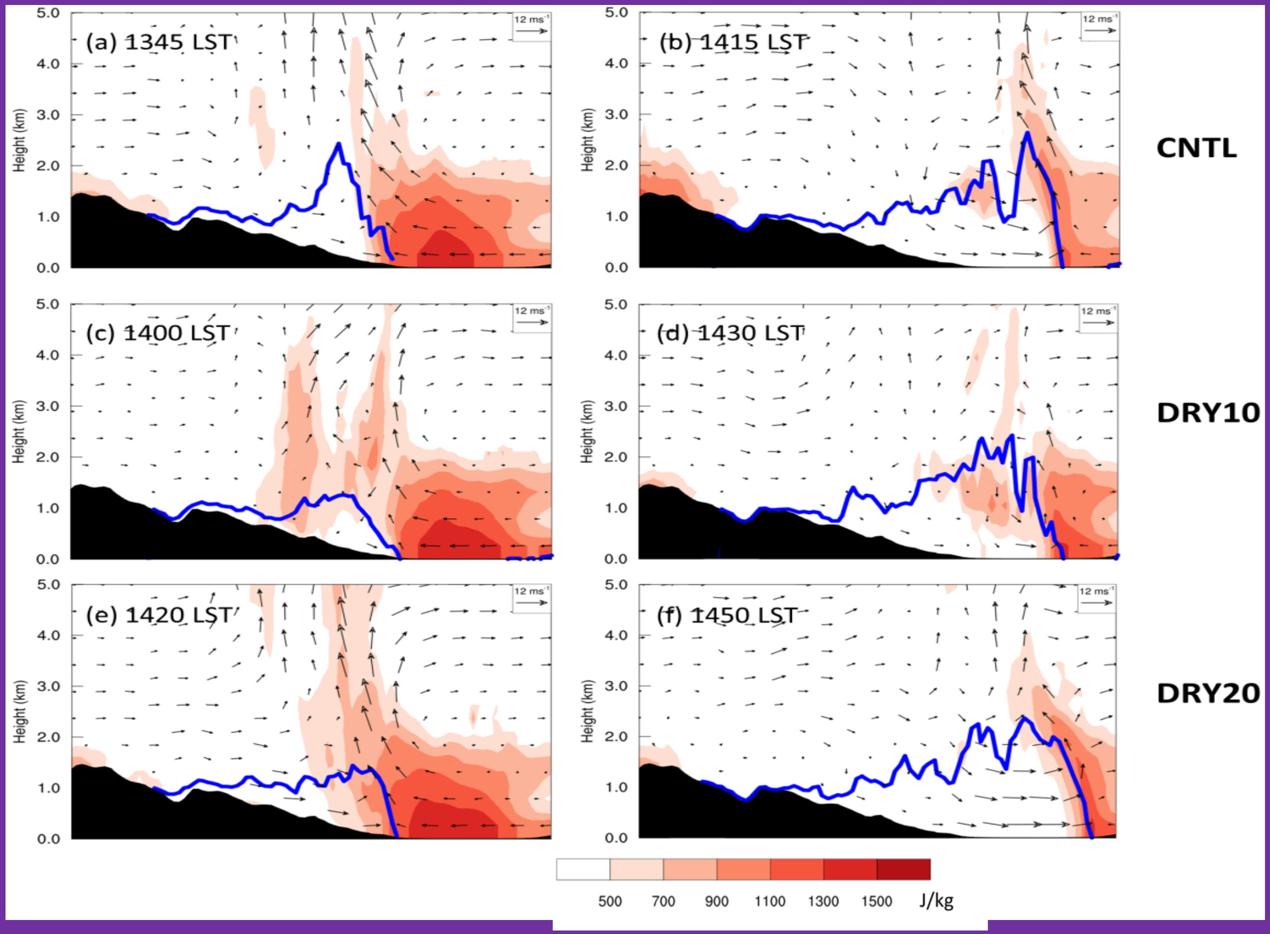

=> CAPE ~ 1500 J/kg in CNTL, DRY10, and DRY20 before the cold pool reached the basin

=> CAPE ~700 J/kg after the cold pool reached the basin

CAPE (colored) and Cold-Pool Height (Contoured)

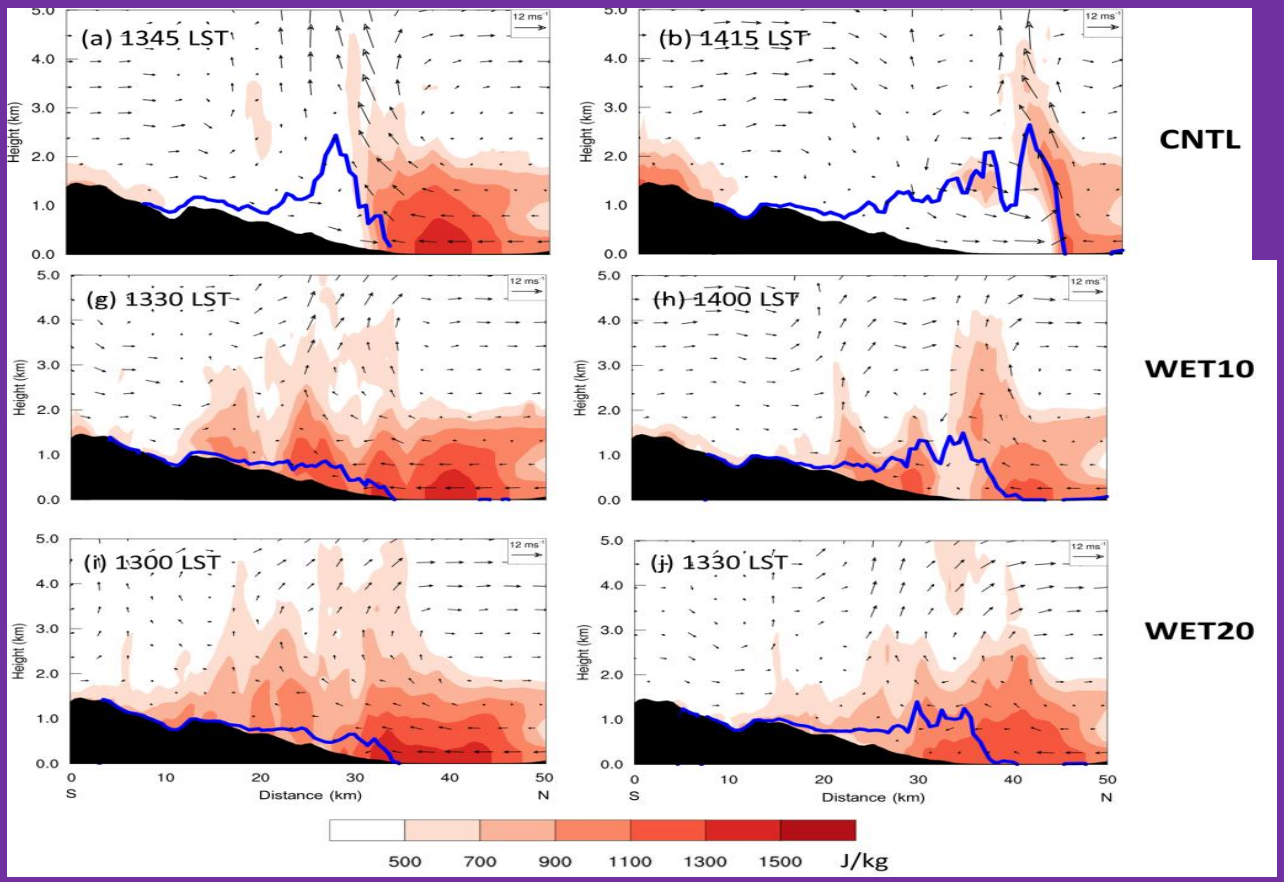

=> CAPE >1100 J/kg in WET10 and WET20 after the cold pool reached the basin

=> Cold pool in WET10 and WET20 were too weak to lift parcels above the gust front

Vertical profiles of mixing ratio of rainwater, graupel, and snow

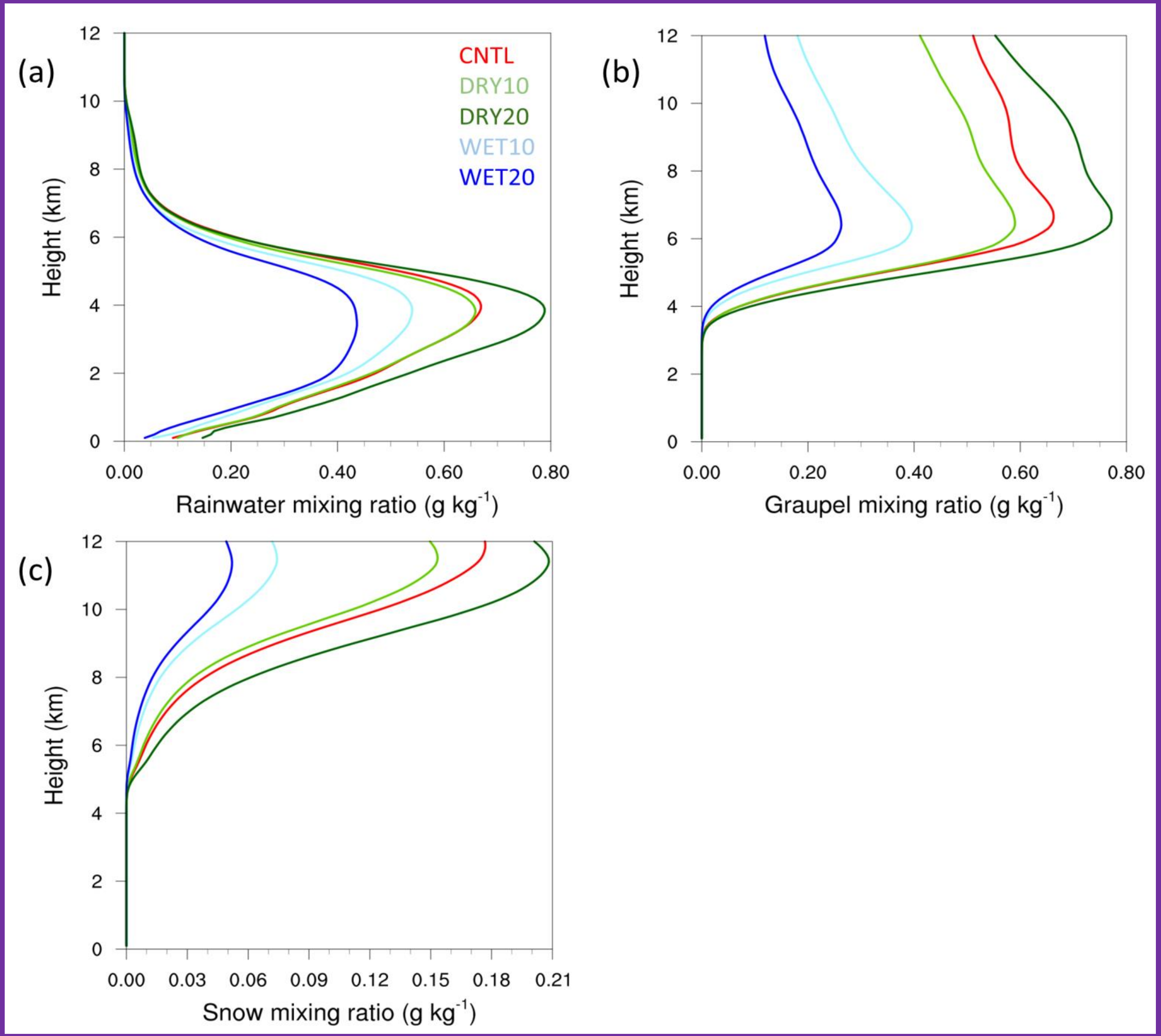

=> DRY20 has the most rainwater, graupel, and snow, followed by CNTL, DRY10, WET10, and WET20

=> Consistent with the results for peak updraft intensity for five experiments

Vertical profiles of latent cooling

=> DRY20 has the strongest evaporative cooling, followed by DRY10, CNTL, WET10, and WET20

=> Ranking for graupel melting cooling is similar to that of evaporative cooling

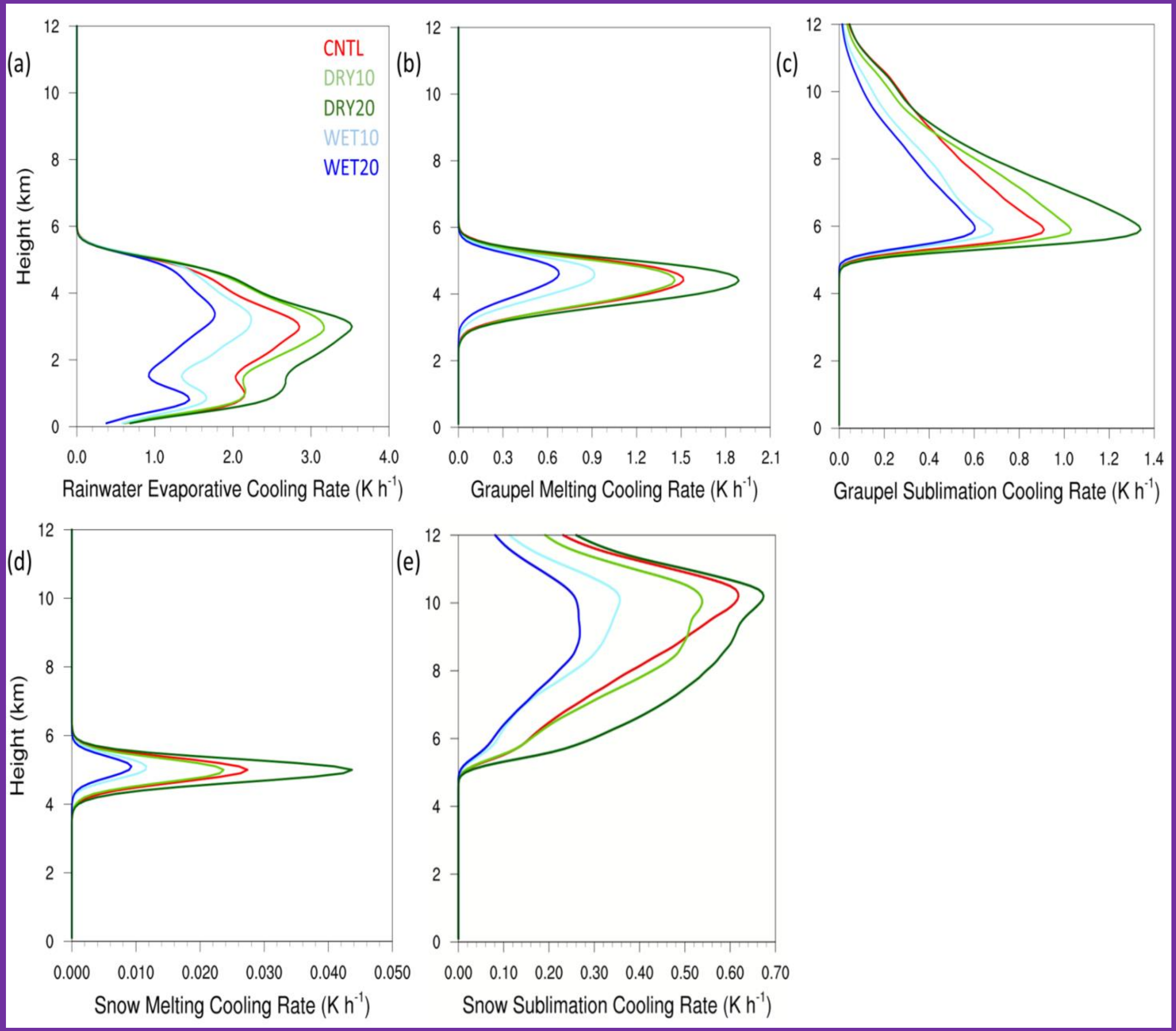

Vertical profiles of net latent heating and cooling

=> DRY20 has the strongest latent heating at mid- to upper levels, followed by CNTL, DRY10, CNTL, WET10, and WET20

=> Similarly, DRY20 has the largest latent cooling at lower levels, followed by CNTL, DRY10, CNTL, WET10, and WET20

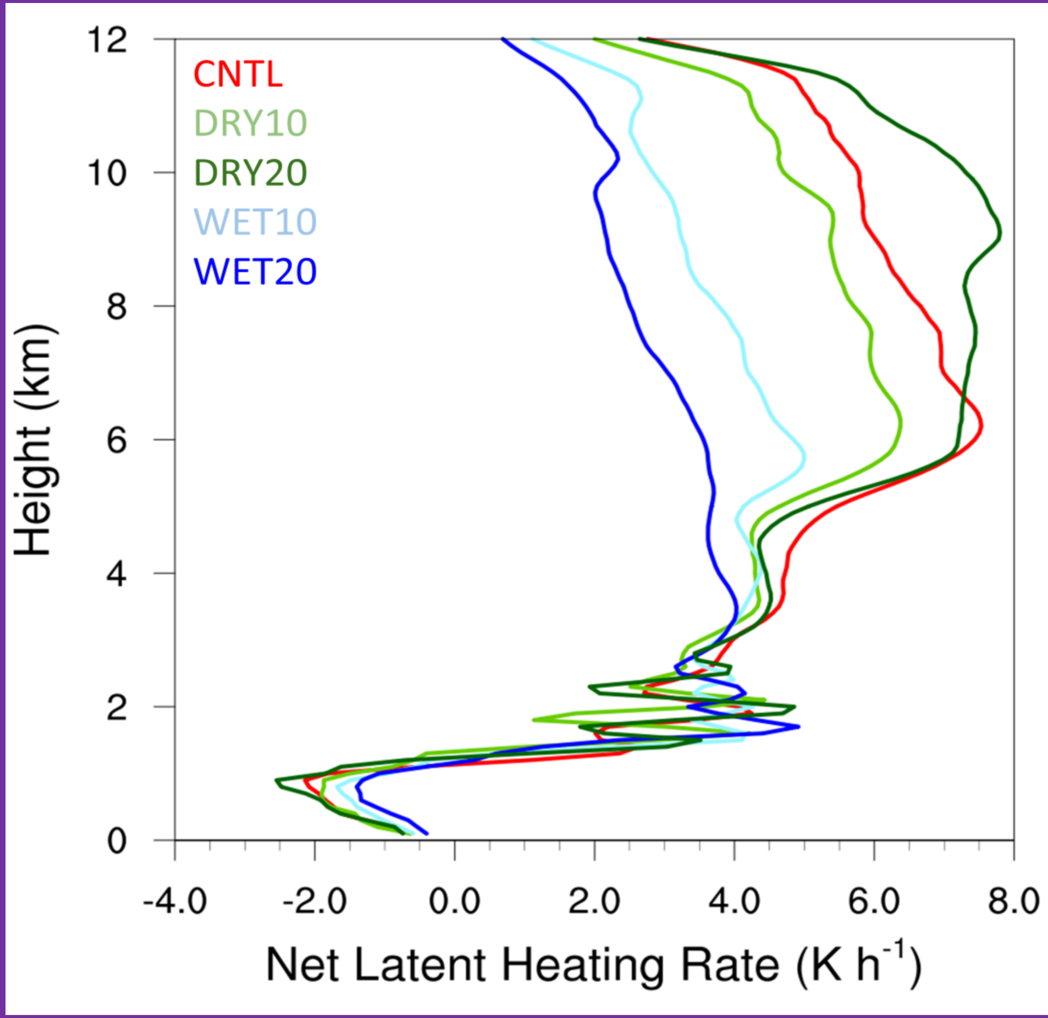

200 backward 1-h trajectories
View from the top

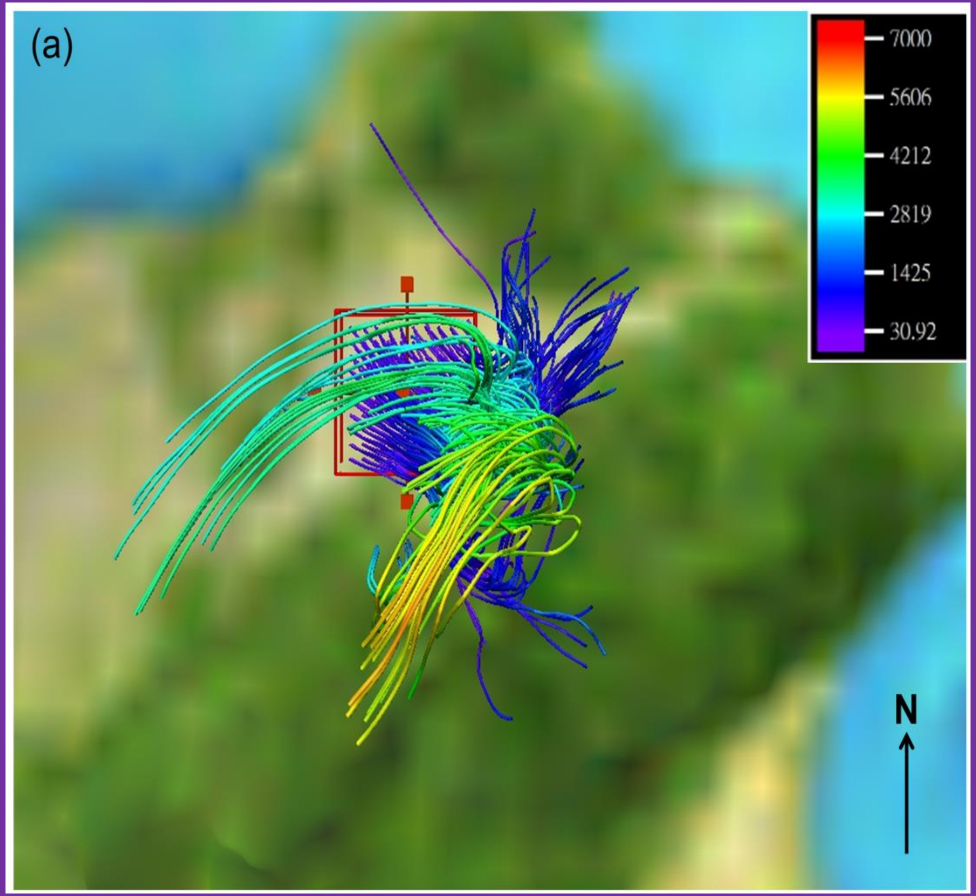

=> 59% of air parcels within the cold pool were above the basin one hour before

200 backward 1-h trajectories
View from the west

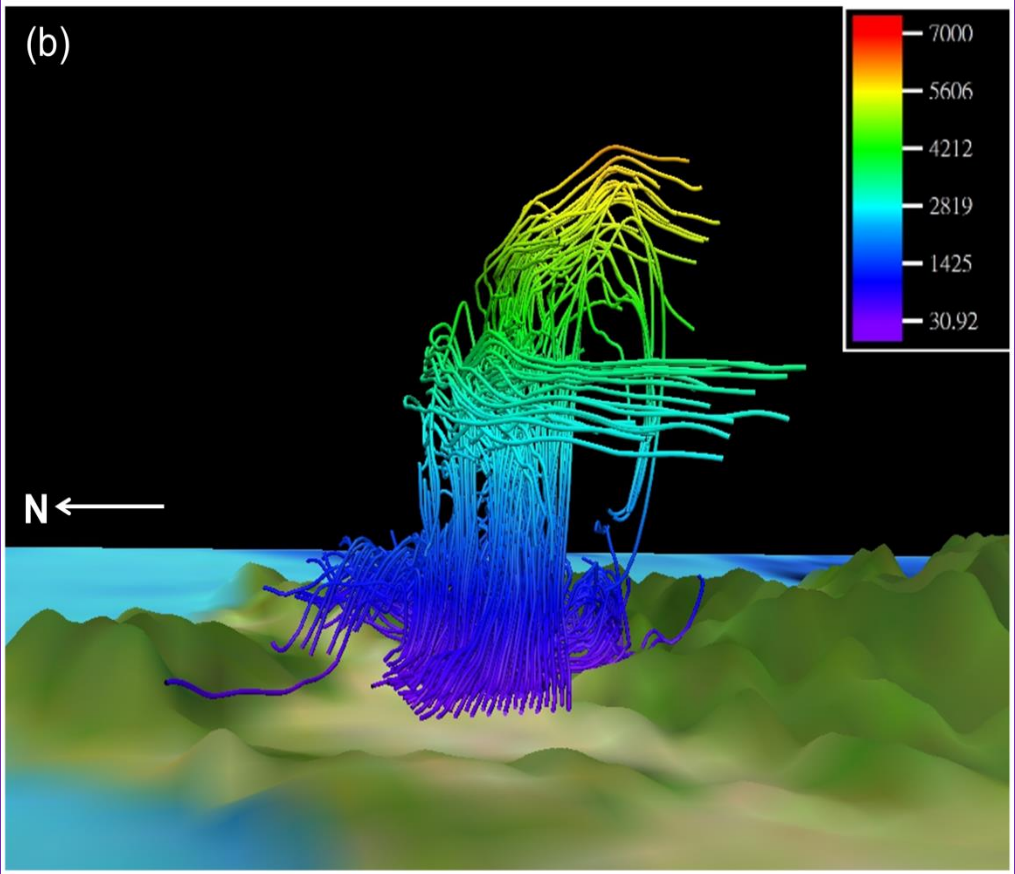

=> Air parcels from the southern slops from transported from 3-7 km levels

Histogram of the heights of backward trajectories at ending time

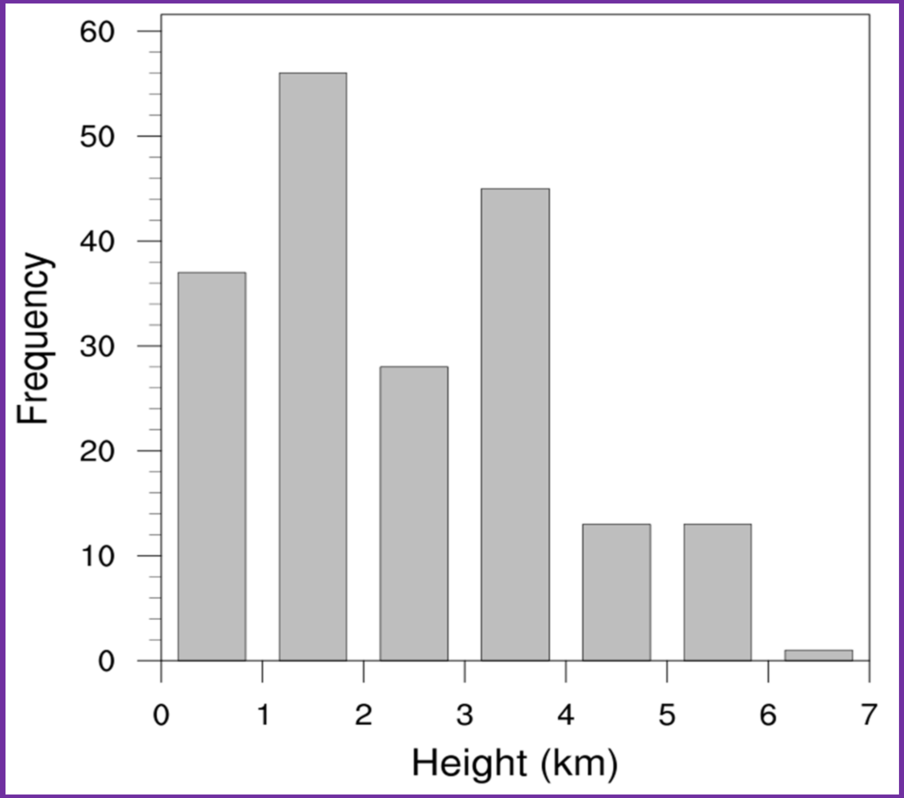

=> 37% of air parcels within the cold pool were descended from 3-km level or higher

=> This explains the reason why the cold-pool intensity was sensitive to mid-level moisture amount!

Conceptual models of thunderstorm in environment with dry and wet mid-level air

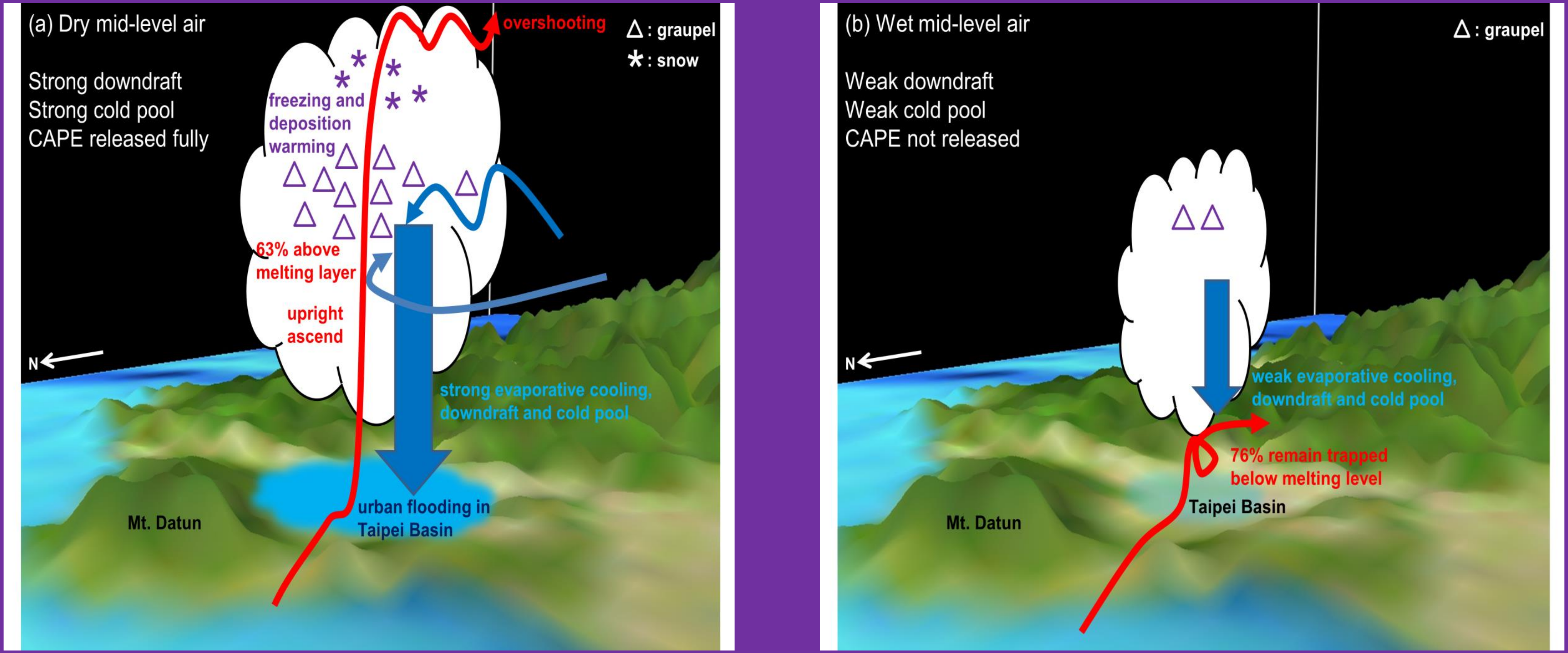

Conclusions (I)

- **Sea-breeze circulation** was responsible for **convection initiation at foothill**, and **mountain-valley circulation** was for **convection initiated at mountain peak**, respectively.

- **CAPE** was increased by **800 to 3200 J/kg** with abundant **moisture transport by the sea breeze from 08 to 12 LST**, providing large thermodynamic instability.

- Two types of cell-merger mechanism, **rear-end and head-on collisions**, are found for this afternoon thunderstorm event.

- **Evaporative cooling of raindrop** played an **major** role in the propagation and intensification of cold-air outflow, while **melting cooling of graupel** played a **minor** role.

- **Mount Datun** produced the **channel effect** along **Danshui River Valley**, **intensified sea-breeze circulation** and transported more moisture, **increased CAPE** and resulted in **stronger thunderstorm** system with **heavier rainfall** inside Taipei City.

Conclusions (II)

- **Decreasing mid-level RH** will enhance **evaporative and sublimative cooling**, producing **stronger downdrafts and cold pools**.

- **Entrainment rate** can be reduced by **stronger cold pool and better convection organization**.

- **Less mid-level RH** in the environment will produce thunderstorms with more **intense rainfall rate**.

- **Accumulated rainfall** is not positively correlated to **rainfall rate**.

- Trajectory analysis showed that **37%** of air parcels within the **cold pool** came from **the middle levels (3-6 km height),** implying that the mid-level RH plays an important role in cold-pool intensity and thunderstorm development.

Reference:

- 繆炯恩、**楊明仁**，2018：2015年6月14日台北盆地劇烈午後雷暴個案研究：對流胞合併機制與強降雨過程探討，*大氣科學*，**46**，427–453。 (in Chinese with English abstract).
- Feng, Z., S. Hagos, A. K. Rowe, C. D. Burleyson, M. N. Martini, and S. P. de Szoeke, 2015: Mechanisms of convective cloud organization by cold pools over tropical warm ocean during the AMIE/DYNAMO field campaign. *J. Adv. Model. Earth Syst.*, **7**, 357–381.
- Kurowski, M. J., K. Suselj, W. W. Grabowski, and J. Teixeira, 2018: Shallow-to-deep transition of continental moist convection: Cold pools, surface fluxes, and mesoscale organization. *J. Atmos. Sci.*, **75**, 4071–4090, https://doi.org/10.1175/JAS-D-18-0031.
- Lin, P.-F., P.-L. Chang, B. J.-D. Jou, J. W. Wilson, and R. D. Roberts, 2011: Warm season afternoon thunderstorm characteristics under weak synoptic-scale forcing over Taiwan Island. *Wea. Forecasting*, **26**, 44–60.
- Lin, P.-F., P.-L. Chang, B. J.-D. Jou, J. W. Wilson, and R. D. Roberts, 2012: Objective prediction of warm season afternoon thunderstorms in northern Taiwan using a fuzzy logic approach. *Wea. Forecasting*, **27**, 1178–1197.
- Miao, J.-E., and M.-J. Yang, 2020: A modeling study of the severe afternoon thunderstorm event at Taipei on 14 June 2015: The roles of sea breeze, microphysics, and terrain. *J. Meteor. Soc. Japan*, **98**, 129–152, doi:10.2151/jmsj.2020-008.
- Miao, J.-E., and M.-J. Yang, 2021: The impacts of mid-level moisture on the structure, evolution, and precipitation of afternoon thunderstorms: A real-case modeling study at Taipei on 14 June 2015. To be submitted.
- Moseley, C., C. Hohenegger, P. Berg, and J. O. Haerter, 2016: Intensification of convective extremes driven by cloud-cloud interaction, *Nat. Geosci.*, **9**, 748– 752.
- **Yang, M.-J.***, and R. A. Houze, Jr., 1995b: Sensitivity of squall-line rear inflow to ice microphysics and environmental humidity. *Mon. Wea. Rev.*, **123**, 3175–3193.

Thanks for your attention!